

MODERN PATHOLOGY

ABSTRACTS

(800-850)

HEAD AND NECK PATHOLOGY

2022



USCAP 111TH ANNUAL MEETING

REAL INTELLIGENCE



MARCH 19-24, 2022 LOS ANGELES, CALIFORNIA

Published by

SPRINGER NATURE

www.ModernPathology.org

 **USCAP**
Creating a Better Pathologist

AN OFFICIAL JOURNAL OF THE
UNITED STATES AND CANADIAN
ACADEMY OF PATHOLOGY

EDUCATION COMMITTEE

Rhonda K. Yantiss
Chair

Kristin C. Jensen
Chair, CME Subcommittee

Laura C. Collins
Chair, Interactive Microscopy Subcommittee

Yuri Fedoriw
Short Course Coordinator

Ilan Weinreb
Chair, Subcommittee for Unique Live Course Offerings

Carla L. Ellis
Chair, DEI Subcommittee

Adebowale J. Adeniran

Kimberly H. Allison

Sarah M. Dry

William C. Faquin

Karen J. Fritchie

Jennifer B. Gordetsky

Levon Katsakhyan, Pathologist-in-Training

Melinda J. Lerwill

M. Beatriz S. Lopes

Julia R. Naso, Pathologist-in-Training

Liron Pantanowitz

Carlos Parra-Herran

Rajiv M. Patel

Charles "Matt" Quick

David F. Schaeffer

Lynette M. Sholl

Olga K. Weinberg

Maria Westerhoff

ABSTRACT REVIEW BOARD

Benjamin Adam
Oyedele Adeyi
Mariam Priya Alexander
Daniela Allende
Catalina Amador
Vijayalakshmi Ananthanarayanan
Tatjana Antic
Manju Aron
Roberto Barrios
Gregory R. Bean
Govind Bhagat
Luis Zabala Blanco
Michael Bonert
Alain C. Borczuk
Tamar C. Brandler
Eric Jason Burks
Kelly J. Butnor
Sarah M. Calkins
Weibiao Cao
Wenqing (Wendy) Cao
Barbara Ann Centeno
Joanna SY Chan
Kung-Chao Chang
Hao Chen
Wei Chen
Yunn-Yi Chen
Sarah Chiang
Soo-Jin Cho
Shefali Chopra
Nicole A. Cipriani
Cecilia Clement
Claudiu Cotta
Jennifer A. Cotter
Sonika M. Dahiya
Elizabeth G. Demicco
Katie Dennis
Jasreman Dhillon
Anand S. Dighe
Bojana Djordjevic
Michelle R. Downes
Charles G. Eberhart
Andrew G. Evans
Fang Fan

Julie C. Fanburg-Smith
Gelareh Farshid
Michael Feely
Susan A. Fineberg
Dennis J. Firschau
Gregory A. Fishbein
Agnes B. Fogo
Andrew L. Folpe
Danielle Fortuna
Billie Fyfe-Kirschner
Zeina Ghorab
Giovanna A. Giannico
Anthony J. Gill
Tamar A. Giordadze
Alessio Giubellino
Carolyn Glass
Carmen R. Gomez-Fernandez
Shunyou Gong
Purva Gopal
Abha Goyal
Christopher C. Griffith
Ian S. Hagemann
Gillian Leigh Hale
Suntrea TG Hammer
Malini Harigopal
Kammi J. Henriksen
Jonas J. Heymann
Carlo Vincent Hojilla
Aaron R. Huber
Jabed Iqbal
Shilpa Jain
Vickie Y. Jo
Ivy John
Dan Jones
Ridas Juskevicius
Meghan E. Kapp
Nora Katabi
Francesca Khani
Joseph D. Khoury
Benjamin Kipp
Veronica E. Klepeis
Christian A. Kunder
Stefano La Rosa

Stephen M. Lagana
Keith K. Lai
Goo Lee
Michael Lee
Vasiliki Leventaki
Madelyn Lew
Faqian Li
Ying Li
Chieh-Yu Lin
Mikhail Lisovsky
Lesley C. Lomo
Fang-I Lu
aDeqin Ma
Varsha Manucha
Rachel Angelica Mariani
Brock Aaron Martin
David S. McClintock
Anne M. Mills
Richard N. Mitchell
Hiroshi Miyamoto
Kristen E. Muller
Priya Nagarajan
Navneet Narula
Michiya Nishino
Maura O'Neil
Scott Roland Owens
Burcin Pehlivanoglu
Deniz Peker Barclift
Avani Anil Pendse
Andre Pinto
Susan Prendeville
Carlos N. Prieto Granada
Peter Pytel
Stephen S. Raab
Emilian V. Racila
Stanley J. Radio
Santiago Ramon Y Cajal
Kaaren K Reichard
Jordan P. Reynolds
Lisa M. Rooper
Andrew Eric Rosenberg
Ozlen Saglam
Ankur R. Sangoi

Kurt B. Schaberg
Qiuying (Judy) Shi
Wonwoo Shon
Pratibha S. Shukla
Gabriel Sica
Alexa Siddon
Anthony Sisk
Kalliopi P. Siziopikou
Stephanie Lynn Skala
Maxwell L. Smith
Isaac H. Solomon
Wei Song
Simona Stolnicu
Adrian Suarez
Paul E. Swanson
Benjamin Jack Swanson
Sara Szabo
Gary H. Tozbikian
Gulisa Turashvili
Andrew T. Turk
Efsevia Vakiani
Paul VanderLaan
Hanlin L. Wang
Stephen C. Ward
Kevin M. Waters
Jaclyn C. Watkins
Shi Wei
Hannah Y. Wen
Kwun Wah Wen
Kristy Wolniak
Deyin Xing
Ya Xu
Shaofeng N. Yan
Zhaohai Yang
Yunshin Albert Yeh
Huina Zhang
Xuchen Zhang
Bihong Zhao
Lei Zhao

To cite abstracts in this publication, please use the following format: **Author A, Author B, Author C, et al. Abstract title (abs#). In "File Title." *Modern Pathology* 2022; 35 (suppl 2): page#**

800 Histological Tumor Regression Grade in Post-Neoadjuvant Treated Oral Squamous Cell Carcinoma: Validation of Proposed Tumor Regression Grade as a Prognostic Indicator

Vishesha Adhvaryu¹, Katha Rabade¹, Swapnil Rane¹, Munita Bal¹, Neha Mittal², Asawari Patil³

¹Tata Memorial Centre, Mumbai, India, ²Tata Memorial Hospital, Mumbai, India, ³ACTREC-Tata Memorial Centre, Thane, India

Disclosures: Vishesha Adhvaryu: None; Katha Rabade: None; Swapnil Rane: None; Munita Bal: None; Neha Mittal: None; Asawari Patil: None

Background: Neoadjuvant chemotherapy (NACT) prior to surgery is successfully used as a therapeutic strategy to achieve resectability and organ preservation in advanced oral squamous cell carcinoma (OSCC). An objective grading system is required to assess the impact of NACT and determine the post-operative line of management. In a previous unpublished study, we assessed a 3-tier tumor regression grading (TRG) system in a cohort of 151 OSCC patients. TRG was significantly associated with disease-free survival (DFS) but not with overall survival (OS). In addition, perineural invasion (PNI) and nodal metastasis showed a significant correlation with DFS. We aim to validate the proposed TRG in NACT-treated OSCC cases.

Design: We evaluated 150 OSCC cases that underwent surgery after NACT (2013-2018) with an adverse event or a minimum event-free follow-up of 24 months. A TRG was assigned based on the percentage of residual viable tumor at the primary site as well as metastatic lymph nodes (TRG1: <5%, TRG2: 5-50%, TRG3: >50%). The cases were divided into two groups: the buccal mucosa group (buccal mucosa, alveolus, lip) and the tongue group. Pathological complete response (PCR) was assessed, defined as the absence of residual tumor at the primary site and in lymph nodes. Statistical correlation of TRG with clinicopathological parameters and survival analysis was done using SPSS version 25.

Results: The mean follow-up, DFS, and OS were 35.58 (range 3-84 months), 33.4 (range 3.42-84.8 months), and 39.4 months (range 4.9-87.8 months), respectively. The distribution of TRG at the primary sites is shown in Table 1. For the buccal mucosa group, TRG was significantly associated with PNI ($p=0.004$), bone and skin involvement ($p<0.001$), nodal metastasis ($p=0.033$), and DFS ($p<0.001$). No significant association of OS was seen with TRG. PCR showed a significant correlation with OS and DFS ($p=0.006$ and 0.023 , respectively). On multivariate analysis, OS and DFS were significantly associated with nodal metastasis ($p=0.041$ and 0.006 , respectively). The tongue group failed to show an association with the above parameters which can be attributed to a smaller number of cases in this group.

Table 1: Distribution of TRG at primary sites

		Tumor Regression Grade			
		1	2	3	Total
Tumor epicenter	Buccal mucosa+Alveolus+Lip	42 (38.8%)	20 (18.5%)	46 (42.5%)	108
	Tongue+Floor of mouth	15 (35.7%)	13 (30.9%)	14 (33.3%)	42
	Total	57	33	60	150

Conclusions: TRG had an impact on DFS when combined with other pathological parameters, thus validating its significance as a component of the model predicting DFS in NACT treated OSCC. This will help us to identify the subset of tumors that fail to respond to therapy, probe into the failure of therapy, and individualize the NACT regimen for this subset.

801 A Case Series of Twenty-Four Head & Neck Squamous Cell Carcinoma Patients with Concomitant Small Lymphocytic Lymphoma/Chronic Lymphocytic Leukemia

Dorukhan Bahceci¹, Annemieke van Zante², Kwun Wah Wen²

¹UCSF Pathology, San Francisco, CA, ²University of California, San Francisco, San Francisco, CA

Disclosures: Dorukhan Bahceci: None; Annemieke van Zante: None; Kwun Wah Wen: None

Background: Cervical nodal metastases can be the first presentation of head and neck (H&N) squamous cell carcinomas (SCC). Lymphomas are the second most common neoplasm in H&N and most are incidental and low-grade. Due to its bland cyto- and histomorphology, small cell lymphoma/chronic lymphocytic leukemia (SLL/CLL) can be missed in H&N SCC patients who undergo fine needle aspiration biopsy (FNAB) of lymph nodes or lymph node dissection.

Design: The pathology database at UCSF was searched to identify 3524 cases of H&N SCC diagnosed between 2000 and 2020. The clinicopathologic data of H&N SCC patients with concurrent diagnosis of SLL/CLL were reviewed.

Results: A total of 24 patients with concomitant SLL/CLL were identified among the 3524 patients with H&N SCC. This high prevalence was not noted for other lymphomas. The 24 patients in this cohort were predominantly male (n = 22), with a mean age of 73 years (range 55 – 86 years) at the time of surgical procedure. WBC counts were elevated (mean: 27 x 10⁹/L and range: 3.5 – 94.5 x 10⁹/L) at diagnosis. Twenty-one patients had concurrent cutaneous SCC of the H&N region, whereas 3 patients had oropharyngeal SCC. Nineteen of 24 patients had nodal metastases. Fifteen of 16 cases had intermediate or high-grade SCC. In 8 cases, SCC grading was not performed due to the fact that only nodal metastasis(es) were excised. P16 immunohistochemistry was positive in 3 (2 cases of oropharyngeal SCC and 1 cutaneous SCC) of 10 tested cases. HPV status was confirmed in these 2 cases using PCR-based test or high-risk HPV in-situ hybridization. All p16-negative SCC cases were of cutaneous origin.

Case Number	Sex	Age	Location	p16/HPV Status	AJCC 8th TNM staging	SCC Grade	WBC Count	FNA Diagnosis
1	F	62	Cutaneous	Not performed	T3N0	G2	7.7	Not performed
2	M	76	Cutaneous	Not performed	Not available	G2	94	Inadequate
3	M	86	Cutaneous	Not performed	T3N0	G2	68.6	Not performed
4	M	78	Cutaneous	Not performed	Not available	G1	Not available	SCC
5	M	74	Cutaneous	p16 negative	T2N3b	G2	5.1	Not performed
6	M	70	Cutaneous	p16 negative	T2N3b	G2	6.5	Necrotic debris
7	M	55	Cutaneous	p16 negative	T3N1	G3	13.5	SCC
8	M	83	Cutaneous	p16 negative	Not available	G2	8.8	CLL
9	M	80	Cutaneous	Not performed	T3N3b	G3	19	Not performed
10	M	82	Cutaneous	p16 negative	N3b	G3	12.9	SCC
11	M	61	Cutaneous	p16 negative	N3b	G3	8.8	SCC
12	M	79	Cutaneous	Not performed	T3N3b	G3	3.5	CLL
13	M	79	Oropharynx	p16 and HRHPV positive	N1	Not applicable	27.8	SCC
14	M	73	Cutaneous	p16 positive	N1	Not applicable	5.9	SCC and CLL
15	M	62	Cutaneous	Not performed	N2a	Not applicable	5.2	CLL
16	M	59	Oropharynx	p16 and HRHPV positive	N1	Not applicable	46.6	Not performed
17	M	64	Cutaneous	Not performed	N3b	Not applicable	16.4	SCC and CLL
18	M	79	Cutaneous	Not performed	N2a	Not applicable	17.3	SCC
19	M	78	Cutaneous	p16 negative	N3b	Not applicable	24	SCC
20	M	80	Cutaneous	Not performed	Not available	G3	94.5	Not performed
21	M	85	Cutaneous	Not performed	T3N0	G1	11.7	Not performed
22	F	83	Oropharynx	Not performed	T4aN2c	G2	71	Not performed
23	M	77	Cutaneous	Not performed	T3N3b	G3	12.5	SCC
24	M	63	Cutaneous	Not performed	Not available	G2	41.6	CLL

Conclusions: SLL/CLL was intriguingly more prevalent in H&N SCC patients (1 per 147) than in the general population (1 per 250,000). Those patients with concurrent SLL/CLL tend to have SCC of cutaneous oropharyngeal origin and nodal metastases. The markedly increased prevalence of SLL/CLL may be related to immunosuppression in these patients. Regardless, background lymphoid tissue should be carefully examined at the time of pathologic examination of H&N SCC FNAB or resection specimens (especially those patients with high WBC counts) to avoid overlooking a second diagnosis of SLL/CLL.

802 Carcinoma Ex-Pleomorphic Adenoma: Reappraising the Pathologic Spectrum of 123 cases

Munita Bal¹, Swati Thorat¹, Neha Mittal², Swapnil Rane¹, Katha Rabade¹, Asawari Patil³

¹Tata Memorial Centre, Mumbai, India, ²Tata Memorial Hospital, Mumbai, India, ³ACTREC-Tata Memorial Centre, Thane, India

Disclosures: Munita Bal: None; Swati Thorat: None; Neha Mittal: None; Swapnil Rane: None; Katha Rabade: None; Asawari Patil: None

Background: Carcinoma ex pleomorphic adenoma (CXPA) is an uncommon malignant epithelial/ myoepithelial neoplasm that arises from a pleomorphic adenoma (PA). The histopathologic spectrum of CXPA is wide-ranging and is continually getting expanded. Herein, we aimed to review the clinical and pathologic features of CXPA diagnosed at our institute.

Design: Clinical data and pathologic material of all CXPA cases (Jan 2005-June 2021) were reviewed after confirming the histologic diagnosis (WHO 2017). Evidence of a benign PA histologically with carcinoma was essential for inclusion. Cases of sarcoma ex-pleomorphic adenoma (n=3) were excluded.

Results: A total of 123 patients were included. The median age was 55 years (range, 22-87 years). The male-to-female ratio was 3.1. The most frequent site was the parotid (65.9%) followed by the submandibular gland (15.5%), hard palate (6.5%), lacrimal gland (4.9%), buccal mucosa, oropharynx, parapharyngeal site (1.6% each, respectively), sublingual, nasal, and nasopharynx (0.8% each, respectively). CXPA cases were either *de-novo* (51.5%) or transformed from recurrent/long-standing PA (48.5%). The median tumor size was 3.4 cm (range, 0.8-30cm). Salivary duct carcinoma and myoepithelial carcinoma were the commonest types among the *de-novo* and transformed cases, respectively. Exceptionally rare dual and triple malignancies were also encountered. The various histologic types of CXPA are enumerated in the table.

Tumors were intracapsular, minimally, and widely invasive in 24.5%, 59.2%, 16.3% cases, respectively. Lymphovascular and perineural invasion was identified in 30.7% and 29.8%, respectively. In 23.5% of patients, the resection margins were involved. Androgen receptor, HER2, and abnormal p53 staining were seen in 54%, 32%, and 44%, respectively. Lymph node metastasis was identified in 39%. Adjuvant radiation/ chemoradiation was administered in 89 patients. Follow-up was available in 79 patients; median 21 months (mean 25.5 months; range 1-84 months). Locoregional recurrence and distant metastases were seen in 34.2% and 37% of patients, respectively. The median time-to-recurrence was 17 months; the median time-to-metastasis was 10 months. The commonest site of distant metastasis was the lung (64.5%) followed by the liver (13.5%).

Histologic types of Carcinoma Ex-Pleomorphic Adenoma	
HISTOLOGIC TYPE	N=123
SINGLE MALIGNANCY	120 (97.6%)
SALIVARY DUCT CARCINOMA (SDC)	63 (51.2%)
SDC, NOS (NOT OTHERWISE SPECIFIED)	55 (44.7%)
SDC, SARCOMATOID	5 (4.1%)
SDC, ONCOCYTIC	2 (1.6%)
SDC, RHABDOID	1 (0.8%)
MYOEPITHELIAL CARCINOMA	29 (23.6%)
ADENOCARCINOMA, NOT OTHERWISE SPECIFIED	19 (15.5%)
ADENOSQUAMOUS CARCINOMA	4 (3.3%)
CARCINOSARCOMA	3 (2.4%)
SQUAMOUS CELL CARCINOMA	1 (0.8%)
MUCOEPIDERMOID CARCINOMA	1 (0.8%)
DUAL MALIGNANCY	2 (1.6%)
SALIVARY DUCT CARCINOMA and SMALL CELL NEUROENDOCRINE CARCINOMA	1 (0.8%)
SALIVARY DUCT CARCINOMA and SARCOMATOID SQUAMOUS CARCINOMA	1 (0.8%)
TRIPLE MALIGNANCY	1 (0.8%)
SALIVARY DUCT CARCINOMA and MYOEPITHELIAL CARCINOMA and UNDIFFERENTIATED CARCINOMA WITH OSTEOCLASTIC GIANT CELLS	1 (0.8%)

Conclusions: CXPA displays a wide pathologic spectrum that may rarely include multiple histologic types. Advanced stage, aggressive histologic types, and wide capsular invasion are poor prognostic features.

803 Reappraisal of p16 Immunohistochemical Staining as a Standalone Test for Determining HPV Status of Squamous Cell Carcinomas Arising in HPV Hot-Spots of the Head and Neck

Swati Bhardwaj¹, Melissa Gitman¹, Siraj El Jamal¹, William Westra¹
¹Icahn School of Medicine at Mount Sinai, New York, NY

Disclosures: Swati Bhardwaj: None; Melissa Gitman: None; Siraj El Jamal: None; William Westra: None

Background: In 2018, the College of American Pathologist recommended p16 immunohistochemistry (IHC) as a standalone test for determining HPV status of primary or metastatic oropharyngeal squamous cell carcinoma (OPSCC) based on its performance as an HPV surrogate marker and predictor of improved patient prognosis. But while its performance was found to be acceptable, it was far from perfect with wide ranging sensitivity and specificity rates plummeting, in some studies, to 43% and 47% respectively. The purpose of this study was to confirm the reliability of p16 IHC for a large group of patients with squamous cell carcinomas (SCC) arising from HPV hot-spot regions of the head and neck, namely the oropharynx (OP) and sinonasal tract (SNT).

Design: Consecutive tissue specimens of OPSCC or sinonasal squamous cell carcinoma (SNSCC) were evaluated for the presence of HPV by p16 IHC and PCR-based HPV DNA testing as part of standard clinical care. For discrepant cases (i.e. p16+/HPV DNA-, p16-/HPV DNA+), high-risk HPV E6/E7 mRNA in-situ hybridization was performed.

Results: From 6/2012 to 9/1/2021, carcinomas from 562 patients underwent HPV testing by p16 IHC and HPV DNA PCR. There were 23 (4.1%) discrepant results including 22 cancers that were p16+/HPV DNA-, and 1 that was p16-/HPV DNA+. A carcinoma was more likely to give discrepant results if it arose in the SNT rather than the OP (7/39, 17.9% vs 15/523, 2.9%; Fischer exact, 0.0003). mRNA ISH demonstrated the presence of high-risk HPV in 12 of 18 (67%) of the discrepant cases available for testing including 9/13 (69%) OPSCCs and 3/5 (60%) SNSCCs. The sensitivity and specificity of p16 staining as a surrogate marker for HPV was 99.8% and 93.2% for OPSCC, and 100% and 84.6% for SNSCC.

Conclusions: p16 immunohistochemistry remains a highly sensitive and specific marker for determining HPV status of SCCs arising in hot-spot regions of the head and neck. Concerns regarding poor specificity (false positive results) of p16 IHC may actually reflect suboptimal performance of PCR- DNA testing previously hyped as the gold standard for HPV testing. Varying prevalence of HPV-associated SCC as a function of anatomic subsite may contribute to lower p16 specificity even for a hot-spot location like the SNT.

804 Oropharyngeal HPV-Mediated Squamous Cell Carcinoma, Basaloid-type (SOX10+): A Variant To Be Highlighted In Our Diagnostic Terminology?

Kari Broder¹, Faisal Saeed², Daniel Lubin², Qiuying (Judy) Shi¹, Kartik Viswanathan¹, Mihir Patel², Nicole Schmitt², Kelly Magliocca¹
¹Emory University, Atlanta, GA, ²Emory University Hospital, Atlanta, GA

Disclosures: Kari Broder: None; Faisal Saeed: None; Daniel Lubin: None; Qiuying (Judy) Shi: None; Kartik Viswanathan: None; Mihir Patel: None; Nicole Schmitt: *Grant or Research Support, Astex Pharmaceuticals; Consultant, Sensorion*; Kelly Magliocca: None

Background: The clinical significance of variant histologic patterns within oropharyngeal HPV-mediated squamous cell carcinoma (OP-HPVSCC) is not well characterized. We report a single institutional experience with OP-HPVSCC basaloid-type, with an emphasis on unique clinical features.

Design: Pathology archives were searched for patients with OP-HPVSCC in which tumor cells were SOX10+ and/or possess a basaloid morphology, jigsaw-like arrangement with reduplicated basement membrane material or hyaline droplets, between 8/1/2017 and 8/31/2021. Slides were retrieved, re-reviewed and cases further characterized clinically.

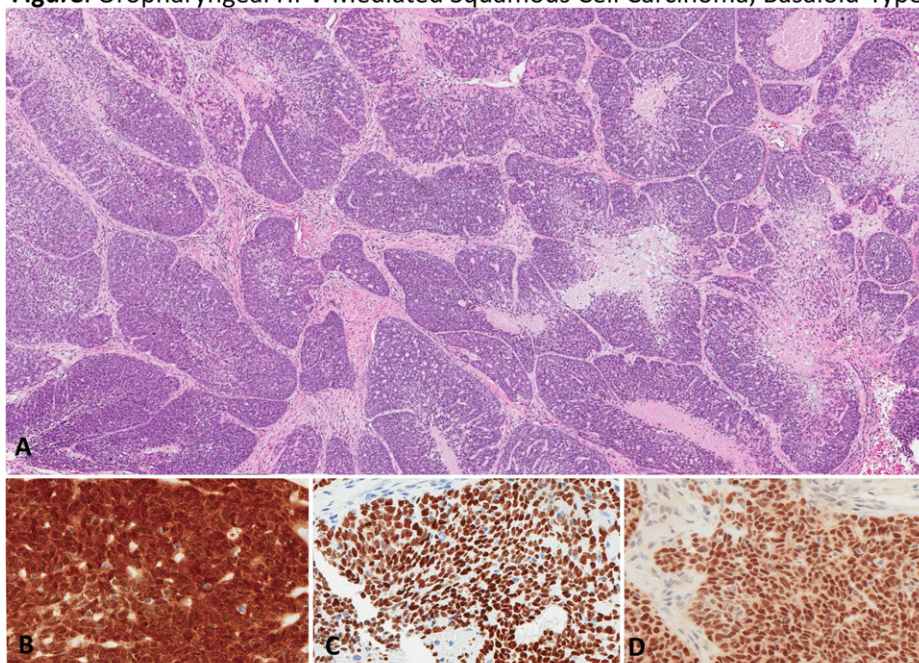
Results: Twelve patients with OP-HPVSCC, basaloid-type were identified. Patients ranged in age from 45 to 72 years, and 11 patients were male. Nine patients initially presented for clinical evaluation of an oropharyngeal mass, and 3 for neck mass. In the latter group, an oropharyngeal mass was readily evident upon clinical examination. No unknown primary scenario was encountered. Seven patients underwent surgical resection and four underwent chemoradiation (CRT) therapy. One patient had regional and distant metastasis (DM) at presentation and was treated with CRT. In the surgical cohort, all 7 patients underwent neck dissection with four (57%) showing no evidence of regional metastasis. In the follow-up period four additional patients

developed DM to lung. In the DM cohort, two patients died of disease 32 months after initial presentation. Three are alive with disease (median follow up 24 months). **Figure and Table.**

Case	Sex	Age	Laterality, Primary site	Primary size (cm)	Largest node (cm)	Initial biopsy site	Treatment	P16	P40	SOX 10	DM	Status	Follow Up (mon)	Stage
1	M	57	L, tonsil	7.6	-	1°	S, CRT	+	+	+	+	DOD	32	T4N0
2	M	72	R, BOT	1.3	3.8	NM	S, RT	+	+	+	-	NED	39	T1N1
3	M	55	R, tonsil	2.7	-	1°	S → pending	+	+	+	+	AWD	16	T2N0
4	M	51	R, tonsil	3.2	-	1°	S, RT	+	+	+	-	NED	31	T2N0
5	M	56	L, GTS	1	6.8	NM	S, RT	+	+	+	-	NED	14	T1N1
6	M	60	L, BOT	1.3	0.4	1°	S, RT	+	+	+	-	NED	16	T1N1
7	M	45	R, tonsil	3	-	1°	CRT	+	ND	ND	-	NED	49	T2N0
8	F	58	R, BOT	4.1*	1.8*	1°	CRT	+	+	+	+	AWD	24	T3N1
9	M	72	L, BOT	3.5*	1.8*	1°	CRT	+	+	+	-	AS	1	T2N1
10	M	66	L, tonsil	3.5*	2.8*	1°	CRT	+	+	ND	+	AWD	14	T2N1
11	M	48	R, tonsil	3.2*	2.2*	1°	CRT	+	+	+	-	NED	12	T2N1
12	M	68	L, tonsil	2.3*	5.5*	NM	CRT	+	+	+	+	DOD	32	T2N1M1

L: left BOT: base of tongue GTS: glossotonsillar sulcus *: radiographic measurement NM: neck mass 1°: primary site S: surgery RT: radiation therapy CRT: chemoradiation ND: not done DM: distant metastasis DOD: died of disease AWD: alive with disease NED: no evidence of disease AS: awaiting surgery

Figure 1 - 804
Figure: Oropharyngeal HPV-Mediated Squamous Cell Carcinoma, Basaloid-Type



A: Basaloid tumor cells with a jigsaw puzzle-like arrangement B-D, Ancillary testing and results in tumor B: p16+ C: p40+ D: SOX10+

Conclusions: Prior studies have confirmed OP-HPVSCC basaloid-type show distinct histologic, immunohistochemical and molecular findings (commonly *CYLD* mutations). Herein, we show the clinical features may also be distinct. In contrast to the characteristic OP-HPVSCC presentation of a neck mass and/or unknown primary, most patients in this series initially presented with a complaint of oropharyngeal mass. Second, primary tumor size exceeded the size of the largest cervical lymph node in all but three cases. Third, nearly 60% of the surgical cohort showed no evidence of regional metastasis. Finally, within a relatively short follow-up interval 4 of 12 patients developed DM. Our results indicate that OP-HPVSCC, basaloid-type may be associated with a distinct clinical presentation and possibly a greater propensity for early distant metastasis. Using ‘basaloid-type’ within diagnostic terminology may be warranted to alert treating physicians.

805 Juvenile Psammomatoid Ossifying Fibroma is Defined by SATB2 Rearrangement

Arjen Cleven¹, Karoly Szuhai¹, David van IJzendoorn², Eline Groen¹, Hans Baelde¹, Pim Schreuder³, Inge Briaire-de Bruijn¹, Stijn Genders¹, Maarten Kleijwegt¹, Herman Kroon¹, Albert Suurmeijer⁴, Dilara Savci-Heijink³, Daniel Baumhoer⁵, Judith Bovee¹

¹Leiden University Medical Center, Leiden, Netherlands, ²Stanford University, Stanford, CA, ³Amsterdam UMC AMC, Amsterdam, Netherlands, ⁴University Medical Center Groningen, Groningen, Netherlands, ⁵University Hospital Basel, Basel, Switzerland

Disclosures: Arjen Cleven: None; Karoly Szuhai: None; David van IJzendoorn: None; Eline Groen: None; Hans Baelde: None; Pim Schreuder: None; Inge Briaire-de Bruijn: None; Stijn Genders: None; Maarten Kleijwegt: None; Herman Kroon: None; Albert Suurmeijer: None; Dilara Savci-Heijink: None; Daniel Baumhoer: None; Judith Bovee: None

Background: Juvenile psammomatoid ossifying fibroma (JPOF) is considered a rare subtype of ossifying fibroma in young patients, predominantly affecting the extra-gnathic bones, particularly the frontal and ethmoid bones. The clinical and morphological features of JPOF may overlap with other fibro-osseous lesions and additional molecular markers would be helpful for accurate diagnostic decision making.

Since a balanced translocation t(X;2)(q26;q33) has been described in two selected cases of JPOF, our aim was to identify the exact genes involved in this translocation and to determine its frequency in JPOF.

Design: We applied whole RNA transcriptome sequencing to a JPOF index case with available fresh frozen tissue and used Defuse (v0.6.2.) for fusion detection. The gene fusion was validated using reverse transcription polymerase chain reaction and FISH. To detect potential recurrent gene rearrangement we screened additional 25 JPOF, 8 juvenile trabecular ossifying fibromas (JTOF) and 11 conventional ossifying fibromas (COF) by fluorescence in situ hybridization.

Results: Fusion detection revealed a gene fusion between SATB2 located on chromosome 2q33.1 and AL513487.1 located on chromosome Xq26 in our JPOF index case. This fusion was validated by reverse transcription polymerase chain reaction and SATB2 fluorescence in situ hybridization. Using SATB2 fluorescence in situ hybridization, we found evidence of SATB2 gene rearrangement in 50% (7/14) of evaluable JPOF cases but not in any of the evaluable JTOF (n=7) and COF (n=7) cases.

Conclusions: We show that SATB2 rearrangement is a recurrent molecular alteration which seems highly specific for JPOF. Our findings add evidence that JPOF is not only morphologically and clinically but also genetically distinct from JTOF and COF and should be considered as an independent craniofacial bone tumour.

806 Tyrosine-Like Crystalloids Occur In Non-Neoplastic True Vocal Fold Tissues

Melad Dababneh¹, Scott Steward-Tharp², Qiuying (Judy) Shi², Kartik Viswanathan², Daniel Lubin³, Faisal Saeed³, Zaid Mahdi³, Kelly Magliocca²

¹Emory University School of Medicine, Atlanta, GA, ²Emory University, Atlanta, GA, ³Emory University Hospital, Atlanta, GA

Disclosures: Melad Dababneh: None; Scott Steward-Tharp: *Advisory Board Member*, Elsevier; Qiuying (Judy) Shi: None; Kartik Viswanathan: None; Daniel Lubin: None; Faisal Saeed: None; Zaid Mahdi: None; Kelly Magliocca: None

Background: Tyrosine-like crystalloids (TC) have been described in association with several head and neck (HN) neoplasms including pleomorphic adenoma, chondroid syringoma, squamous cell carcinoma and meningioma. In an index case, we incidentally identified TC within the anterior macula flava (AMF) toward the anterior commissure of the larynx. The presence of TC within non-neoplastic tissue of the larynx was unexpected. This objective of this study was to evaluate a series of laryngectomy specimens for the presence of TC and if present, characterize the anatomic location and patient demographics.

Design: Consecutive laryngectomy specimens in which sampling included parasagittal sections of the right and left vocal folds and an anterior commissure sagittal section were retrieved for review. Data collection included presence/absence of TC, laterality and anatomic location of TC, patient age, sex, underlying diagnosis leading to laryngectomy, history of HN radiation, history of vocal fold injections and serum calcium at presentation.

Results: Within 86 laryngectomy specimens, 16 patients were found to have TC and formed the study cohort. Thirteen patients showed TC in a sectioned labeled anterior commissure, two from the left vocal cords, one from the right vocal cords. In all cases,

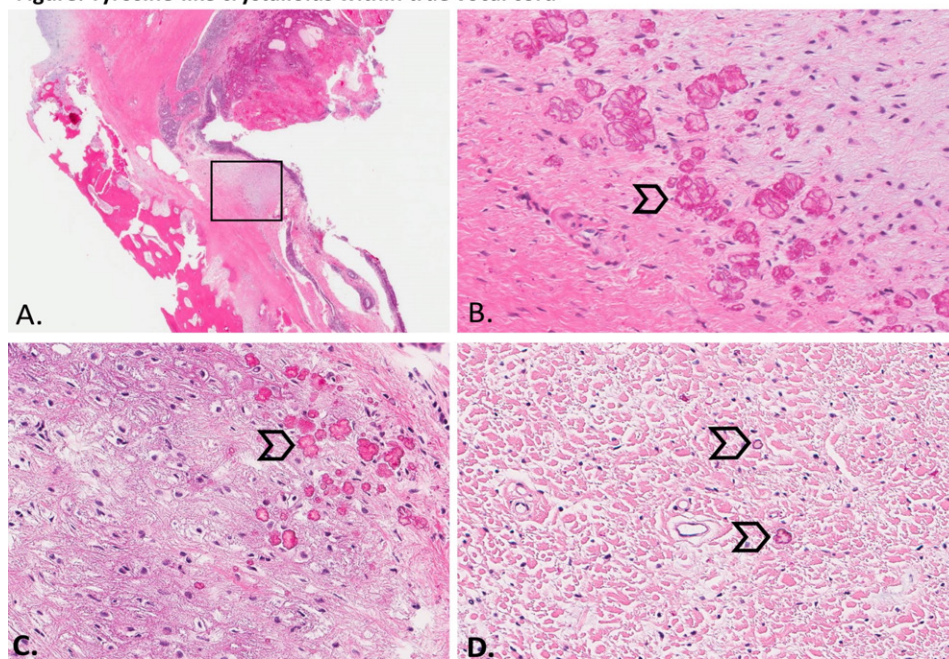
TC localized to the true vocal fold (TVF) or its tendinous attachments: 12 within the AMF or adjacent vocal ligament and 4 cases within the anterior commissure tendon (ACT). Figure. Patients ranged in age from 37 to 85 (mean 62 y), and 11 were male. Laryngectomy was performed for advanced stage untreated SCCa (7), recurrent SCCa (7) neuroendocrine carcinoma (1) and non-functional larynx after irradiation (1). Table.

	Age	Sex	Diagnosis	Primary site	Prior XRT	TC Laterality/General	Anatomic Subsite	Specific Area	SCCa invades TVF	History TVF Injection	Serum Calcium mg/dL
1	53	M	NF(SCCa)	Supraglottis	Y	Ant ML	TVF	AMF/V.Lig	N	0	9.4
2	72	M	SCCa	R TVF	N	Ant ML	TVF	AMF	Y	0	9
3	60	F	SCCa	Supraglottis	N	Ant ML	TVF	AMF	N	0	9.7
4	56	M	SCCa	Supraglottis	N	Ant ML	TVF	AMF/V.Lig	N	0	9.5
5	37	M	SCCa	Left TVF	Y	Ant ML	TVF	AMF/ACT	N	0	8.9
6	77	M	SCCa	Supraglottis	N	Ant ML	TVF	AMF/V.Lig	N	0	8.8
7	68	F	SCCa	Supraglottis	Y	Ant ML	TVF	V.Lig	N	0	9.1
8	66	M	SCCa	R TVF	Y	Ant ML	TVF	ACT	Y	0	8.9
9	64	M	SCCa	Supraglottis	Y	Ant ML	TVF	AMF	N	0	8.9
10	44	M	SCCa	Supraglottis	N	Left	TVF	V.Lig	N	0	9.3
11	70	M	SCCa	Supraglottis	N	Ant ML	TVF	ACT	Y	0	8.8
12	65	F	SCCa	R TVF	Y	Ant ML	TVF	AMF	N	0	10.3
13	62	M	SCCa	L TVF	Y	Ant ML	TVF	ACT	N	0	9.5
14	54	F	SCCa	Supraglottis	Y	Left	TVF	AMF	Y	0	9.3
15	52	F	SCCa	Supraglottis	N	Ant ML	TVF	ACT	N	0	9.7
16	85	M	NEC	Supraglottis	N	Right	TVF	V.Lig	N	0	9.8

NF: Non functional SCCa: Squamous cell carcinoma NEC: Neuroendocrine carcinoma R: Right L: Left TVF: True vocal fold Ant ML: Anterior midline V.Lig: Vocal ligament Y: Yes N: No XRT: Radiation therapy

Figure 1 - 806

Figure: Tyrosine-like crystalloids within true vocal cord



A. Rectangle highlights true cord, higher magnification view in Panel B. Tyrosine-like crystalloids (arrows) within true cord tissues from Case 5 (A-B), Case 1 (C) and Case 11 (D).

Conclusions: The presence of TC in non-neoplastic tissue is uncommon. In this study, TC appears to occur most frequently in anterior midline commissure area and tends to localize within structures related to the true vocal fold. The conspicuous association of TC with the midline ACT region raises the possibility that TC may preferentially develop in areas under tension or other forces. The impact of regional tumor altering the laryngeal mechanics and/or impact of aging remain as confounding factors. Nevertheless, the reproducibility of this distinctive finding represents a useful gross and microscopic teaching point for students and resident trainees. The presence of TC may also represent a useful way to confirm the accuracy of the selected sections in a laryngectomy specimen cassette summary.

807 Retrospective Clinico-Pathologic Analysis of Primary Lymphoepithelial Carcinoma of the Parotid Gland: A case series

Liz Edmund¹, Adel El-Naggar¹

¹The University of Texas MD Anderson Cancer Center, Houston, TX

Disclosures: Liz Edmund: None; Adel El-Naggar: None

Background: Lymphoepithelial carcinoma is a very rare salivary gland malignancy. Although it has been associated with EBV infection, particularly in endemic areas, its etiology, pathogenesis, and biologic behavior remains unclear. Here we examine the morphologic and immunophenotypic features of primary lymphoepithelial carcinoma of the parotid gland (LECp) and assess its clinical behavior in a series of 16 patients.

Design: Our institutional archives were queried for all cases of LECp from 01/2010 to 09/2021. All available glass slides and digital images were retrieved for review. Each case was assessed for salient morphologic and immunophenotypic features (see table) by two pathologists, LNE and AEN. Histologic indicators of adverse outcome were also noted (see table). The medical records of each patient was also reviewed in order to assess post-surgical management and follow up data (see table).

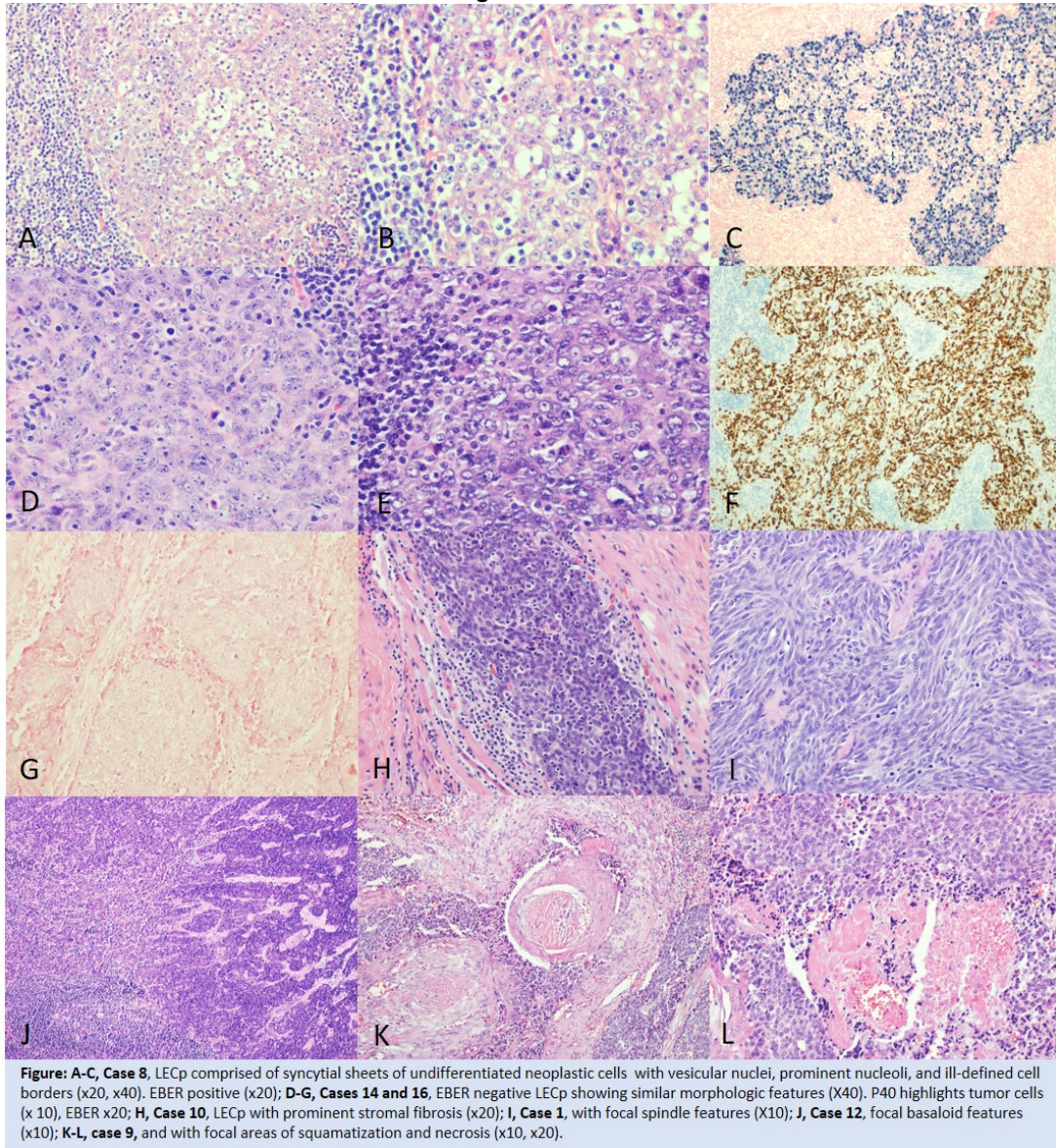
Results: Our LECp cohort comprised 16 patients, with median age 57 years (28-81 years) and a slight female predominance of 1.6:1. LECp developed more often in the right parotid (69%) and the average tumor size was 2.8 cm. The tumors exhibited a predominantly syncytial growth pattern, with a dense lymphoid background (87.5%)(figure). Significant sclerosis of the background stroma was seen in 2 cases (12.5%) (Fig H). Basaloid features, rare squamatization and necrosis were seen focally in 2 cases (12.5%) and 1 case (6.3%) and 2 cases (12.5%) respectively (Fig J-L). An associated lymphoepithelial precursor was present in 3 cases. Keratins or p63/p40 were expressed in 8 of 8 cases where immunohistochemistry (IHC) was performed to aid diagnosis of carcinoma. EBER-ISH was positive in only 3 of 16 cases (18.6%). All cases were negative for p16. Lymph node metastasis was seen in 5 cases (31.3%) at the time of diagnosis. Post-surgical therapy data was available for 12 patients (see table). Follow-up data was available for 9 cases, of which 3 showed local recurrence, with distant metastasis and disease related death in 1 case. There was no evidence of disease in 7 of 9 cases (77.8%) with median follow up of 5 years. Seven cases were lost to follow up.

Table: Clinicopathologic features of lymphoepithelial carcinoma of the parotid gland in 16 patients

Case No.	Age at diagnosis (yrs)	Sex	Tumor site	Tumor size (cm)	Pattern of growth	EBER	LEL	Lymph node status	Follow up	Post-operative therapy
1	83	F	RP	1.5	syncytial, spindled	-	-	+	Recurrence	CRT
2	58	F	LP	5	syncytial	-	+	+	LFU	
3	73	F	LP	2	syncytial	-	+	NA	NED	XRT
4	55	F	RP	5.6	syncytial	-	-	+	LFU	CRT
5	50	F	LP	2.5	syncytial	-	-	+	NED	XRT
6	64	F	RP	3.6	syncytial	-	-	-	NED	none
7	28	F	RN	2.8	syncytial, sclerotic stroma	+	-	+	Recurrence, metastasis, DRD	CRT, biotherapy
8	28	M	LP	1.8	syncytial	+	-	+	LFU	
9	65	F	RP	2.6	syncytial, focal basaloid and squamous features, focal necrosis	-	-	-	NED	CRT
10	81	M	RP	1.6	syncytial with sclerotic stroma	-	-	NA	LFU	XRT
11	68	M	RP	2	syncytial	-	-	NA	NED	XRT
12	53	M	RP	2.1	focal basaloid, necrosis	-	+	-	NED	XRT
13	54	M	RP	NA	syncytial	+	-	NA	LFU	NA
14	35	F	RP	2.5	syncytial	-	-	-	LFU	
15	69	M	LP	NA	syncytial	-	-	NA	NED	CRT
16	56	F	RP	3	syncytial	-	-	NA	NED	None

Abbreviations: RP-right parotid, LP-left parotid, LEL- lymphoepithelial lesion, LFU-lost to follow up, NED-no evidence of disease, DRD-disease related death, CRT-chemotherapy and radiation, XRT-radiation therapy, NA-not available

Figure 1 - 807



Conclusions: In our institutional study, LECp exhibited a predominantly syncytial pattern of growth, with a minority of cases showing prominent stromal sclerosis, focal basaloid and rare squamous differentiation, and necrosis. The LECp were predominantly EBV-negative tumors, with median time to 1st recurrence of 1.5 years, and 77.8% 5y-disease free survival.

808 Enrichment Analysis of the Amplified Genes by Array-based Comparative Genomic Hybridization in the Carcinoma Ex Pleomorphic Adenoma

Erika Egal¹, João Scarini², Wellington Lima Sabino³, My Helms¹, Reydson de Lima-Souza², Rogerio Gondak⁴, Luiz Kowalski⁵, Albina Altemani⁶, Ana Cristina Victorino Krepischi⁷, Fernanda Mariano⁸

¹The University of Utah, Salt Lake City, UT, ²State University of Campinas (Unicamp), Campinas, Brazil, ³School of Medical Sciences, State University of Campinas (Unicamp), Campinas, Brazil, ⁴Universidade Federal de Santa Catarina, Florianopolis, Brazil, ⁵Faculdade de Medicina da USP, Campinas, Brazil, ⁶UNICAMP - Brazil, Brazil, ⁷Faculdade de Medicina da USP, Sao Paulo, Brazil, ⁸Campinas, Brazil

Disclosures: Erika Egal: None; João Scarini: None; Wellington Lima Sabino: None; My Helms: None; Reydson de Lima-Souza: None; Rogerio Gondak: None; Luiz Kowalski: None; Albina Altemani: None; Ana Cristina Victorino Krepischi: None; Fernanda Mariano: None

Background: Carcinoma Ex Pleomorphic Adenoma (CXPA) is a rare and aggressive neoplasm originated from Pleomorphic Adenoma (PA). By definition, CXPA must present histological evidence of coexisting benign residual area (residual PA) or pre-existing history of PA.

Design: Our goal was to identify the profile of the genetic changes by array-based comparative genomic hybridization (aCGH) between the benign residual area (n=14) and the CXPA (n=27) transformed area. The amplified genes identified in the study groups were subjected to enrichment analysis using STRING database. The related genes were annotated and enriched by KEGG pathway analysis.

Results: Ten biological processes and pathways were found to be important in the malignant counterpart of the CXPA. Five processes were directly related to the tumor immune response: IFNA and MEF2 family genes in the processes of NK cell (p = 1.10e-18), T cell (p = 1.75e-12) and B cell (p = 8.10e-11) activation, as well as involved in the process's differentiation (p = 4.98e-11) and proliferation (p = 5.33e-16) of B cell. RIG-I-like receptor signaling pathway (p = 4.76e-12), Jak-STAT signaling pathway (p = 6.25e-11), NOD-like receptor signaling pathway (p = 5.39e-09), Toll-like receptor signaling pathway (p = 9.01e-09), and cytokine-cytokine-receptor interaction (p = 9.01e-09) play importance roles in the CXPA carcinogenesis. Enrichment analysis on amplified genes in residual PA did not show statistically significant biological processes and KEGG pathways.

Conclusions: Our findings emphasize that genes amplified in CXPA were enriched for biological processes related to innate and adaptive immune signaling. Studies of the immune microenvironment in CXPA are scarce. Further studies are needed to better understand the immunological aspects of CXPA carcinogenesis.

809 Detection of Novel Fusions in Salivary Gland Type Tumors Using a Custom NGS RNA Sequencing Fusion Panel

Hasanain Hasan¹, Issa Hindi¹, Fang Zhou², George Jour³, Cheng Liu¹, Tamar Brandler¹

¹NYU Langone Health, New York, NY, ²NYU School of Medicine, New York, NY, ³New York University, New York, NY

Disclosures: Hasanain Hasan: None; Issa Hindi: None; Fang Zhou: *Stock Ownership*, MRNA, DOCS; George Jour: None; Cheng Liu: None; Tamar Brandler: None

Background: Fusion gene detection plays an important role in salivary gland tumor diagnosis. In our study we used a custom-designed Archer Anchored Multiplex PCR (AMP™) technology-based NGS test FusionSeq, including most reported gene fusions, to investigate fusions in various salivary gland type tumors.

Design: We performed a retrospective review of 32 tumors that underwent FusionSeq testing in 12/4/2013-08/20/2021. Patients' demographics, surgical pathology diagnoses, and molecular results were analyzed.

Results: Out of the 32 cases, male:female was 20:12. Mean age was 51.4 years. Most cases were of parotid (16/32) or submandibular gland (5/32) origin. Eight (8/32) cases were from other head/neck sites: buccal x3, cheek x1, nasopharynx x1, lip x1, ethmoidal sinus x1, orbit x1, hard palate x1. One case was found in the lung and one in the trachea.

The most common surgical pathology diagnosis was adenoid cystic carcinoma (6/32): 2/6 had *MYB:NFIB*; 1/6 had *MYBL1:NFIB*; 3/6 were negative. Secretory carcinomas (5/32) showed *ETV6:NTRK3* (4/5) and dual *ETV6:RET* & *EGFR:SEPT14* fusions (1/5).

Three cases (3/32) of mucoepidermoid carcinoma showed *CRTC1:MAML2* (3/3). Pleomorphic adenoma showed varying fusions: *LINC00681:PLAG1* x1, *HMGA2:WIF1* x2, *CTNNB1:PLAG1* x1. One case of intraductal carcinoma showed the common *NCOA4:RET* fusion; one tumor with features of papillary cystadenocarcinoma demonstrated *ETV6:NTRK3*. Basal cell adenocarcinoma x1 showed *FBXO32:PLAG1*, Warthin tumor with extensive cystic change showed *CRTC1:MAML2* x1, and clear cell carcinoma *EWSR1-ATF1* x1 (negative on FISH). Eleven tumors tested negative for fusions (see Table 1) (see Fig. 1)

Table 1: 32 Salivary gland type tumors with demographics, histopathology diagnoses, & FusionSeq results

#	Age	Sex	Location	Laterality	Diagnosis	Fusion
1	35	F	Parotid	Right	Acinic cell carcinoma	Negative
2	24	F	Parotid	Left	Acinic cell carcinoma	Negative
3	48	F	Submandibular	Left	Adenoid cystic carcinoma	<i>MYB:NFIB</i>
4	38	M	Lung	Left	Adenoid cystic carcinoma	Negative
5	65	M	Submandibular	Left	Adenoid cystic carcinoma	Negative
6	63	M	Ethmoidal sinus	NA	Adenoid cystic carcinoma	Negative
7	50	F	Trachea	NA	Adenoid cystic carcinoma	<i>MYB:NFIB</i>
8	73	F	Orbital	Left	Adenoid cystic carcinoma	<i>MYBL1:NFIB</i>
9	63	M	Buccal	Left	Adenosquamous carcinoma	Negative
10	60	F	Submandibular	Right	Basal cell adenocarcinoma	<i>FBXO32:PLAG1*</i>
11	19	F	Parotid	Left	Carcinoma ex-pleomorphic adenoma, minimally invasive	Negative
12	29	M	Parotid	Left	Cellular pleomorphic adenoma	<i>HMGA2:WIF1</i>
13	28	F	Parotid	Right	Cellular pleomorphic adenoma	<i>CTNNB1:PLAG1</i>
14	28	F	Parotid	Right	Low grade intraductal carcinoma	<i>NCOA4:RET</i>
15	73	F	Parotid	Right	Secretory carcinoma	<i>ETV6:NTRK3</i>
16	78	M	Parotid	Left	Secretory carcinoma	<i>ETV6:NTRK3</i>
17	41	M	Buccal	Right	Secretory carcinoma	<i>ETV6:NTRK3</i>
18	26	M	Parotid	Left	Secretory carcinoma	<i>ETV6:NTRK3</i>
19	19	M	Parotid	Right	Secretory carcinoma	<i>ETV:RET* & GFR:SEPT14*</i>
20	74	M	Cheek	Right	Mucoepidermoid carcinoma	<i>CRTC1:MAML2</i>
21	63	M	Nasopharynx	Right	Mucoepidermoid carcinoma	<i>CRTC1:MAML2</i>
22	36	M	parotid	Right	Mucoepidermoid carcinoma	<i>CRTC1:MAML2</i>
23	43	M	Submandibular	Left	Oncocytoma	Negative
24	74	M	Parotid	Right	Papillary cystadenocarcinoma	<i>ETV6:NTRK3</i>
25	67	M	Parotid	Left	Pleomorphic adenoma	<i>LINC00681:PLAG1*</i>
26	59	M	Buccal	Right	Polymorphous adenocarcinoma with high grade transformation	Negative
27	62	M	Lip	Right	Poorly differentiated adenocarcinoma	Negative
28	77	M	Submandibular	Left	Salivary duct carcinoma	Negative
29	71	M	Parotid	Left	Salivary duct carcinoma	Negative
30	31	F	Parotid	Right	Spindle cell mesenchymal neoplasm with myopericytoma	Negative
31	72	M	Parotid	Right	Warthin tumor with extensive cystic change	<i>CRTC1:MAML2^{&}</i>
32	56	F	Hard palate	Left	Clear cell carcinoma	<i>EWSR1-ATF1⁺</i>

Legend:

* Novel fusion, never before reported in this type of salivary gland tumor

& Only rarely reported before in this type of salivary gland tumor

+ Case was initially negative for EWSR1 fusion by FISH testing.

Figure 1 - 809
Gene fusion / Histopathology diagnosis

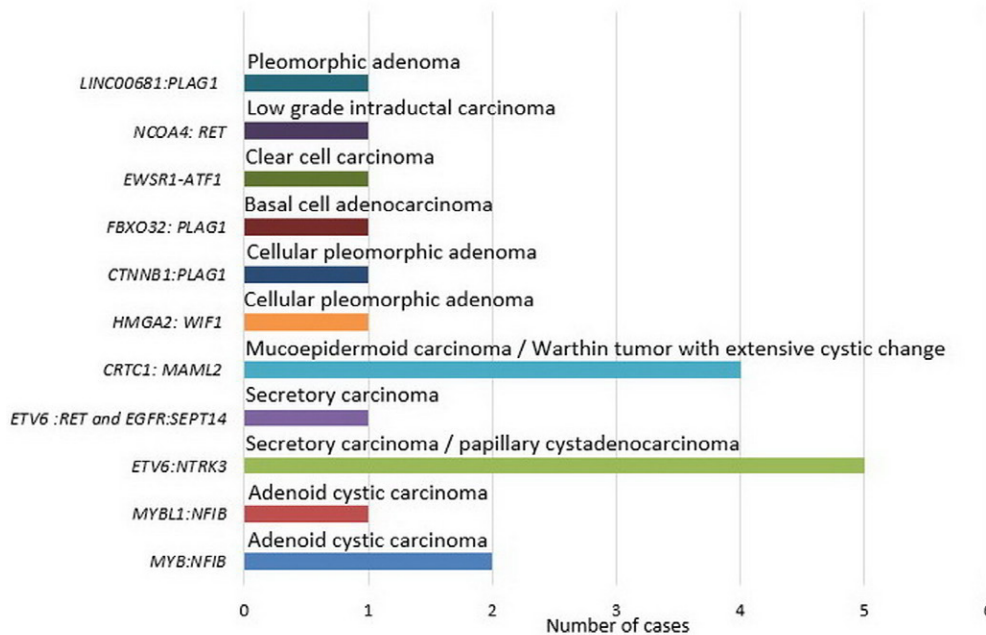


Figure 1: Gene fusions tallied by histopathology diagnosis

Conclusions: Our results expand the genomic landscape of salivary gland type tumors. Rarely or never-before reported fusions were found in basal cell adenocarcinoma (*FBXO32:PLAG1* fusion), secretory carcinoma (dual fusions *ETV6-RET* and *EGFR-SEPT14*), Warthin tumor (*CRTC1:MAML2*), and pleomorphic adenoma (*LINC00681:PLAG1*).

One case of clear cell carcinoma failed to demonstrate fusions by FISH while subsequently an *EWSR1-ATF1* fusion was discovered using the FusionSeq method, suggesting that multiplexed targeted RNA NGS based testing is superior to conventional methods. Further validation of NGS findings in a larger cohort is warranted, as well as continued modification of the genetic panel to include the most up to date known mutations, which may eventually help to uncover prognostic and therapeutic targets.

810 Genotypic–phenotypic Correlation of Papillary Epithelial Neoplasms (PEN) of the Middle Ear and Temporal Bone (ME/T)

Juan Hernandez-Prera¹, Daryoush Saeed-Vafa¹, Bruce Wenig¹
¹H. Lee Moffitt Cancer Center & Research Institute, Tampa, FL

Disclosures: Juan Hernandez-Prera: None; Daryoush Saeed-Vafa: None; Bruce Wenig: None

Background: The classification of PEN of the ME/T represent a histologically mixed group of tumors carrying various terminologies including middle ear adenoma (MEA) with papillary features and aggressive papillary tumor (APT). Among the central controversies revolving around these tumors is whether they represent distinct/independent entities, a single tumor with varying morphologies or whether there is a relationship with endolymphatic sac tumor (ELST) or MEA/middle ear neuroendocrine tumor (MeNET). Herein, we provide evidence of a possible genotypic-phenotypic correlation this group of neoplasms.

Design: 6 PEN of the ME/T were identified in our files. The clinico-pathological features are summarized, and four cases were subjected to targeted next generation sequencing (NGS).

Results: There were 5 women and 1 man with a mean age for 69 years (range 42-82). Tumors affected the middle ear (3), mastoid (2) or Eustachian tube (1). Morphologically, all tumors were characterized by papillary architecture with variable tubuloglandular component. In 5 cases the cells lining the papillae were columnar with variable mucinous cytoplasm, highlighted by mucicarmine and/or D-PAS. 1 case showed oncocytic cells with features reminiscent to oncocytic/cylindrical sinonasal papilloma. Except for 1

case, all tumors showed minimal nuclear pleomorphism, no significant increased mitotic activity and no necrosis. 2 mucinous tumors showed extensive histological evidence of invasion of which 1 recurred over a period of 3 years. Tumors were immunoreactive for AE1/AE3, CAM5.2 and CK7 and negative for CK20, CDX2, PAX8, CAIX and neuroendocrine makers. NGS was successful in 3 cases: the oncocytic tumor harbored a *BRAF-MKRN1* fusion; 1 mucinous tumor had *KRAS* (p.Q61H) and *BRAF* (p.D594N) mutations, and another mucinous tumor showed *HRAS* (p.Q61R), *PIK3CA* (p.H1047R), and *SMAD4* (p.L498*) mutations.

Conclusions: Our study highlights 2 possible subtypes of PEN including a mucinous subtype with mutations in the *RAS* family of genes and an oncocytic subtype harboring *BRAF-MKRN1* fusion. The *RAS* mutations in the mucinous subtype and its ability to invade support the designation of adenocarcinoma, and may encompass tumors previously diagnosed as APT. Similarities to sinonasal papillomas are noted in the oncocytic subtype but absence of *KRAS* mutations and the presence of the *BRAF-MKRN1* fusion allow for their distinction. The overall findings provide evidence that PEN are distinct from ELST and MEA/MeNET.

811 Next-generation Sequencing (NGS) of Low-grade Nasopharyngeal Papillary Adenocarcinoma (LGNPA): Absence of Confirmatory *ROS1* Fusion Transcripts

Juan Hernandez-Prera¹, Daryoush Saeed-Vafa¹, Theresa Boyle¹, Bruce Wenig¹
¹H. Lee Moffitt Cancer Center & Research Institute, Tampa, FL

Disclosures: Juan Hernandez-Prera: None; Daryoush Saeed-Vafa: None; Theresa Boyle: None; Bruce Wenig: None

Background: LGNPA is a surface-derived malignant glandular neoplasm characterized by prominent papillary architecture and indolent behavior. Recently, *ROS1-GOPC* fusion was documented in a single case. We undertook this study to determine whether *ROS-GOPC* fusion is a defining recurrent driver event of LGNPA.

Design: Five cases of LGNPA were identified in our consultation files. The morphological and immunohistochemistry features were summarized, and all cases were subjected to DNA and RNA-based NGS assay with the ability of identifying *ROS1* fusion transcripts.

Results: The five tumors were characterized by an admixture of papillary and glandular architecture. The papillary growth was the predominant pattern characterized by complex (back-to-back) glandular and cribriform/microcystic growth with arborization and fibrovascular cores. The tumor cells ranged from pseudostratified columnar to cuboidal and exhibit eosinophilic cytoplasm with round to oval vesicular nuclei some with optical clearing resembling nuclei in papillary thyroid carcinoma. In all cases there was mild nuclear pleomorphism. Scattered squamoid and spindle cell areas were appreciated. Neoplastic cells were diffusely immunoreactive for cytokeratins and TTF1, while negative for thyroglobulin and PAX8. Four cases with adequate DNA/RNA concentration had successful NGS runs that showed an absence of *ROS1* fusion transcripts or other molecular driver events. Various variants of unknown significance, most of which were likely germline, were reported in all cases.

Conclusions: *ROS1* fusion transcripts were not identified in our cohort of cases. The small sample size and a possible low frequency of this alteration in this tumor could explain the negative results. Nevertheless, we could not confirm *ROS1* fusions as a driver event in the development of LGNPA, the molecular underpinnings of which remain unknown and yet to be determined.

812 Sinonasal Adenosquamous Carcinoma- Morphology and Genetic Drivers Including Low and High-Risk HPV mRNA, *DEK-AFF2* Fusion, and *MAML2* Rearrangement

Dean Holliday¹, Mitra Mehrad¹, Kim Ely¹, Jen-Fan Hang², Ying-Ju Kuo², Fangjia Tong³, Xiaowei Wang³, James Lewis Jr.¹
¹Vanderbilt University Medical Center, Nashville, TN, ²Taipei Veterans General Hospital, Taipei, Taiwan, ³University of Illinois at Chicago, Chicago, IL

Disclosures: Dean Holliday: None; Mitra Mehrad: None; Kim Ely: None; Jen-Fan Hang: None; Ying-Ju Kuo: None; Fangjia Tong: None; Xiaowei Wang: None; James Lewis Jr.: None

Background: Adenosquamous carcinoma of the sinonasal tract is a rare entity with less than 100 reported cases in the English literature. Due to its rarity, there are almost no studies detailing morphology or characterizing genetic driver events such as transcriptionally-active human papillomavirus (HPV) status or *DEK-AFF2* fusion. Further, many authors have termed sinonasal tumors with glands and squamous carcinoma combined as "mucoepidermoid carcinomas", but no studies have examined for the

presence of MAML2 rearrangement in these patients. In this study, we examined 8 cases of sinonasal adenosquamous carcinoma, characterized their morphology, and evaluated for key driver events.

Design: A natural language search of pathology reports at our institution identified cases of sinonasal adenosquamous carcinoma diagnosed from 2014-2020. These cases were examined microscopically and confirmed as adenosquamous carcinoma using WHO diagnostic criteria. After confirmation, cases were tested for p16 expression by immunohistochemistry (70% cutoff), DEK-AFF2 fusion by FISH and immunohistochemistry for AFF2, MAML2 rearrangement by FISH, and low and high-risk HPV by RNA in situ hybridization and reverse transcription PCR, respectively. Detailed morphologic characterization was also performed, and clinical and demographic data were reviewed.

Results: There were 4 male and 4 female patients ranging from 52-74 years of age (median, 69) with 7 of 8 patients being Caucasian and 1 African American. Most were active smokers (6/8, 75%) and they typically presented with epistaxis, a visible nasal mass, or facial pain prompting biopsy. The average follow-up time was 14.7 months (range 2 weeks- 28 months) with 1 patient lost to follow up and 1 who died secondary to disease in the follow up period. Two of 8 patients suffered disease recurrence, one of whom required re-operation and one for whom the patient elected to undergo palliative therapy and hospice.

Tumors had a highly variable morphology with a squamous component that was variably keratinizing, nonkeratinizing, or mixed, and nuclear pleomorphism ranged from mild to marked. Three tumors arose in a background of benign sinonasal papilloma and two, interestingly, showed ciliated tumor cells. Driver events were largely exclusive with 6/8 (75%) of patients having an identified driver, whether low or high risk HPV or DEK-AFF2. All tumors were negative for MAML2 gene rearrangement.

	Precursor lesion	Squamous Differentiation	Cilia	MAML2 FISH	DEK-AFF2 FISH/IHC	p16 IHC	lrHPV mRNA	hrHPV mRNA
1	None	NK*	+	-	+	-	+	-
2	None	K	-	-	-	+	-	+
3	Inverted papilloma	NK	-	-	-	-	-	-
4	None	NK	-	-	-	+	-	+
5	Inverted papilloma	NK*	-	-	-	+	-	+
6	None	K	-	-	-	+	-	+
7	None	K	-	-	-	-	-	-
8	Exophytic papilloma	K	+	-	-	-	+	-

K= Keratinizing, NK= Non-keratinizing, NK*= Non-keratinizing with maturation

Conclusions: In summary, sinonasal adenocarcinoma is a rare and somewhat heterogenous tumor frequently arising ex papilloma and having various drivers including hrHPV, and occasionally DEK-AFF2 or lrHPV. It is not, despite previous reports of MEC of the sinonasal tract, a MAML2 rearrangement salivary type tumor when surface mucosa is involved.

813 Sinonasal Bacteroma/ Bacterial-Related Concretions- A Distinct and Previously Uncharacterized Pathologic Entity of the Sinonasal Tract

Dean Holliday¹, James Lewis Jr.¹, Mitra Mehrad¹, Kim Ely¹
¹Vanderbilt University Medical Center, Nashville, TN

Disclosures: Dean Holliday: None; James Lewis Jr.: None; Mitra Mehrad: None; Kim Ely: None

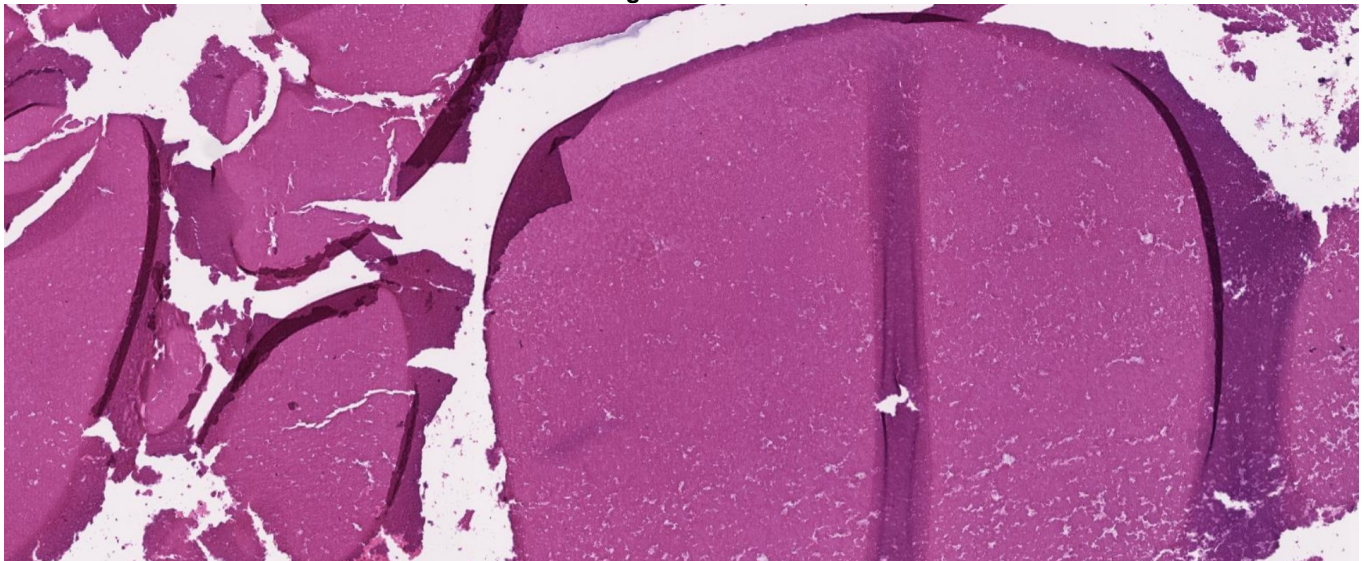
Background: On the routine head and neck surgical pathology service, we identified cases described clinically as “fungal debris”, “mycetoma”, or “mass-like obstruction” of the sinonasal tract with suspicion for fungal infection that microscopically lacked fungus

and instead had bacterial colonies and distinct morphology. Here we report 15 cases of this entity compared to 15 randomly selected cases of mycetoma to characterize the clinical and pathologic features of these patients.

Design: A natural language search of pathology reports from 2016-21 at our institution was performed to identify potential cases. All candidate cases were examined microscopically and included if they had granular debris with negative GMS staining for fungus or excluded if they were another specific disease process. Additionally, 15 cases of mycetoma were randomly selected from the same time period. Clinical and demographic data were reviewed for all patients.

Results: There were 7 males and 8 females ranging from 21 to 78 years old. Imaging frequently revealed opacification of the paranasal sinuses with some cases showing occlusion of outflow tracts. Operative reports showed all to have paranasal sinus involvement and only 2 involving the nasal cavity. Most were unilateral (13/15, 87%). The maxillary sinus was involved in eleven (11/15, 73%) cases, sphenoid sinus in two (2/15, 13%), and frontal and ethmoid sinuses in one each (1/15, 7%). Bacteroma patients frequently had a history of allergic rhinitis (8/15, 53%) which was significantly more common than for mycetoma patients ($p=0.0142$). The most common presenting symptoms were facial pain (13/15, 87%) and rhinorrhea (8/15, 53%). The modalities for treatment were antibiotics, steroids, excision, or a combination of these. Morphologically, cases consisted of large aggregates of paucicellular to acellular debris with a characteristic densely eosinophilic granular appearance, commonly associated with bacteria (Figure 1). Ten cultures were taken and 9 grew a non-contaminant bacterial organism, with 4/10 growing *Pseudomonas aeruginosa*. The concretions grossly did not appear to represent actual stones (rhinoliths). Clinical course post-treatment ranged from symptom resolution 1-week post-operatively to others with recurrent infections and symptoms 23 months from the initial operation.

Figure 1 - 813



Conclusions: In summary “bacteroma” is a heretofore undescribed pathologic entity that appears to be related to chronic bacterial infection and is distinct from mycetoma and rhinolithiasis.

814 Application of the Milan System for Reporting Salivary Gland Cytopathology to Core Needle Biopsies of the Parotid Gland

Anna-Karoline Israel¹, Christopher Griffith¹

¹Cleveland Clinic Foundation, Cleveland, OH

Disclosures: Anna-Karoline Israel: None; Christopher Griffith: None

Background: The Milan System for Reporting Salivary Gland Cytopathology was developed by an international consortium of experts in the field and published in 2018 to enable standardized reporting of salivary aspirates. There are seven categories with distinct corresponding risks of malignancy (non-diagnostic 25%, non-neoplastic 10%, atypia of undetermined significance (AUS) 25%, benign neoplasm <5%, salivary gland neoplasm of uncertain malignant potential (SUMP) 35%, suspicious for malignancy

60% and malignant 90%). Core needle biopsies (CNB) of salivary glands are also common but reporting varies and lacks standardization. Here we explore the feasibility of a Milan-like reporting system on CNB of the parotid gland.

Design: Our laboratory information system was searched for parotid gland CNB from 2010-2021. Reports were reviewed and translated into a Milan-like reporting system. Non-diagnostic - normal salivary gland tissue and insufficient biopsy material. Non-neoplastic - Lymph node without atypia, granulomatous inflammation without atypia, epithelial cysts without atypia, and sialadenitis. AUS - findings suspicious for neoplasm, keratin debris, atypical lymphocytes/cells. Benign neoplasm – definitive diagnosis of a benign neoplasm including those with modifiers such as “consistent with...”. SUMP - cases with a differential diagnosis including benign and malignant entities. Any case were only malignant entities were considered in the report or clearly identified as a specific malignant diagnosis were classified as suspicious for malignancy or malignant, respectively. CNB findings were correlated with cytology and resection specimens when available. Risk of neoplasia (RON) and risk of malignancy (ROM) was calculated for CNB Milan categories using cases with follow-up resection.

Results: 95 CNB of the parotid gland were identified. The table summarizes demographic and Milan categorization. The most common CNB Milan categories included malignant, benign neoplasm non-diagnostic and non-neoplastic. A specific diagnosis was provided in 46% (44/95) of CNB cases. AUS, SUMP and suspicious for malignancy were less common. 48 cases had a corresponding aspiration and 27 cases had follow-up resection. RON was high for all categories of at least AUS and ROM showed some differentiation between categories.

Milan categories	Total (n)	%	Resected (n)	Neoplastic (n)	RON (%)	Malignant (n)	ROM (%)	Diagnoses on Resection (n)
Non-diagnostic	17	18	0	n/a	n/a	n/a	n/a	n/a
Non-neoplastic	12	13	1	0	0	0	0	Nodular oncocytic hyperplasia
AUS	9	9	4	3	75	2	50	Met CA, Lymphoma, oncocytoma, lymphoid hyperplasia
Benign Neoplasm	22	23	6	6	100	0	0	WT (4), PA, meningioma
SUMP	5	5	5	5	100	2	40	SDC, myoepithelial CA, WT, BCA, myoepithelioma
Suspicious for malignancy	1	1	1	1	100	1	100	Lymphoma
Malignant	29	31	10	10	100	10	100	Met CA (3), SDC (2), AdCC (2), CAexPA, EMCA, HG NEC

Malignant Dx on core biopsy	Total (n)	Benign Nx on core biopsy	Total (n)	Non-Neoplastic Diagnoses on core biopsy	Total (n)
Lymphoma	13	WT	15	Lymph node	4
Met CA	5	PA	4	Sarcoidosis	2
SDC	2	Oncocytoma	1	Epithelial lined cyst	2
AdCC	2	Schwannoma	1	Chronic sialadenitis	2
EMCA	1	Meningioma	1	IgG4 Disease	1
Melanoma	1			Abscess	1
Metastatic Adenocarcinoma	1				

Table 1: Characteristics of Milan categories in salivary gland core needle biopsies: AUS- atypia of undetermined significance, SUMP- Salivary gland neoplasm of uncertain malignant potential, RON- rate of neoplasia, ROM- rate of malignancy, Met CA- metastatic carcinoma (squamous cell and basal cell carcinoma), WT- Warthin tumor, PA- Pleomorphic adenoma, SDC- salivary duct carcinoma, CA- carcinoma, BCA- basal cell adenoma, AdCC- adenoid cystic carcinoma, CAexPA- carcinoma ex pleomorphic adenoma, EMCA- epithelial-myoepithelial carcinoma, HG NEC- high-grade neuroendocrine carcinoma.

Conclusions: This study confirms the feasible of using a Milan-like system in the setting of parotid gland CNB with differentiation in RON and ROM. CNB allows assessment of architectural features that may allow more specific diagnoses in some cases.

815 Frequent PLAG1 Alterations in Epithelial Myoepithelial Carcinoma

Aanchal Kakkar¹, Chetna Sarma¹, Kavneet Kaur¹, Ria Mahendru¹, Alok Thakar¹
¹All India Institute of Medical Sciences, New Delhi, India

Disclosures: Aanchal Kakkar: None; Chetna Sarma: None; Kavneet Kaur: None; Ria Mahendru: None; Alok Thakar: None

Background: Epithelial myoepithelial carcinoma (EMC) is a low grade salivary gland neoplasm characterized by a biphasic cell population i.e. ductal cells and abluminal (basal, myoepithelial) cells, and infiltrative growth. Recently, a proportion of EMCs were proven to originate from pre-existing pleomorphic adenoma (PAs), which are known to harbor rearrangements involving Pleomorphic Adenoma Gene1 (PLAG1). We aimed to evaluate alterations in PLAG1 in a cohort of EMC and correlate the results with histological features.

Design: EMC cases diagnosed between 2014 and 2021 were retrieved. Histomorphological features were evaluated, particularly for evidence of preexisting PA. Fluorescence in situ hybridization was performed on paraffin-embedded whole tissue sections using a dual color break apart probe for PLAG1. Signals were scored in at least 100 non-overlapping intact nuclei. PLAG1 rearrangement was defined as split signals in >10% of cells. Presence of >2 PLAG1 signals in >75% of cells was considered as amplification.

Results: Twenty EMC cases were identified. Eight cases (40%) showed PLAG1 alterations, with PLAG1 rearrangement in 5 cases (25%) and PLAG1 amplification in 3 cases (15%). PLAG1 alterations were absent in 12 cases. PLAG1 altered EMC were more frequently located in the parotid. On histology, all EMCs showed typical biphasic architecture at least focally. All PLAG1 rearranged tumors had evidence of a preexisting PA, while all cases with PLAG1 amplification showed solid growth pattern; both these features were uncommon in cases with normal PLAG1.

	PLAG1 rearrangement	PLAG1 amplification	No PLAG1 alteration
No. of cases	5 cases	3 cases	12 cases
Epidemiology			
Age distribution	47 to 69 years	29 to 47 years	21 to 66 years
Mean age	49.6 years	47.5 years	47.3 years
Sex ratio	1:1.5	2:1	1.4:1
Location			
Parotid	4 (80%)	2 (67%)	7 (58%)
Minor salivary glands	1 (20%)	Nil	3 (25%)
SMG	Nil	Nil	2 (17%)
Orbit	Nil	1 (33%)	Nil
Histology			
Oncocytic	2 (40%)	1 (20%)	3 (25%)
Clear cell	3 (60%)	3 (60%)	5 (42%)
Solid	2 (40%)	3 (100%)	2 (17%)
Preexisting PA	5 (100%)	1 (33%)	4 (33%)
High grade transformation	Nil	1 (33%)	Nil

Conclusions: EMC is a molecularly heterogeneous entity. Consistent with previous data, a proportion of EMCs arise ex PA, and harbor PLAG1 gene rearrangements. In addition, a subset of EMCs show PLAG1 amplification. Further genetic testing is indicated in the normal PLAG1 group to ascertain the molecular pathway to its pathogenesis.

816 Loss of SMARCA4 Immunoexpression in a Subset of Olfactory Neuroblastomas

Aanchal Kakkar¹, Diya Roy¹, Kavneet Kaur¹, Deepali Jain¹, Rajeev Kumar¹, Alok Thakar¹, Raja Pramanik¹
¹All India Institute of Medical Sciences, New Delhi, India

Disclosures: Aanchal Kakkar: None; Diya Roy: None; Kavneet Kaur: None; Deepali Jain: None; Rajeev Kumar: None; Alok Thakar: None; Raja Pramanik: None

Background: Molecular analysis of sinonasal carcinomas has led to the identification of several novel entities that harbor specific genetic alterations, including NUT carcinoma, SWI/SNF complex-deficient sinonasal carcinoma and isocitrate dehydrogenase 2 (IDH2)-mutant SNUC, which were previously diagnosed as sinonasal undifferentiated carcinoma (SNUC), neuroendocrine carcinoma (NEC) or poorly differentiated carcinomas, and have prognostic implications. Olfactory neuroblastoma (ONB) is a

neuroectodermal neoplasm whose rarity has precluded its inclusion in high throughput molecular analyses, with occasional studies till date. Also, there is significant morphological overlap between high grade (III/IV) ONB, SNUC and NEC. We recently identified SMARCA4 loss in a cohort of poorly differentiated/undifferentiated sinonasal carcinomas and teratocarcinomas (TCS), including one case with ONB-like areas with neurofibrillary matrix, prompting us to evaluate a series of ONB for SMARCA4 loss to identify cases of SMARCA4-deficient carcinoma.

Design: Cases of ONB diagnosed over an 11-year period (2010-2020) were retrieved. Sections were reviewed, and cases were assigned Hyams grades. Immunohistochemistry for SMARCA4 was performed on whole tissue sections. Cases with loss of nuclear staining in tumor cells with intact staining in endothelial cells were considered as SMARCA4-deficient.

Results: Fifty cases of ONB were evaluated. Fourteen ONBs (28%) showed loss of SMARCA4 expression. Of these, 10 cases (20%) showed complete SMARCA4 loss, three cases showed complete SMARCA4 loss in certain areas of the tumor with retained expression in others i.e. partial loss, and one showed heterogeneous staining with loss of immunoreactivity in approximately 50% of tumor cells. On reviewing the morphology, all 10 cases with complete loss, and two cases with partial loss were of high Hyams grade; one case with partial loss and the case with heterogeneous loss were of low Hyams grade. On morphology, eight cases were ONB-like, four were more akin to NEC, and two were TCS-like.

Conclusions: SMARCA4 loss in a significant proportion of ONBs is indicative of molecular heterogeneity within this entity. Most cases with SMARCA4 loss resemble high grade ONBs, with only a few bearing resemblances to morphologically similar tumors viz. NEC and TCS. These findings warrant confirmation by molecular testing, and indicate that SMARCA4 immunohistochemistry should be performed on all ONBs to facilitate identification of SMARCA4 deficient carcinoma.

817 Prognostic Significance of Extent of Extracapsular Extension in Metastatic Nodes in Advanced Oral Cavity Squamous Carcinoma: Evidence for Inclusion in the Existing Nodal Staging

Ramandeep Kaur¹, Neha Mittal¹, Swapnil Rane², Asawari Patil³, Munita Bal², Katha Rabade²

¹Tata Memorial Hospital, Mumbai, India, ²Tata Memorial Centre, Mumbai, India, ³ACTREC-Tata Memorial Centre, Thane, India

Disclosures: Ramandeep Kaur: None; Neha Mittal: None; Swapnil Rane: None; Asawari Patil: None; Munita Bal: None; Katha Rabade: None

Background: The extracapsular extension (ECE) is an established prognostic parameter in the overall survival of oral cavity squamous carcinoma (OCSCC) and is a part of the 8th edition AJCC classification. However, extent of ECE (micro- versus macro-ECE) has not been factored into classification yet. We undertook a survival-based analysis of the significance of the extent of ECE as a prognostic parameter in stage IV OCSCC.

Design: A cohort of 162 patients (staged according to AJCC 7th edition) from an earlier clinical trial (CTRI/2012/10/ 003062), all with stage IV OCSCC, uniformly treated with surgery and adjuvant CTRT, and histologically proven metastatic nodes with extracapsular extension (ECE) were re-classified for pT and pN categories according to AJCC 8th edition. The cases were divided into metastatic nodes with micro-ECE(≤ 2 mm) & macro-ECE(> 2 mm). Survival analysis was done using the Kaplan Meyer graphs and the significance of ECE was established using the Log-rank test.

Results: The mean age was 43.79 years, with a distinct male preponderance (M: F=7.5:1) & median overall survival of 39 months for the entire cohort. Primary tumor parameters included tongue (35%) followed by buccal mucosa (32%) as the most common sites; pT4 tumors in 51%, depth of invasion > 10 mm in 58% cases, high tumor budding in 41%, perineural invasion in 61% and tumor-infiltrating-lymphocytes $> 25\%$ in 51% cases. The mean number of sampled nodes per case was 37 (range:12-88). The mean metastatic nodal burden was 3 (range:1-14), staged as pN2a (20%) and pN3b (80%) according to AJCC 8th edition. Size of largest metastatic focus ranged from 0.3 to 4.2 cm (mean:1.6 cm). ECE was present in 100% of cases; sub-stratified as micro-ECE in 53% & macro-ECE in 47% of cases. The median 3-year overall survival (OS) was 45 months for macro-ECE, however, it was not reached for cases with micro-ECE (P value=0.013). The median 3-year progression-free survival (PFS) was significantly worse for cases with macro-ECE than micro-ECE (p value=0.017). In addition, subgroup analysis showed that 52% of pN2a cases with macro-ECE progressed in the first year as compared to only 10% with micro-ECE (P value=0.026).

Parameters		Number of cases (Percentage)
Tumor parameters (n=159)		
T Stage	pT1 pT2 pT3 pT4	13 (8) 36 (23) 29 (18) 81 (51)
Epicentre of tumor	Tongue and Floor of mouth Buccal mucosa GBS Lower alveolus RMT Palate Lip	57 (35) 51(32) 22(14) 15 (10) 8 (5) 2 (1) 4 (3)
Depth of invasion (DOI)	DOI <=5mm 5-10mm >10mm	16 (10) 46 (28) 86 (53)
Worst pattern of invasion	2 3 4 5	1 (0.6) 5(3) 118 (73) 35 (22)
Perineural invasion (PNI) (n=99)	Density >1 (>4 foci of PNI) Size of involved nerve>1mm	35 (22) 6 (4)
Tumor-infiltrating lymphocytes- Stromal	<=5 5-10 10-25 25-50 50-100	1(0.6) 10(6.2) 18(11) 36(23.2) 94 (59)
Tumor budding	Absent- Low High	30 (19) 63 (40) 66 (41)
Grade	Well Mod Poor Sarcomatoid	20 (12) 65 (41) 36 (23) 38 (24)
Markers for advanced T stage	Bone involvement Skin involvement	52(33) 17(11)
Nodal parameters		
Number of nodes with metastasis	<=7 >8	150 (93) 12(07)
Laterality of node involvement	Ipsilateral Contralateral Bilateral	140 (86.4) 01 (0.6) 21(13)
Level of nodes involved	I to III IV, V	113(70) 49 (30)
Number of nodes with ECE	<=4 >5	152(94) 10(6)
Extent of ECE	Micro --≤2mm Macro - >2mm	85(53) 77(47)
N stage (n=162)	pN2a (single metastatic ipsilateral node with ECE) pN3b (Any node with ECE with >/=2 metastatic nodes)	32 (20) 130 (80)
Survival parameters (n=162)		
Median PFS	Micro ECE Macro ECE	29 months 22 months
Median OS	Micro ECE Macro ECE	32 months 25 months

Figure 1 - 817

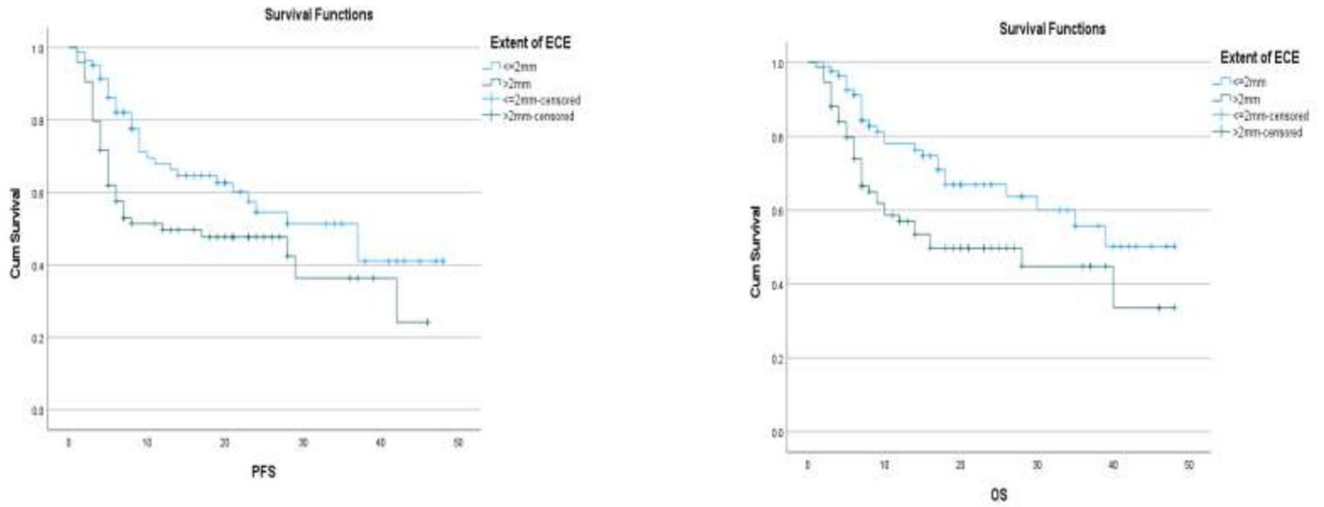
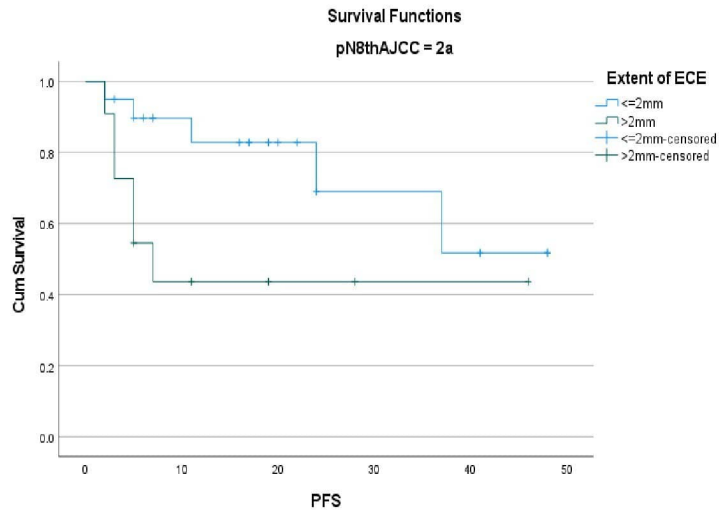


Figure 2 - 817



Conclusions: The extent of extracapsular extension is an independent prognostic factor for OS and PFS in advanced OSCC. Nodal stage pN2a with macro-ECE has a survival comparable to pN3b. Thus, a case-in-point is made for the inclusion of the extent of ECE in the current nodal staging for a better-informed decision for adjuvant therapy, and prognostication.

818 Nuclear Expression of AFF2 C-terminus as a Sensitive and Specific Ancillary Marker for DEK-AFF2 Fusion-Associated Carcinoma of the Sinonasal Tract

Ying-Ju Kuo¹, James Lewis Jr.², Rebecca Chernock³, Tra Truong⁴, Changwen Zhai⁵, Yun-An Chen⁶, Chien-Kuan Lee⁷, Qiuying (Judy) Shi⁸, Min-Shu Hsieh⁹, Ilan Weinreb¹⁰, Jen-Fan Hang¹

¹Taipei Veterans General Hospital, Taipei, Taiwan, ²Vanderbilt University Medical Center, Nashville, TN, ³Washington University School of Medicine, St. Louis, MO, ⁴Sunnybrook Health Sciences Centre, Toronto, Canada, ⁵Fudan University, Shanghai, China, ⁶Taichung Veterans General Hospital, Taichung, Taiwan, ⁷Kuan-Tang General Hospital, Taiwan, ⁸Emory University, Atlanta, GA, ⁹National Taiwan University Hospital, Taipei, Taiwan, ¹⁰University Health Network, Toronto, Canada

Disclosures: Ying-Ju Kuo: None; James Lewis Jr.: None; Rebecca Chernock: None; Tra Truong: None; Changwen Zhai: None; Yun-An Chen: None; Chien-Kuan Lee: None; Qiuying (Judy) Shi: None; Min-Shu Hsieh: None; Ilan Weinreb: None; Jen-Fan Hang: None

Background: *DEK-AFF2*-fusion associated carcinoma of the sinonasal tract is an emerging entity. The tumor is characterized by papillary proliferation of non-keratinizing squamous epithelial cells with monotonous and bland cytologic features, which may mimic other tumors with similar morphology. The confirmation of the gene fusion solely relied on next-generation sequencing, fluorescence in situ hybridization (FISH), or reverse transcription polymerase chain reaction (RT-PCR) in previous studies. This current study aimed to validate an immunohistochemical assay for AFF2 C-terminus and to evaluate its performance as an ancillary marker in diagnosing *DEK-AFF2*-fusion associated carcinoma.

Design: Immunohistochemistry (IHC) with an anti-AFF2 C-terminus antibody was optimized for the staining protocol using a selection of normal control tissues. After optimization, the AFF2 IHC was performed on 13 *DEK-AFF2*-fusion associated carcinomas and 23 *DEK* FISH-negative sinonasal tumors, including five poorly-differentiated carcinomas, eight non-keratinizing squamous cell carcinomas, two basaloid squamous cell carcinomas, and eight adenosquamous carcinomas.

Results: In the normal control tissues, AFF2 IHC showed strong cytoplasmic staining in plasma cells and serous acinar cells of the salivary gland, and moderate cytoplasmic staining in pancreatic islet cells and cytotrophoblasts. In *DEK-AFF2* fusion-associated carcinomas, seven cases had a "low-grade papillary Schneiderian carcinoma-like" appearance, five showed nonkeratinizing squamous cell carcinoma features, and one demonstrated adenosquamous carcinoma morphology. All of the 13 cases were positive for nuclear expression with strong staining in three (Figure 1) and moderate staining in ten (Figure 2). The staining was present in more than 50% of tumor cells in seven cases, 25-50% of the tumor cells in three, and less than 25% of the tumor cells in three. In *DEK* FISH-negative sinonasal tumors, all 23 cases were negative for nuclear expression. There were only two cases of adenosquamous carcinoma showing focal and weak cytoplasmic staining in 1% to 2% of the tumor cells. Nuclear expression of AFF2 IHC showed 100% sensitivity and specificity in diagnosing *DEK-AFF2* fusion-associated carcinoma.

Figure 1 - 818

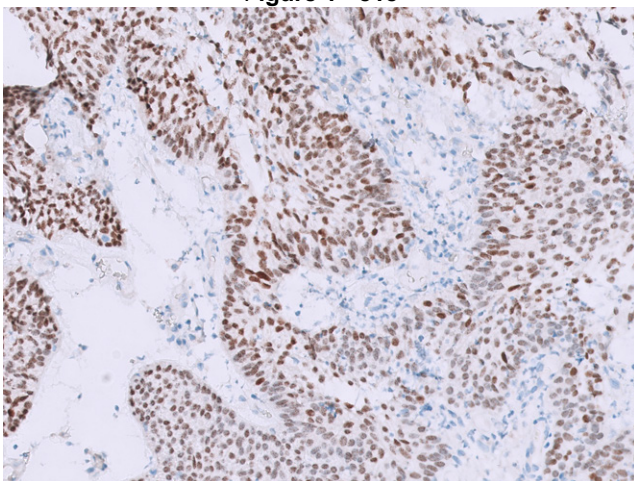
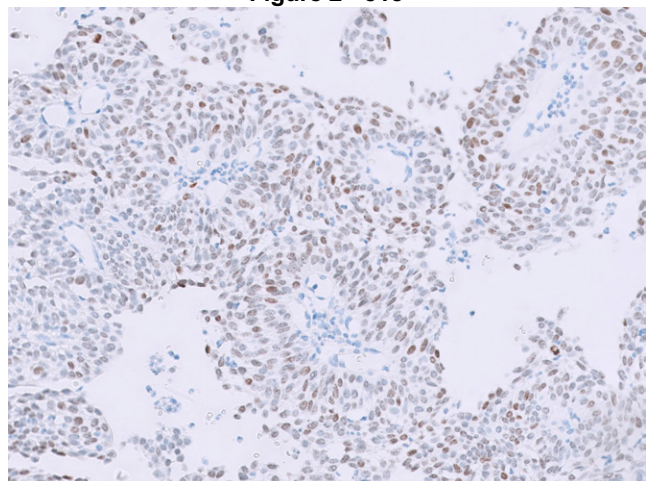


Figure 2 - 818



Conclusions: The AFF2 IHC is a sensitive and specific ancillary marker and distinguishes *DEK-AFF2* fusion-associated carcinoma from the other sinonasal tumors with overlapping morphological features.

819 Is Salivary Duct Carcinoma an Apocrine Carcinoma of the Salivary Glands? Immunohistochemical Evaluation for AR, GCDFF-15, GATA3, p62(sequestosome1) and FABP7 in 106 Cases

Kimihide Kusafuka¹, Tomohiro Iwasaki¹, Kaori Ueda², Hiroshi Inagaki², Junya Itakura³, Yoshiro Otsuki⁴, Tsutomu Daa⁵, Kensuke Suzuki⁶, Hiroshi Iwai⁶, Naoto Kuroda⁷, Koji Yamanegi⁸, Ichiro Ito⁹, Yoshiaki Imamura¹⁰, Mei Hamada¹¹, Masanori Yasuda¹², Yoko Sato¹³, Makoto Suzuki¹

¹Shizuoka General Hospital, Shizuoka City, Japan, ²Nagoya City University, Nagoya City, Japan, ³Kurashiki Central Hospital, Kurashiki, Japan, ⁴Seirei Hamamatsu General Hospital, Hamamatsu, Japan, ⁵Oita University Faculty of Medicine, Yufu, Japan, ⁶Kansai Medical University, Hirakata City, Japan, ⁷Kinrou Hospital, Kochi City, Japan, ⁸Hyogo College of Medicine, Nishinomiya, Japan, ⁹Nagano Red Cross Hospital, Nagano, Japan, ¹⁰Fukui University, Yoshida-gun, Japan, ¹¹Saitama Medical University International Medical Center, ¹²Saitama Medical University International Medical Center, Hidaka, Japan, ¹³Shizuoka Graduate University of Public Health, Shizuoka city, Japan

Disclosures: Kimihide Kusafuka: None; Tomohiro Iwasaki: None; Kaori Ueda: None; Hiroshi Inagaki: None; Junya Itakura: None; Yoshiro Otsuki: None; Tsutomu Daa: None; Kensuke Suzuki: None; Hiroshi Iwai: None; Naoto Kuroda: None; Koji Yamanegi: None; Ichiro Ito: None; Yoshiaki Imamura: None; Mei Hamada: None; Masanori Yasuda: None; Yoko Sato: None; Makoto Suzuki: None

Background: The up-regulation of p62 (sequestosome1) and brain fatty acid binding protein (FABP7) was reported in apocrine carcinoma of the breast (ACB). On the other hands, GATA3 is well-known markers for urothelial and breast carcinomas. Salivary duct carcinoma (SDC) is a relatively rare malignancy in the salivary glands, but it is frequently seen as carcinomatous component of carcinoma ex pleomorphic adenoma (CXPA). We aim to elucidate the expression states of androgen receptor (AR), gross cystic disease fluid protein (GCDFF)-15, p62, GATA3 and FABP7 in SDC, in comparison with pleomorphic adenoma (PA) and to elucidate the significance of these molecules and relationship with its outcomes in SDC.

Design: We selected SDC cases and PA cases from a pathology file of 12 institutions during 2000-2020, immunostained them for p62, GATA3 and FABP7, adding to AR, GCDFF-15, and Ki-67. In the assessment for p62, nuclear signals were estimated as N type, whereas cytoplasmic signals were estimated as CY type. We estimated (-),negative or <10% positive cancer cells and (+), ≥10% of positive cancer cells. All statistical analyses were made using R version 3.6.2 software. (The R Foundation for Statistical Computing, Vienna, Austria)

Results: One hundred six cases were finally selected as SDC (Table), including 59 cases of CXPA (20 cases of intracapsular type, 8 cases of minimally invasive type and 31 cases of widely invasive type). Thirty-two cases of PA, including 6 cases of atypical PA, were randomly selected as benign control. Ninety-two percent of SDC was positive for p62 (N type, 58%; CY type, 13%; N+CY type, 21%) (Figure 1), whereas 54% of PA was focally positive for p62 (only N type). Seventy-six percent, 78%, 34%, and 54% of SDC were positive for AR, GCDFF-15, GATA3, and FABP7, respectively (Figure 2 and Table). Thirty-four percent, 22%, 12%, and 25% of PA were focally positive for AR, GCDFF-15, GATA3, and FABP7, respectively. Despite no statistical significance, the expression status of p62 CY type (+) and (-) was related to worse outcome of SDC patients (P>0.05), whereas the GATA3(+) cases were related to better outcome (P>0.05).

Table. Background of the Patients with SDC in This Study and the Results of Immunohistochemical Examinations for Apocrine Markers

	n=106	percentage	alive n=56 (%)	death n=35 (%)
Age: mean=66y/o (28-91y/o)				
<50y/o	9	14%	6(11%)	2(6%)
50-59y/o	18	17%	8(14%)	8(23%)
60-69y/o	32	30%	20(36%)	9(26%)
≥70y/o	47	44%	22(39%)	16(46%)
Gender				
female	17	16%	11(20%)	4(11%)
male	89	84%	45(80%)	31(89%)
Location				
parotid	81	76%	45(80%)	25(71%)
SMG	20	19%	6(11%)	10(29%)
others	5	5%	5(1%)	0(0%)
CXPA				
(-)	39	37%	20(36%)	12(34%)

(-)SDCIS	2	2%	0(0%)	1(3%)
(+)IC	20	19%	16(29%)	4(11%)
(+)MinI	8	8%	5(9%)	2(6%)
(+)WI	31	29%	13(23%)	14(40%)
unknown	6	6%	2(4%)	2(6%)
pT factor				
pTis	2	2%	1(2%)	1(3%)
pT1	25	24%	20(36%)	4(11%)
pT2	22	21%	13(23%)	7(20%)
pT3	27	25%	9(26%)	11(31%)
pT4	23	22%	13(50%)	9(26%)
pTx	7	7%	0(0%)	3(9%)
pN factor				
pN0	39	37%	27(48%)	10(29%)
pN1	13	29%	5(9%)	6(17%)
pN2	44	42%	19(34%)	17(49%)
pN3	2	2%	1(2%)	0(0%)
pN(+)	5	5%	1(2%)	1(3%)
pNx	3	3%	3(5%)	1(3%)
cM factor				
cM0	93	88%	52(93%)	30(86%)
cM1	10	10%	4(7%)	4(11%)
cMx	3	3%	0(0%)	1(3%)
pStage				
pStage 0	2	2%	1(2%)	0(0%)
pStage I	23	22%	19(34%)	4(11%)
pStage II	7	6.6%	4(7%)	2(6%)
pStage III	15	14%	8(14%)	5(14%)
pStage IVA	41	38%	19(34%)	16(46%)
pStage IVB	1	1%	1(2%)	0(0%)
pStage IVC	11	10%	4(7%)	5(14%)
pStage X	6	6%	0(0%)	3(9%)
No.of LN meta				
0	39	37%	25(45%)	11(31%)
1~3	24	23%	10(18%)	8(23%)
4~10	20	19%	6(11%)	9(26%)
≥11	14	13%	8(14%)	6(17%)
Unknown	9	8.5%	7(13%)	1(2.9%)
Therapy				
S	35	33%	21(38%)	9(26%)
S+POT	55	52%	32(57%)	20(57%)
S+unknown	4	4%	0(0%)	2(6%)
only ND	3	3%	0(0%)	1(3%)
Bx/others	9	9%	3(5%)	4(11%)
apocrine markers				
p62 N(+)	61	58%	42(75%)	8(23%)
p62 CY(+)	14	13%	3(5%)	11(31%)
p62 N+CY(+)	22	21%	10(18%)	12(34%)
p62 (-)	9	8%	1(2%)	4(11%)
AR (+)	81	76%	49(75%)	25(71%)
AR (-)	25	24%	7(13%)	10(29%)
GCDFP-15(+)	83	78%	45(80%)	25(71%)
GCDFP-15(-)	23	22%	6(11%)	10(29%)
GATA3(+)	36	34%	20(56%)	13(37%)
GATA3(-)	70	66%	36(64%)	22(63%)
FABP7(+)	57	54%	34(61%)	21(60%)
FABP7(-)	49	40%	22(39%)	14(40%)
				loss of follow-up: n=15
SMG, submandibular gland; IC, intracapsular type; MinI, minimally invasive type; WI, widely invasive type; S, surgery; POT, postoperative therapy; ND, neck dissection; Bx, biopsy.				

Figure 1 - 819

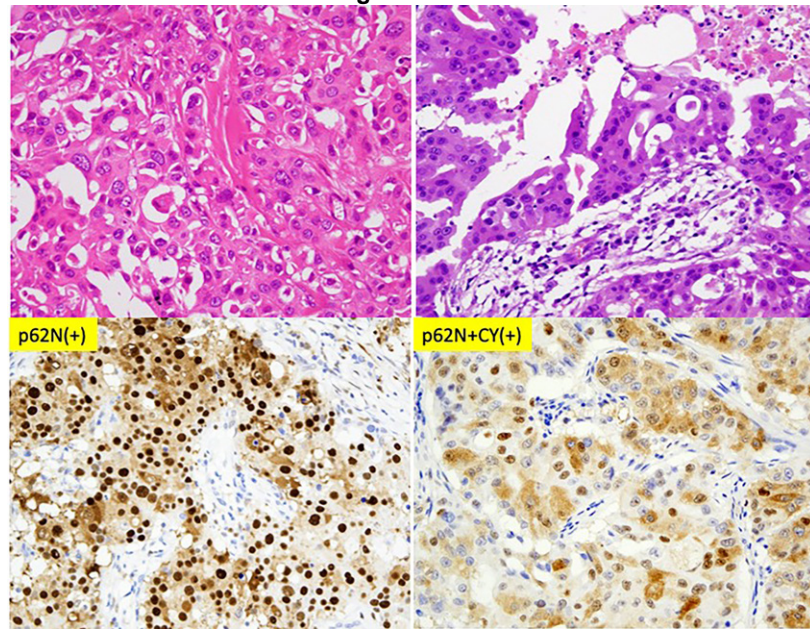
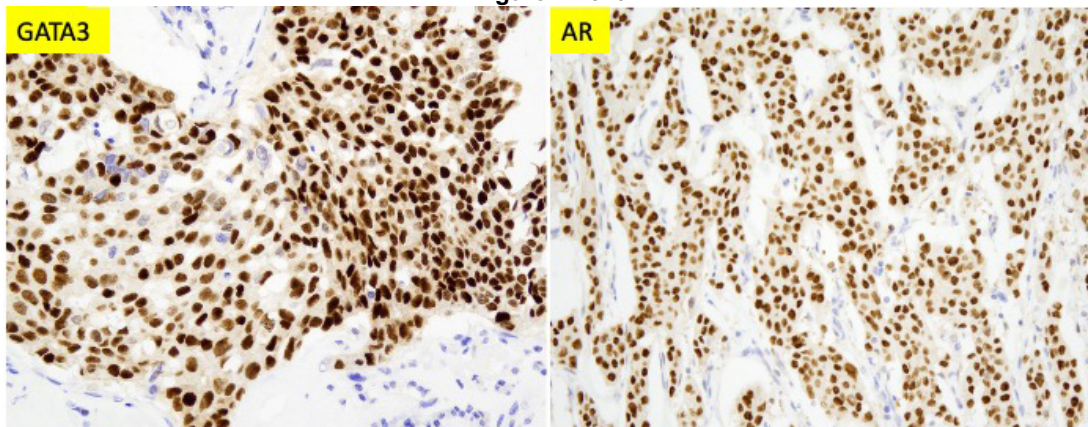


Figure 2 - 819



Conclusions: In conclusion, some subgroup of SDC should be called “apocrine carcinoma of the salivary glands”, due to the positivity for AR, GCDFP-15, p62, GATA3 and FABP7, such as ACB. In the cases of CXPA, the luminal cells of PA may acquire the malignant features of SDC, accompanying the apocrine differentiation, especially, in the progression process from atypical PA to early phase of CXPA (intracapsular subtype): This process is related to “adenoma-carcinoma sequence” of salivary glands.

820 Whole Exome Sequencing Revealed that Assessment of TP53 and CDKN2A Status can be a Predictive Marker of Malignant Transformation of Sinonasal Inverted Papilloma

Soohyeon Kwon¹, Jee Hye Wee², Hyojin Kim³

¹Seoul National University Bundang Hospital, Seongnam-si, South Korea, ²Hallym University Sacred Heart Hospital, Anyang, South Korea, ³Seoul National University Bundang Hospital, Seongnam, South Korea

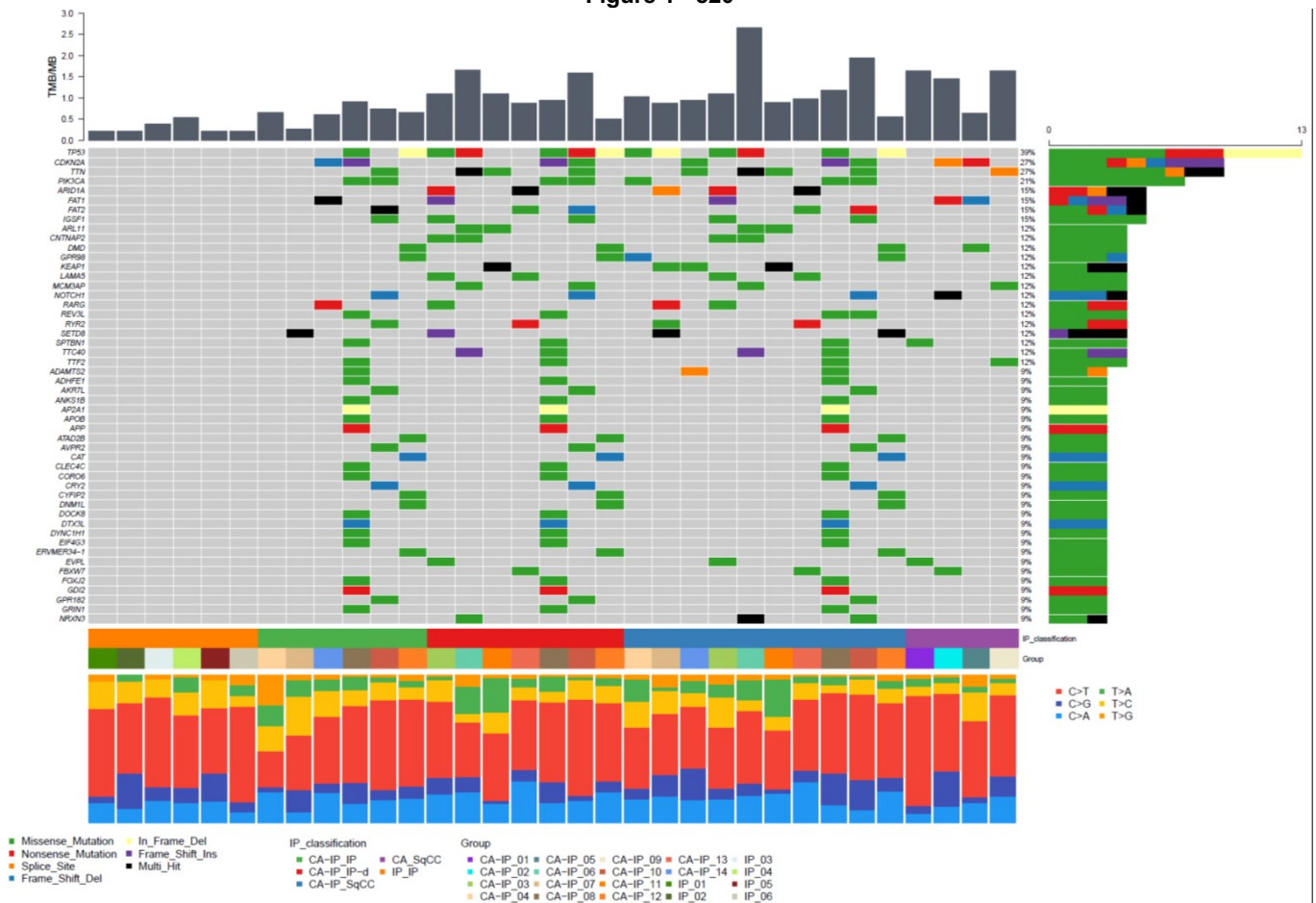
Disclosures: Soohyeon Kwon: None; Jee Hye Wee: None; Hyojin Kim: None

Background: Sinonasal inverted papilloma (IP) has the potential to transform into squamous cell carcinoma (SCC), but the mechanism is still uncertain and there are no diagnostic methods to predict malignant transformation. We investigated genetic mutations involved in stepwise progression of IP-SCC and explored biomarkers that can predict malignant transformation of IP.

Design: Fourteen patients diagnosed with SCC arising in IP and six IP patients who did not undergo malignant transformation were included. DNA was extracted from IP, IP with dysplasia, and SCC, respectively, and whole exome sequencing was performed. Of the 14 patients with IP that progressed to SCC, 4 had both IP and SCC lesions, 4 had dysplastic IP and SCC lesions, and 3 had both IP, dysplastic IP and SCC lesions. The remaining 3 patients had IP lesions, but they were so small that macrodissection was impossible, so DNA was obtained only from SCC samples. Immunohistochemistry for TP53 and p16 was also performed.

Results: Major oncogenic mutations were observed with high frequency in the stepwise progression from IP to SCC. *TP53* was the most frequently mutated gene (39%), followed by *CDKN2A* (27%), *TTN* (27%), *ARID1A* (21%), and *PIK3CA* (15%). Mutations in *TP53* and/or *CDKN2A* were observed in 3 out of 6 IPs with malignant transformation, whereas none of the mutations were observed in IPs that did not undergo SCC. Tumor mutational burden increased from IP to SCC (0.65/Mb for IP, 1.1/Mb for dysplasia, and 1.25 for SCC group, respectively), and IPs with malignant transformation showed higher TMB than pure IP group (0.65/Mb versus 0.27/Mb). As a result of TP53 and CDKN2A IHC, three of six IPs with malignant transformation showed a diffuse strong or null pattern in p53, and one showed a total loss of p16 which is distinct pattern of pure IPs.

Figure 1 - 820



Conclusions: Our result suggests that assessment of TP53 and CDKN2A status can be a predictive marker of malignant transformation of IP.

821 Oral Cavity Human Papillomavirus-Associated Squamous Cell Carcinoma: “Yes It Happens and It is Different!” - A Case Series Showing Unique Morphologic and Clinicopathologic Features

James Lewis Jr.¹, Molly Smith², Kim Ely¹, Mitra Mehrad¹, Fangjia Tong³, Xiaowei Wang³, Krystle Kuhs⁴
¹Vanderbilt University Medical Center, Nashville, TN, ²University of Kentucky College of Dentistry, Lexington, KY, ³University of Illinois at Chicago, Chicago, IL, ⁴University of Kentucky, Lexington, KY

Disclosures: James Lewis Jr.: None; Molly Smith: None; Kim Ely: None; Mitra Mehrad: None; Fangjia Tong: None; Xiaowei Wang: None; Krystle Kuhs: None

Background: While human papillomavirus (HPV) dominates oropharyngeal squamous cell carcinoma (SCC) in Western countries, a minority of non-oropharyngeal SCCs are HPV-associated. These are not well-characterized in the literature and their clinical significance is also poorly understood.

Design: We gathered a cohort of oral cavity (OC) SCC which had nonkeratinizing morphology, either in the primary tumor or in situ carcinoma (or both), from institutional files and tested them for p16 by immunohistochemistry with a 70% nuclear and cytoplasmic staining cutoff as well as for high risk HPV E6/E7 mRNA by RTPCR (the well established reference standard for transcriptionally-active high risk HPV). Patients with involvement of the oropharynx or history of oropharyngeal SCC were excluded. Detailed morphologic and clinicopathologic data was also collected.

Results: Nine patients were identified and proven to be HPV-associated by combined p16 and high risk HPV mRNA positivity. HPV types were 16 (8/9 89%) and 33 (1/9 11%). All 9 (100%) were men, average age was 63 (range 53 to 69), and all underwent primary surgical resection. All 9 patients (100%) were heavy smokers and 7/9 (78%) were active drinkers. Tumors had a striking predilection for the floor of mouth (FOM) and/or ventral tongue (7/9 78% FOM +/- tongue, and 2/9 22% tongue only). Tumors were large (avg 3.6 cm - range 1.6 to 5.2 cm) or had bone invasion (6/9 66% were T4a tumors), and most (6/9 66%) had extensive carcinoma in situ (CIS) which was clinically hard to appreciate with all 6 of these patients having margins positive for CIS after resection. Nodal metastases were present in 4/9 (44%) of patients. All of the tumors had nonkeratinizing features, but in highly variable amounts (range 10 to 100, avg 62%), with cells with high N:C ratios and larger nests, frequently with pushing borders and less (or no) stromal desmoplasia. The CIS was nonkeratinizing with high N:C ratio cells, full or nearly full thickness loss of maturation, and abundant apoptosis and mitosis.

Conclusions: HPV-associated OCSCC is an uncommon entity, but when well characterized with mRNA-based HPV testing has distinct clinical and pathologic features including predilection for the floor of mouth, high rates of heavy smoking and drinking, frequent bone invasion, nonkeratinizing morphology, and extensive nonkeratinizing CIS which is clinically hard to recognize and resect. Recognition of these features may aid in pathologic diagnosis and clinical management.

822 Simple as a Blood Test? Serology as a Diagnostic Test for High Risk HPV Status in Oropharyngeal SCC Patients at Presentation

James Lewis Jr.¹, Tim Waterboer, Kim Ely¹, Mitra Mehrad¹, Xiaowei Wang³, Daniel Faden⁴, Seth Davis¹, Krystle Kuhs⁵
¹Vanderbilt University Medical Center, Nashville, TN, ²German Cancer Research Center, Heidelberg, Germany, ³University of Illinois at Chicago, Chicago, IL, ⁴Massachusetts Eye and Ear Infirmary, Harvard Medical School, Boston, MA, ⁵University of Kentucky, Lexington, KY

Disclosures: James Lewis Jr.: None; Tim Waterboer: *Consultant*, MSD (Merck) Sharp & Dohme; Kim Ely: None; Mitra Mehrad: None; Xiaowei Wang: None; Daniel Faden: None; Seth Davis: None; Krystle Kuhs: None

Background: Human papillomavirus (HPV) status in oropharyngeal squamous cell carcinoma (OPSCC) patients, by p16 immunohistochemistry, with or without HPV specific testing, is recommended by the CAP expert panel on HPV testing in head and neck carcinomas. HPV RNA in situ hybridization (ISH) is emerging as a preferred HPV specific test on tissue specimens and cell blocks. Easier assessment of HPV status in OPSCC patients would be useful. Since patients develop a robust immune response to high risk HPV E6 and E7 proteins, serology for IgG anti-E6 and E7 has been suggested for screening and follow up in OPSCC patients. We sought to explore its potential use as a diagnostic test for HPV status compared to the reference standard tissue hrHPV RNA ISH.

Design: A cohort of 84 OPSCC patients with blood drawn for research was accumulated. All had serology for IgG anti-HPV E6/E7 types 16,18,31,33,35,45,52,58. Patients were considered positive when either E6 and E7 IgG were detected for a given

hrHPV type. High risk HPV RNA ISH with RNAscope using a cocktail of 18 different high risk HPV types was performed on a tissue microarray of the cases and read semiquantitatively as 1 to 3+. Results were correlated with clinical and pathologic variables.

Results: Of the 84 patients, 74 (88.1%) were hrHPV RNA ISH positive while 10 (11.9%) were negative. All 10 HPV negative patients were seronegative (100% specificity) while 66/74 of HPV positive patients were seropositive (89.2% sensitivity) including 53 HPV type 16, 3 type 33, 2 type 18, and 1 type 52 tumors, while 7 had multiple hrHPV types. Of the 8 serology false negative patients, 4/8 (50.0%) had 1+ (low level) RNA ISH compared to 30/66 (45.5%) of the true positive patients ($p=0.43$) arguing that low transcription rates for HPV proteins do not result in lower seroconversion. Of the 74 seropositives, 13 underwent neck FNA initially which was positive for SCC. Only 4/13 (30.8%) had HPV status (p16 on cell blocks) ascertained on those specimens. If serology as a simple blood test for HPV status had been available in clinical practice, then 4 surgeries for tissue biopsy could have been avoided and the HPV status ascertained on all 13 without additional procedures.

Conclusions: High risk HPV serology is a specific and relatively sensitive test for high risk HPV status at presentation in OPSCC patients. Serology is promising as a non-invasive test method for laboratory assessment of HPV status in OPSCC patients.

823 SSTR2 Receptor Expression Increased in Recurrent and Metastatic Hürthle Cell Carcinoma: Implications for Treatment

Manuel Lora Gonzalez¹, Dezhi Wang¹, Rachael Guenter¹, Rui Zheng-Pywell¹, J. Bart Rose¹, Renata Jaskula-Sztul¹, Ricardo Lloyd², Diana Lin¹

¹The University of Alabama at Birmingham, Birmingham, AL, ²University of Wisconsin, Madison, WI

Disclosures: Manuel Lora Gonzalez: None; Dezhi Wang: None; Rachael Guenter: None; Rui Zheng-Pywell: None; J. Bart Rose: None; Renata Jaskula-Sztul: None; Ricardo Lloyd: None; Diana Lin: *Consultant, Proteocyte*

Background: Somatostatin receptors (SSTR) are often overexpressed in neuroendocrine tumors, allowing for targeted treatment with receptor-specific analogues. Recent studies have shown SSTR2 expression in papillary thyroid carcinoma and anaplastic carcinoma, but to our knowledge, SSTR2 has not yet been studied in Hürthle cell neoplasms.

Design: Following approval by Institutional Review Board, a retrospective search for Hürthle cell neoplasms diagnosed from 2012 to 2019 was performed in the pathology laboratory information system (Cerner Millennium). Clinical information and slides were reviewed and formalin-fixed paraffin embedded (FFPE) tissue blocks were pulled for tissue microarray (TMA) construction. Slide marking and digital analysis (Galileo TMA CK3600 Tissue Arrayer) were used to punch 2 mm cores from FFPE blocks. An average of 3 cores per tumor were used for TMA assembly with negative control cores (normal thyroid) and positive control cores (pancreatic neuroendocrine tumor). TMA blocks were cut into 5 micron sections and stained with anti-SSTR2 antibody (Abcam). Immunostains were analyzed by 3 independent pathologists and cytoplasmic staining in at least 10% of tumor cells was considered positive. Chi-squared analysis was used to assess statistical significance ($p<0.05$).

Results: 41 Hürthle cell carcinoma (HC) cases (34 primary, 5 localized recurrences, 2 metastatic [1 lymph node, 1 lung]) and 14 Hürthle cell adenoma (HA) cases were identified. SSTR2 positivity was noted in 2 HA (17%) and 14 HC cases (34%), including 9 primary HC and 5 recurrent/metastatic HC. SSTR2 was significantly more expressed in recurrent/metastatic HC (71%) compared to primary HC (26%) ($p=0.02$), but not all HC cases compared to HA ($p>0.05$).

Conclusions: Significantly higher SSTR2 expression identified in recurrent/metastatic HC has promising treatment implications, especially for patients who fail first-line radioactive iodine therapy. Efficacy of targeted SSTR therapies in this patient population should be investigated.

824 The Genomic and Immune Landscape of Highly-aggressive, Treatment-resistant HPV-positive Oropharyngeal Tumors

Lily Mahapatra¹, Neal Andruska¹, Mena Mansour²

¹Barnes-Jewish Hospital/Washington University, St. Louis, MO, ²Washington University Medical Center, St. Louis, MO

Disclosures: Lily Mahapatra: None; Neal Andruska: None; Mena Mansour: None

Background: The majority of Human papillomavirus (HPV)-positive oropharyngeal squamous cell carcinoma (OPSCC) have a favorable prognosis; however, there is a subset within this group that are aggressive, non-responsive to chemoradiation, with poor clinical outcomes. Identification of “average-risk (AR)” versus “high risk (HR)” HPV-positive OPSCC tumors is required to distinguish which patients benefit from escalated upfront therapy.

Design: A retrospective review of institutional medical and pathology records from 2011-2019 was completed with a total of 18 AR and HR HPV OPSCC patients identified. Young patients, typically with minimal to no smoking history, were selected based on the natural course of HPV-positive OPSCC. HR patients represented those with an unusually aggressive clinical course characterized by rapid development of locoregional recurrence and metastatic disease, typically associated with distant metastases at sites outside the lungs, which is associated with poorer prognosis. These patients were resistant to standard-of-care therapy and salvage therapies, and rapidly died from their disease. We matched HR patients to AR HPV-positive patients that were free of disease with long-term follow-up after definitive therapy. RNA sequencing, CIBERSORTX to characterize immune cell subsets, cytokine profiling of HR tumors, and histological evaluation of tumor infiltrating lymphocytes (TILs) was performed.

Results: All HR HPV OPSCCs were in men, with a median disease-free survival and overall survival of 6 and 18 months, respectively. There were no significant differences in viral mRNA expression, nor were there differences in the ratio of full-length versus truncated E6 mRNA in the AR and HR HPV OPSCC tumors. RNA sequencing identified PRAME and MAGE-A1, tumor associated antigens (TAAs), upregulated in HR patients. CIBERSORTX analysis demonstrated that CD8 T cells are decreased in HR patients. Preliminary data suggests a trend towards a decreased TILs by immunohistochemical analysis.

Conclusions: Further understanding the molecular basis of highly aggressive HPV-positive OPSCC is paramount to the long-term goal of identifying new therapeutic strategies for this patient population. Here we report a distinct genomic landscape, immune microenvironment, and cytokine profile representing high-risk HPV-positive tumors.

825 Genomic Alterations in the Malignant Transformation of Pleomorphic Adenoma: A Comprehensive Analysis by Whole Exome Sequencing

Fernanda Mariano¹, João Scarini², Erika Egal³, Sheila Nagamatsu², Rodrigo Maioral², Reydson de Lima-Souza², Marcelo Carazzolle², Luiz Coutinho⁴, Luiz Kowalski⁵, Albina Altemani⁶

¹Campinas, Brazil, ²State University of Campinas (Unicamp), Campinas, Brazil, ³The University of Utah, Salt Lake City, UT, ⁴Piracicaba, Brazil, ⁵Faculdade de Medicina da USP, Campinas, Brazil, ⁶UNICAMP - Brazil, Brazil

Disclosures: Fernanda Mariano: None; João Scarini: None; Erika Egal: None; Sheila Nagamatsu: None; Rodrigo Maioral: None; Reydson de Lima-Souza: None; Marcelo Carazzolle: None; Luiz Coutinho: None; Luiz Kowalski: None; Albina Altemani: None

Background: Among the tumors that can affect the salivary glands, two constitute an interesting model for the study of the mechanism of malignant transformation, given that the first one, the most common benign tumor in the salivary gland, Pleomorphic Adenoma (PA), can undergo genetic transformations resulting in its malignant counterpart, Carcinoma Ex-Pleomorphic Adenoma (CXPA). CXPA is a rare and aggressive salivary gland malignancy, leading to different biological behavior and prognosis.

Design: WES was successfully performed on DNA samples from 13 CXPA, 7 PA, and 5 residual PA individuals. Sequencing reads were aligned to the hg38 reference genome. Single nucleotide polymorphisms (SNPs) were identified for all samples. Quality and variant frequency filters were applied to the data.

Results: A comprehensive analysis identified a total of 10,088 genes that underwent non-synonymous mutations. Of these, 2735 (27.3% of them) were unique to CXPA, 2520 (25.2%) were unique to PA, and 848 (8.5%) were unique to residual PA. In the adenoma-carcinoma transition, we noticed that mutations in 1463 of them (16.4%) were seen in the PA and remained in the carcinoma counterpart. The mutation profile seen in residual AP was more similar to carcinoma than PA. Furthermore, almost 10% of all mutated genes found were present throughout the entire adenoma-carcinoma sequence (973 of them). The extracellular matrix-receptor interaction pathway was the main target of mutations in the adenoma-carcinoma ex-PA transition, whose 15

mutated genes were correlated to collagen (*COL4A2*, *COL6A3*, *COL6A5*), integrins (*ITGA10*, *ITGB4*, *ITGB7*), laminins (*LAMA1*, *LAMA4*, *LAMA5*, *LAMB3*, *LAMC1*) and other glycoproteins/proteoglycans (*HSPG2*, *RELN*, *TNR*, *TNXB*). Among the known mutations in cancer, somatic alterations in *CDH1*, *FGFR2*, *FGFR3*, *RET*, *SPEN* were found only in PA samples. Changes in *ATM*, *NCoR-1* and *Rb1* were shared between the PA and the CXPA. Furthermore, two genes were found only in the residual PA (*BRAF* and *PIK3CA*) and only one was shared between the residual PA and the CXPA (*TP53*). On the other hand, four were unique to CXPA only (*SMARCB1*, *FBXW7*, *ARID1A* and *Notch-1*) and five were shared among all groups (*BRIP1*, *FANCA*, *LRP1B*, *PALB2* and *TSC2*).

Conclusions: Taken together, the findings presented here suggest that malignant transformation of PA is a sequential process, with multiple alterations in oncogenes and tumor suppressor genes.

826 ERBB2 Gene Amplification Correlates Positively with HER2 Immunohistochemical Staining but has an Inverse Relationship with Androgen Receptor Staining in Salivary Duct Carcinoma

John McAfee¹, Raza Hoda¹, Carrie Hoyle¹, Lauren McCoy¹, Cathy Sprague¹, Miglena Komforti¹, Christopher Griffith²
¹Cleveland Clinic, Cleveland, OH, ²Cleveland Clinic Foundation, Cleveland, OH

Disclosures: John McAfee: None; Raza Hoda: None; Carrie Hoyle: None; Lauren McCoy: None; Cathy Sprague: None; Miglena Komforti: None; Christopher Griffith: None

Background: Salivary duct carcinoma (SDC) is an aggressive neoplasm. A subset of SDC display HER2 overexpression by immunohistochemistry (IHC) and/or *ERBB2* gene amplification by fluorescence in situ hybridization (FISH). Definitive HER2 IHC scoring is not established for SDC to predict *ERBB2* amplification and guide anti-HER2 treatment decisions.

Design: Fifty-one cases of SDC resected at our institution between 2004 and 2020 were included. Androgen receptor (AR), HER2 IHC and *ERBB2* FISH was performed in all cases. AR expression was scored for percent positive cells and categorized as positive (>10% of cells), low positive (1-10%) or negative (<1%). HER2 staining levels and patterns were recorded and scored using 2018 ASCO/CAP HER2 guidelines. FISH probes were enumerated by at least two observers and interpreted by a breast pathologist.

Results: Table 1 summarizes the findings. The figures show representative *ERBB2*-amplified (Fig 1) and non-amplified (Fig 2) cases. The median age was 70 years with a male predominance. Parotid gland was the most common site (82%). Twenty-nine (57%) were exPA with eight (16%) exclusively *in situ*/encapsulated carcinoma exPA. Tumors showed ductal carcinoma *in situ* (DCIS)-like or diffusely invasive architectural patterns, or often both. Perineural invasion was more common in non-amplified cases ($p=0.011$, Fisher’s exact test). The majority of lesions displayed HER2 protein expression, most often in a membranous pattern. However, the percentage of cells showing HER2 expression was significantly higher in amplified cases (Fig 1C, 1D, 2C, 2D) ($p=0.00003$, Wilcoxon rank-sum test). While expression levels were uniformly high among *ERBB2*-amplified cases, they varied dramatically among non-amplified cases. HER2 IHC Score 3+ was only identified in *ERBB2*-amplified tumors, while a score 2+ was common among non-amplified cases. AR expression correlated negatively with *ERBB2* amplification (Fig 1B, 2B) ($p=0.001$, Wilcoxon rank-sum test).

	All cases n = 51	<i>ERBB2</i> Amplified n = 11	<i>ERBB2</i> Non-amplified n = 40
CLINICAL FEATURES			
Age at diagnosis (years)			
Median (IQR)	70 (58-76)	64 (57-72)	72.5 (60-76)
Sex			
Male	38 (75%)	7 (64%)	31 (78%)
Female	13 (25%)	4 (36%)	9 (23%)
M:F	2.9	1.75	3.4
Site			
Parotid gland	43 (84%)	9 (82%)	34 (85%)
Submandibular gland	6 (11%)	1 (9%)	5 (13%)
Other	2 (4%)	1 (9%)	1 (3%)
PROGNOSTIC FEATURES			
Angiolymphatic invasion	35 (74%)	7 (64%)	28 (70%)
Perineural invasion	34 (76%)	4 (36%)*	30 (75%)*
pN1+	40 (78%)	8 (73%)	32 (80%)
LN _s involved, Median (IQR)	4.5 (1-14)	6 (0-28)	4.5 (1-13)
IMMUNOHISTOCHEMICAL			

FEATURES			
Androgen Receptor			
Positive (>10%)	42 (83%)	5 (45%)	37 (93%)
Low positive (1-10%)	6 (12%)	5 (45%)	1 (3%)
Negative (<1%)	3 (6%)	1 (9%)	2 (5%)
Percent cells, mean (SD)	66% (37%)	26% (35%)**	77% (29%)**
Percent cells, median (IQR)	80% (28-95%)	5% (5-28%)	88% (79-99%)
HER2 strong circumferential staining			
Percent cells, mean (SD)	17% (35)	74% (38)	0 (0.9)
Percent cells, median (IQR)	0% (0-2)	95% (55-99)	0 (0-0)
HER2 ASCO/CAP 2018 Score			
3+	9 (19%)	9 (82%)	0
2+	25 (52%)	2 (18%)	23 (58%)
1+	8 (16%)	0	8 (20%)
0	5 (10%)	0	5 (13%)
Indeterminate	4 (8%)	0	4 (10%)
HER2 any staining			
Percent cells, mean (SD)	64% (38%)	96% (6%***)	55% (38%***)
Percent cells, median (IQR)	80% (15-95%)	99% (95-99%)	73% (10-90%)
HER2 staining pattern			
Membranous	43 (84%)	11 (100%)	32 (80%)
Granular	2 (4%)	0	2 (5%)
Granular and membranous	1 (2%)	0	1 (3%)
Cytoplasmic	1 (2%)	0	1 (3%)
Entirely negative, not applicable	4 (8%)		4 (10%)
ARCHITECTURAL PATTERN			
All invasive	22 (43%)	5 (45%)	17 (43%)
DCIS-like and invasive	25 (49%)	6 (55%)	19 (48%)
DCIS-like only	4 (8%)	0	4 (10%)
SD, standard deviation; IQR, interquartile range			
Percentages may not add to 100 due to rounding.			
*p=0.011, Fisher's exact test			
**p=0.001, Wilcoxon rank-sum test			
***p=0.00003, Wilcoxon rank-sum test			

Figure 1 - 826

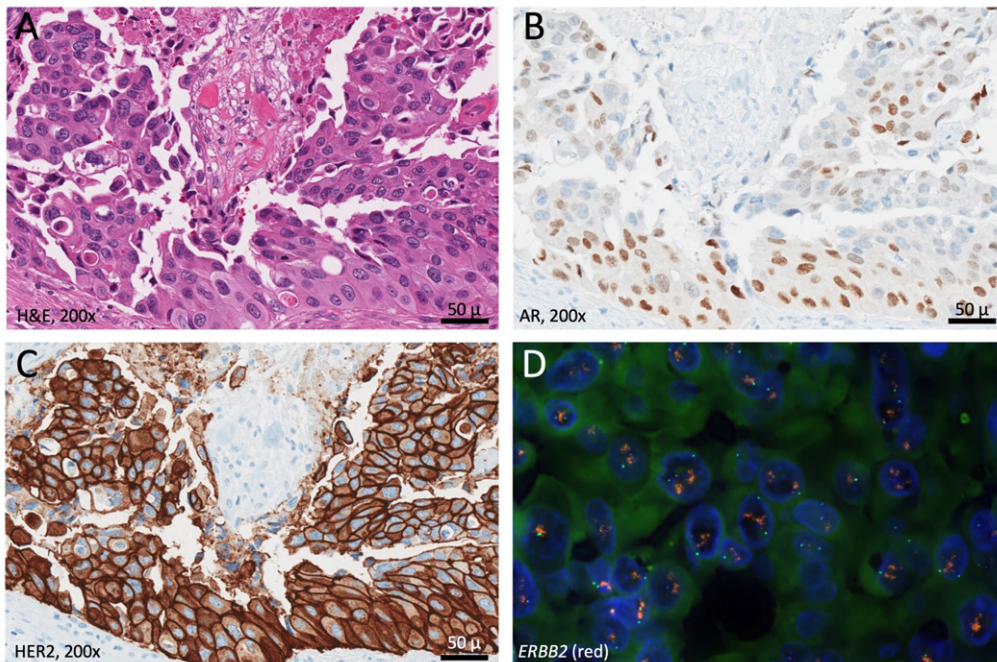
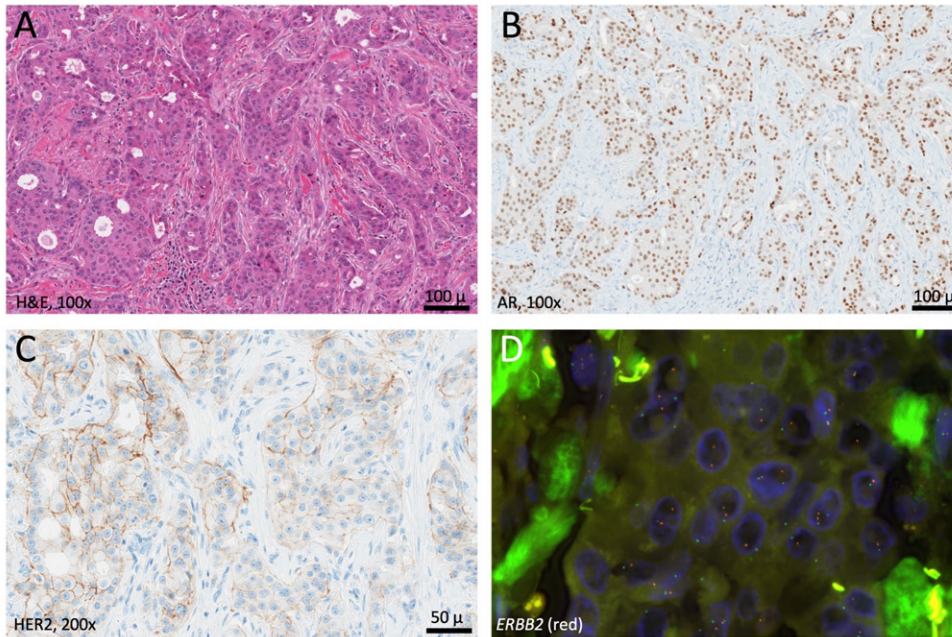


Figure 2 - 826



Conclusions: Complete strong circumferential (3+) HER2 IHC staining was only observed in *ERBB2*-amplified cases suggesting HER2 IHC is an appropriate surrogate marker for *ERBB2* gene status. Although most cases with 2+ staining were not *ERBB2*-amplified, the few amplified cases with 2+ staining support reflexive evaluation of such tumors with FISH. The inverse association between AR expression and *ERBB2*-amplification is intriguing and could suggest SDC subsets with different pathogenesis or disease biology, ultimately guiding treatment.

827 Sinonasal High Grade Neuroendocrine Carcinomas: A Clinicopathological and Immunohistochemical Re-Appraisal

Michael Mikula¹, Qiuying (Judy) Shi², Sam Sirotnikov³, Justin Bishop⁴, Lisa Rooper⁵

¹Johns Hopkins University, Baltimore, MD, ²Emory University, Atlanta, GA, ³Emory School of Medicine, Atlanta, GA, ⁴University of Texas Southwestern Medical Center, Dallas, TX, ⁵Johns Hopkins Hospital, Baltimore, MD

Disclosures: Michael Mikula: None; Qiuying (Judy) Shi: None; Sam Sirotnikov: None; Justin Bishop: None; Lisa Rooper: None

Background: Historically, sinonasal neuroendocrine carcinomas (NEC) were assumed to be analogous to NEC at other sites. However, recent studies have suggested that these tumors lack molecular hallmarks of other NEC, raising the possibility that they are a distinct group. Although some sinonasal NEC have been linked to high-risk human papillomavirus (HPV) and others show overlap with IDH2-mutant and SMARCA4-deficient carcinomas, the incidence of these drivers is unclear. This study aims to re-appraise the clinicopathologic and immunohistochemical features of sinonasal NEC to better understand their pathogenesis and classification.

Design: We identified 27 sinonasal carcinomas with diffuse neuroendocrine (NE) differentiation from 2 academic medical centers and the authors' consultation files. Tumors with non-NE components (i.e. mixed squamous cell) were excluded. All tumors were histologically classified as small cell NEC (SCNEC), large cell NEC (LCNEC), or high grade NEC not otherwise specified (HGNEC-NOS). We performed immunohistochemistry for AE1/AE3, synaptophysin, chromogranin, CD56, INSM1, Ki67, p16, IDH2, and SMARCA4 and RNA in-situ hybridization (ISH) for high-risk HPV as tissue availability permitted.

Results: Patients included 17 men and 10 women with a median age of 59 years (range 15-86); 5 (19%) were younger than 40 and 10 (56%) were never-smokers. There were 10 SCNEC (37%), 3 LCNEC (11%), 2 mixed SCNEC/LCNEC (7%) and 12 HGNEC-NOS (44%). All cases expressed AE1/AE3 (27/27, 100%) and at least one NE marker including INSM1 (15/15, 100%), CD56 (17/18, 94%), synaptophysin (24/27, 89%), or chromogranin (11/21, 52%); Ki67 ranged from 50-100%. 8/21 cases (38%)

overexpressed p16, 5/9 (40%) were positive for high-risk HPV RNA ISH, 2/12 (17%) expressed mutant IDH2, and 1/12 (8%) had SMARCA4 loss. Of 17 patients with follow-up (median 12 months), 6 (35%) died of disease and 7 (41%) are alive with disease.

Conclusions: Sinonasal NEC are a heterogeneous group including a significant subset of HPV-positive tumors and occasional cases that can be reclassified as IDH2-mutant or SMARCA4-deficient sinonasal carcinomas. Many remaining tumors do not fit into conventional SCNEC or LCNEC categories, and many patients lack common risk factors for developing NEC. These findings are concordant with molecular evidence that sinonasal NEC may be a unique category.

828 Recurrent MAPK Pathway Alterations Define a Subset of Warthin Tumors

Jeffrey Mito¹, Lynette Sholl², Vickie Jo³

¹Brigham and Women's Hospital, Boston, MA, ²Harvard Medical School, Boston, MA, ³Brigham and Women's Hospital, Harvard Medical School, Boston, MA

Disclosures: Jeffrey Mito: None; Lynette Sholl: *Consultant*, Genentech, Lilly; *Grant or Research Support*, Genentech; Vickie Jo: *Stock Ownership*, Merck and Co

Background: Warthin tumors (WT) are the second most common benign salivary gland neoplasm and are characterized by a distinct oncocytic epithelial component and lymphoid stroma. Despite a strong association with cigarette smoking, little is known about the pathogenesis of WT. Prior cytogenetic studies have shown few recurrent copy number changes in a subset of cases, but to our knowledge, no one has evaluated the landscape of somatic alterations by next generation sequencing (NGS).

Design: A cohort of 17 cases from 15 patients diagnosed as WT on surgical resection (n = 6) or fine needle aspiration (FNA) (n = 11) was identified. Cases were considered suitable for NGS with a minimum 30% estimated cellularity of the epithelial component. We utilized our institutional targeted sequencing platform which examines >300 cancer related genes for somatic mutations and copy number alterations. One FNA case showed a *CRTC1-MAML2* fusion. This case was reclassified as mucoepidermoid carcinoma and excluded from further analysis.

Results: In 16 WT samples from 14 patients, 5 somatic mutations were identified in 3 genes. Known oncogenic mutations in *KRAS* (3 of 16) and *BRAF* (1 of 16) were present in a subset. One additional case showed a truncating somatic mutation in *BCOR* (1 of 16). No somatic mutations were identified in the remaining 10 cases. No copy number alterations were identified.

Conclusions: In keeping with a benign neoplasm, our cohort demonstrated few somatic mutations and no copy number alterations in WT. Our data is reminiscent of prior array CGH studies that demonstrated a population of genomically stable WTs and a second group with limited copy number alterations. We identified a subset of cases with recurrent alterations in *KRAS* and a known activating mutation in *BRAF*. This data suggests a potential role for MAPK pathway activation in the tumorigenesis of WTs. Different (undetected) driver events may account for the WTs that lacked pathogenic alterations by the present targeted sequencing panel.

829 Revisiting Sinonasal Teratocarcinomas for the Diagnostic Congruity of SMARCA4 – a “New-Age Marker”

Neha Mittal¹, Swapnil Rane², Munita Bal², Katha Rabade², Asawari Patil³

¹Tata Memorial Hospital, Mumbai, India, ²Tata Memorial Centre, Mumbai, India, ³ACTREC-Tata Memorial Centre, Thane, India

Disclosures: Neha Mittal: None; Swapnil Rane: None; Munita Bal: None; Katha Rabade: None; Asawari Patil: None

Background: Sinonasal teratocarcinomas (SNTCS) harbor a unique combination of teratomatous and malignant epithelial and mesenchymal elements. Recent molecular underpinnings revealed bi-allelic somatic inactivation of SMARCA4 (BRG1), with a corresponding immuno-negativity for SMARCA4 by immunohistochemistry(IHC).

Design: All the diagnosed cases of SNTCS 2008-till date were subjected to SMARCA4 IHC,(SMARCA4/anti BRG1, Abcam, clone EPNCIR111A) following a review of clinico-pathological findings.

Results: A total of 58 patients (50 male, 8 female, M:F= 6.25:1) diagnosed as SNTCS (6 cases each of recurrent and metastatic) with an age range of 16-91 years (mean,45.7; median, 45 years) were evaluated. Salient clinic-radiological findings were symptoms of nasal obstruction and bleeding in 72.8%, naso-ethmoid origin in 100%, cribriform plate erosion in 56.8%, and intracranial extension in 34.5% patients. On histology, nodular pattern with a malignant neuroectodermal/neuroendocrine component admixed with benign glandular epithelium in 100% cases, fetal-type squamous cells in 54%, squamous carcinoma, and adenocarcinoma in 3.4% and 5.17% respectively. Rhabdomyosarcomatous differentiation was seen in 65%, undifferentiated sarcoma (3.4%), and osteosarcoma-like areas in 1.72% cases. Teratomatous components were seen in 75% of recurrent and 55.6% of metastatic cases as well. Of the 50 cases in which SMARCA4 IHC was performed, 34 showed complete loss(68%), 9 (18%) partial loss, and 7 (14%) showed retained expression of SMARCA4. Cases with complete loss showed loss of staining in all three components (teratomatous, stromal, and epithelial), with a 100% correlation between biopsy and resected specimens, and pre-and post-chemotherapy samples for the pattern of loss of SMARCA4 staining. One case showed heterogeneity with complete loss in neuroectodermal areas and partial loss in sarcomatous areas. All but one case of partial SMARCA4 loss had rhabdomyosarcomatous differentiation. SMARCB1/INI1 was retained in all cases (n=20). In addition, Pan-CK and synaptophysin were positive in 100% cases, albeit to varying degrees; NUT and p16 were negative (n=16).

Parameter	SNTCS cases
1. Benign glands	58(100%)
2. Benign fetal-like squamous cells	31(54%)
3. Malignant round cell component(RC)	58(100%)
4. Fibrocellular mesenchyme	50(93.3%)
5. Rhabdomyosarcomatous differentiation	38(65%)
6. Cartilage	2 (3.4%)
7. Smooth muscle	2 (3.4%)
8. Osteosarcoma-like	1(1.72%)
9. Glial areas	2 (3.4%)
10. CK/AE1/AE3- RC component	58(100%) (dot-like positivity, cytoplasmic in glands)
11. SMARCA4 immunohistochemistry	Complete Loss= 34 (68%) Partial loss =9 (18%) Retained =7 (14%)
12. P40 in Squamous component	30 (54%)
13. Neuroendocrine marker positivity (synaptophysin, chromo, CD56)	58(100%)
14. NUT IHC	0/15 (0%)
15. Desmin in mesenchymal component	38 (65%)
16. Myogenin	8(13.8%)
17. Multimodality therapy	30/50 (60%)
18. Recurrence/ Locoregional metastasis	8 cases
19. Distant metastasis	6 cases

Conclusions: Naso-ethmoid mass in a male with divergent differentiation on histology and a characteristic immunonegativity (complete or partial) for SMARCA4 defines SNTCS. SMARCA4 loss was seen in 86% cases. SMARCA4 immunohistochemistry is a useful addition to the panel of IHC markers in sinonasal tumors, especially for the diagnosis of SNTCS in small biopsies.

830 CDKN2A/B Loss in High-Grade Transformation of Salivary Gland Carcinoma: High-Grade Malignant Potential in Histologically Low-Grade Component

Masato Nakaguro¹, William Faquin², Matija Snuderl³, Zubair Baloch⁴, Richard Cantley⁵, Margaret Compton⁶, Kim Ely⁶, Brittany Holmes⁷, Rong Hu⁸, Darcy Kerr⁹, Kathleen Montone¹⁰, Michiya Nishino¹¹, Liron Pantanowitz¹², Esther Rossi¹³, Toshitaka Nagao¹⁴, Peter Sadow²

¹Nagoya University Hospital, Nagoya, Japan, ²Massachusetts General Hospital, Harvard Medical School, Boston, MA, ³New York University, New York, NY, ⁴Hospital of the University of Pennsylvania, Philadelphia, PA, ⁵Michigan Medicine, University of Michigan, Ann Arbor, MI, ⁶Vanderbilt University Medical Center, Nashville, TN, ⁷Stanford Medicine/Stanford University, Los Altos, CA, ⁸University of Wisconsin School of Medicine and Public Health, Madison, WI, ⁹Dartmouth-Hitchcock Medical Center, Geisel School of Medicine at Dartmouth, Lebanon, NH, ¹⁰University of Pennsylvania, Philadelphia, PA, ¹¹Beth Israel Deaconess Medical Center, Harvard Medical School, Boston, MA, ¹²University of Michigan, Ann Arbor, MI, ¹³Fondazione Policlinico Universitario Agostino Gemelli IRCCS-Università Cattolica del Sacro Cuore, Rome, Italy, ¹⁴Tokyo Medical University

Disclosures: Masato Nakaguro: None; William Faquin: None; Matija Snuderl: None; Zubair Baloch: None; Richard Cantley: None; Margaret Compton: None; Kim Ely: None; Brittany Holmes: None; Rong Hu: None; Darcy Kerr: None; Kathleen Montone: None; Michiya Nishino: None; Liron Pantanowitz: None; Esther Rossi: None; Toshitaka Nagao: None; Peter Sadow: None

Background: High-grade transformation (HGT) is a process whereby conventional low- to intermediate-grade salivary gland carcinomas (SGC) transform into high-grade carcinomas with variable loss of their original histologic features. It is unclear whether there are common pathogenic pathways in HGT. Here, we performed histologic, immunohistochemical and copy number analysis in a large series of SGCs with HGT.

Design: Thirty-four HGT cases were retrieved from institution cases and consultation files (acinic cell carcinoma [AcCC], 15 cases; adenoid cystic carcinoma [AdCC], 14 cases; epithelial-myoepithelial carcinoma [EMC], 5 cases). A component of conventional tumor (low-grade: LG) and a high-grade component (HG) were analyzed separately. Fourteen conventional salivary gland carcinomas without HGT were also selected from institution cases. Histologic evaluation and immunohistochemical staining for p53 and Ki-67 were performed. Using extracted DNA from formalin-fixed paraffin-embedded sections, copy number analysis was performed.

Results: The patients were 24-87 years old (mean 63.4 years), and the male/female ratio was 18:15. The most frequent primary site was parotid gland (55%). Necrosis, bizarre nuclei, brisk mitotic activity, perineural invasion, and lymphovascular invasion was observed in 53%, 21%, 36%, 72%, and 53% of the cases, respectively. Diffuse and strong p53 expression suggesting a *TP53* mutation was detected in the HG component of 5 HGT cases (15%) (Fig. 1). Ki-67 labelling index (LI) was higher in the HG component than the LG component (44% vs 10%, P=0.00), and, in AcCC, the Ki-67 LI of the LG component was higher than in conventional AcCC cases (12% vs 2.4%, P=0.048, Fig. 2a). *CDKN2A/B* loss was identified in both the LG and HG components in 8 HGT cases (40%), and in the HG component in 1 case (5%) (Fig. 2b). *CDKN2A/B* loss was not detected in conventional tumors without HGT.

Figure 1 - 830

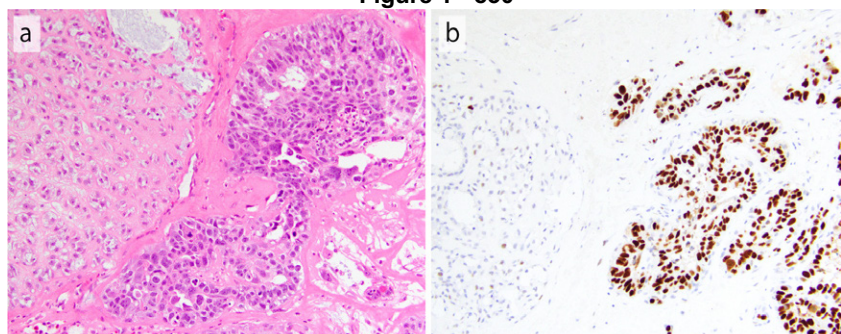


Figure 1:
(a) High-grade transformation (right) of epithelial-myoepithelial carcinoma (left). (b) Diffuse and strong p53 immunoreactivity in high-grade component.

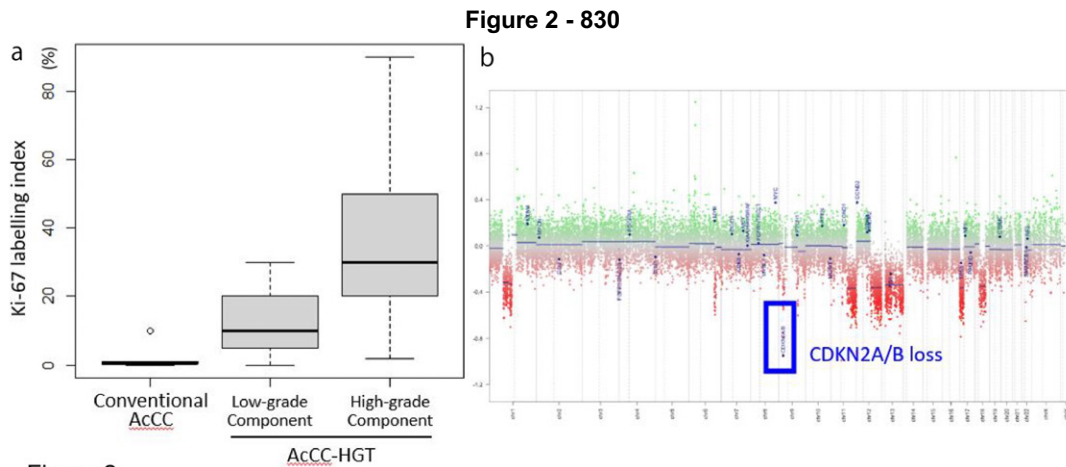


Figure 2: (a) Ki-67 labelling index of conventional acinic cell carcinoma (AcCC) and AcCC with high-grade transformation (HGT). (b) CDKN2A/B loss in AcCC with HGT.

Conclusions: *TP53* mutation appears to contribute to HGT in a subset of SGCs, but alternative pathways are also likely. The presence of *CDKN2A/B* loss and higher Ki-67 LI in the LG component may represent an early step in HGT.

831 Primary Mucoepidermoid Carcinoma of the Thyroid: Perspectives from Institutional and Population-Level Data

Tam Ngo¹, Truong Nguyen², Mitsuyoshi Hirokawa³, Kennichi Kakudo⁴, Huy Vuong⁵
¹Pham Ngoc Thach University of Medicine, Ho Chi Minh, Vietnam, ²Cho Ray Hospital, ³Kuma Hospital, Kobe, Japan, ⁴Izumi City General Hospital, ⁵Oklahoma University Health Sciences Center, Oklahoma University, OK

Disclosures: Tam Ngo: None; Truong Nguyen: None; Mitsuyoshi Hirokawa: None; Kennichi Kakudo: None; Huy Vuong: None

Background: Mucoepidermoid carcinoma (MEC) is the most common salivary gland malignancy, accounting for less than 10% of all tumors of the salivary gland. Primary MEC of the thyroid is a very rare entity. This study aimed to investigate demographic, clinical, histopathological features and prognostic outcomes of MEC.

Design: We searched for MEC in our institutional databases and the Surveillance, Epidemiology, and End Result (SEER) database. We retrospectively enrolled 5 from our institutional databases.

Results: The median age of MEC subjects was 66 years (interquartile range (IQR), 54 to 80 years; range, 44 to 89 years), and all cases were females. The mean tumor size at presentation was 51.3 ± 12.8 with a range of 38 to 65 mm. Histopathologically, tumors were composed of varying proportions of epidermoid, intermediate, and mucous cells which were positive with alcian blue staining. Three cases were noted to have a mixture of eosinophils. The extrathyroidal extension was found in three patients whereas nodal/ distant metastases were absent in all cases. Hashimoto thyroiditis was the most common associated lesion accompanying with MEC. Immunohistochemically, most cases were positive for CK, TTF1, and PAX8 whereas thyroglobulin was not expressed in any cases. Mitoses were rare and the median Ki67 index was 2%. Three patients underwent total thyroidectomy, and two patients underwent subtotal thyroidectomy. Neoadjuvant radiotherapy was administered in two patients, while no patients received neoadjuvant chemotherapy. After a median follow-up of 64.5 months (IQR, 19.3-191.5), 4 patients were alive and 1 patient died of disease at 6 months of follow-up. Further, from the SEER database, we also identified 45 MEC patients. Integrating with the institutional data, our multivariable analysis found that age was a significant predictor of all-cause mortality (HR, 1.06, 95% CI, 1.01-1.12, $p = 0.01$). Noticeably, receiving chemotherapy (HR, 1.98, 95% CI, 0.26-15.1, $p = 0.51$) and radiation (HR, 1.06, 95% CI, 0.40-2.83, $p = 0.91$) were not significantly associated with clinical outcome.

Conclusions: Our study reported the clinical and histopathological characteristics, and prognostic outcomes of MEC of the thyroid. Combining with data from the SEER database, age has been found as the only important predictor of mortality in MEC patients.

832 MAPK Activation is Associated with BRAF V600E Protein Expression in Ameloblastoma but Occurs in a BRAF-independent manner in Ameloblastic Fibroma and Ameloblastic Fibro-Odontoma

Kyu-Young Oh¹, Ji-Hoon Kim¹, Sung-Dae Cho¹, Hye-Jung Yoon¹, Jae-Il Lee¹, Seong-Doo Hong¹
¹Seoul National University School of Dentistry and Dental Research Institute, Seoul, South Korea

Disclosures: Kyu-Young Oh: None; Ji-Hoon Kim: None; Sung-Dae Cho: None; Hye-Jung Yoon: None; Jae-Il Lee: None; Seong-Doo Hong: None

Background: Although several types of odontogenic tumors (OTs) share the same BRAF V600E mutation, its effects on the MAPK pathway in each tumor type are not well studied. This study aimed to determine the association between MAPK activation and BRAF V600E mutations at the gene and protein levels in OTs.

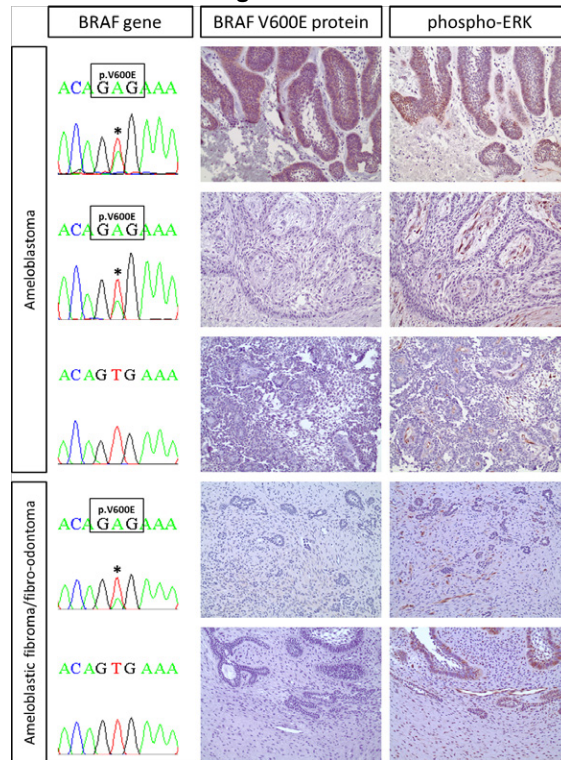
Design: A total of 32 OTs included in this study consisted of 16 ameloblastoma and 16 benign mixed OTs (9 ameloblastic fibroma and 7 ameloblastic fibro-odontoma). Sanger sequencing was performed to detect mutations in exon 15 of the *BRAF* gene. BRAF V600E protein expression and MAPK activation were investigated by immunohistochemistry using antibodies against VE1 and phospho-extracellular signal-regulated kinase (p-ERK), respectively. The associations of p-ERK expression with BRAF mutation status and VE1 expression were analyzed by Fisher exact test.

Results: BRAF V600E mutations were observed in 12/16 (75.0%) ameloblastomas and 6/16 (37.5%) benign mixed OTs. Of the 12 BRAF^{V600E}-ameloblastomas, VE1 expression was confirmed in nine cases, while all six BRAF^{V600E}-benign mixed OTs were VE1-negative. Half of all ameloblastomas showed high p-ERK expression, which was significantly associated with VE1 expression ($P=0.041$) but not with BRAF gene mutation status ($P=0.569$). In benign mixed OTs, BRAF V600E mutations were not associated with p-ERK expression in both epithelial (p-ERK-high in 43.8%; $P=0.633$) and mesenchymal (p-ERK-high in 50.0%; $P=1.000$) components.

Tumor type	Component	p-ERK	BRAF gene			BRAF V600E protein		
			WT	V600E	P	Neg	Pos	P
Ameloblastoma	Epithelial	Low	3	5	0.569	6	2	0.041*
		High	1	7		1	7	
AF & AFO	Epithelial	Low	5	4	0.633	9	0	NA
		High	5	2		7	0	
	Mesenchymal	Low	5	3	1.000	8	0	NA
		High	5	3		8	0	

AF, ameloblastic fibroma; AFO, ameloblastic fibro-odontoma; NA, not analyzable; Neg, negative; Pos, positive; WT, wild-type.

Figure 1 - 832



Conclusions: These findings suggest that BRAF V600E mutations may lead to MAPK activation in a BRAF V600E protein-related manner in ameloblastoma. In contrast, MAPK can be activated irrespective of BRAF mutations in ameloblastic fibroma and ameloblastic fibro-odontoma.

833 Molecular Characterization of Secretory Myoepithelial Carcinoma (SMCA)

Simmi Patel¹, Abigail Wald², Jassem Bastaki³, Aatur Singhi², Raja Seethala⁴

¹University of Pittsburgh Medical Center Presbyterian Shadyside, PA, ²University of Pittsburgh Medical Center, Pittsburgh, PA, ³Ministry of Health of Kuwait, Kuwait, ⁴University of Pittsburgh School of Medicine, Pittsburgh, PA

Disclosures: Simmi Patel: None; Abigail Wald: None; Jassem Bastaki: None; Aatur Singhi: *Consultant*, Foundation Medicine; Raja Seethala: None

Background: SMCA are rare, mucin producing myoepithelial tumors that characteristically show a signet ring morphology. While many mucinous/secretory salivary gland entities have now been molecularly characterized (i.e. *SS18* fusions in microsecretory adenocarcinoma, and *AKT1* mutations in mucinous adenocarcinomas), key drivers in SMCA have yet to be elucidated. Here, we report molecular features on four SMCA cases.

Design: Total nucleic acid from four SMCAs (all previously *ETV6*, *EWSR1*, and *ALK1* fusion negative) was evaluated using a targeted 161 gene panel OncoPrint™ Comprehensive Assay v3 using Ion Torrent™ next generation sequencing (NGS) platform (ThermoFisher Scientific). Additional immunohistochemical studies (including: p53, PTEN, and NKX 3.1) and (breakapart) fluorescence in situ hybridization for *SS18* (*SYT*) rearrangements were performed using established methodologies.

Results: Clinicopathologic features and ancillary findings are summarized in Table 1. All cases were strongly positive for NKX3.1, a homeodomain transcription factor required for minor salivary development that is strongly expressed in normal mucous acini. Case 1 failed OncoPrint due to possible tissue degradation. Case 2 failed hybridization but the other 3 cases were negative for *SS18* rearrangements. NGS was successful in two cases (Cases 3 and 4). Case 3 demonstrated a *PTEN* c.655C>T p.Q219* mutation and a *SEC16A/NOTCH1* fusion, which was previously reported in breast carcinoma. Case 4 (the only case with nodal metastasis) demonstrated a *PTEN* c.1026+1G>A p.K342 splice variant, *TP53* c.524G>A p.R175H mutation and a fairly high tumor

mutation burden of 29 per Mb. Both cases 3 and 4 also showed PTEN loss by immunohistochemistry (IHC), while cases 1 and 2 showed retention. Case 4 also showed focal strong staining for p53.

Table 1. Summary of clinicopathologic features and ancillary findings

Case #	Age	Sex	Site	Tumor Size (cm)	Nodal Status	IHC	SS18 (SYT) FISH	Molecular Features
1	18	M	Left buccal	4.5	-	PTEN retention	Negative	n/a
2	81	F	Left deep parotid	2.0	-	PTEN retention	n/a	n/a
3	61	M	Left buccal	n/a	-	PTEN loss	Negative	<i>PTEN</i> c.655C>T p.Q219* mutation; <i>SEC16A/NOTCH1</i> fusion
4	65	M	Left soft palate	1.5	+	PTEN loss; p53 (focally +)	Negative	<i>PTEN</i> c.1026+1G>A p.K342 splice variant, <i>TP53</i> c.524G>A p.R175H mutation

Conclusions: The frequency of *PTEN* mutations in SMCA suggests some commonality with salivary mucinous adenocarcinomas given the shared alterations of the PTEN/PI3K/AKT pathway. Strong NKX3.1 expression suggests that SMCA may recapitulate a mucous acinar phenotype. One aggressive case shows some molecular features of progression. We document the first extramammary tumor with *SEC16A/NOTCH1* fusion.

834 INSM1 Staining in SNUC and SMARCB1-deficient Carcinoma in the Absence of Other Neuroendocrine Markers

Ashley Patton¹, Abberly Lott Limbach²

¹The Ohio State University Wexner Medical Center/James Cancer Hospital, Columbus, OH, ²The Ohio State University Wexner Medical Center, Columbus, OH

Disclosures: Ashley Patton: None; Abberly Lott Limbach: None

Background: Insulinoma-associated protein 1 (INSM1) has been suggested as a novel marker for neuroendocrine differentiation in a variety of anatomic locations including the head and neck. However, the utilization of INSM1 as a stand-alone marker in the diagnostic evaluation of neuroendocrine differentiation in undifferentiated tumors of the head and neck has not been well elucidated. There is emerging literature that INSM1 may stain tumors without neuroendocrine differentiation, leading to confusion and the performance of additional immunostains. The present study evaluates the staining pattern of INSM1 in a series of sinonasal undifferentiated carcinomas (SNUC) and SMARCB1-deficient carcinomas in conjunction with chromogranin and synaptophysin.

Design: There were 27 cases of SNUC and 9 cases of SMARCB1-deficient carcinoma identified. SNUC cases were verified by the retention of INI-1 and a panel of immunostains. SMARCB1-deficient carcinoma cases were verified by loss of INI-1 expression. The cases were reviewed for confirmation of diagnosis and block selection. Immunoreactivity for INSM1, chromogranin, and synaptophysin was evaluated in both tumors using histoscores (H-score) which were calculated based on intensity of INSM1 staining and percentage of positive tumor cells.

Results: Table 1 demonstrates the distribution of H-scores of INSM1 staining in both tumor types (Figure 1). Diffuse, low-intensity nuclear staining of INSM1 in tumor cells of both SNUC and SMARCB1-deficient carcinoma was seen. INSM1 staining was observed in the absence of synaptophysin and chromogranin positivity (Figure 2). Of note, focal to diffuse, low-intensity nuclear staining was observed in nontumor cells of the uninvolved epithelium and submucosa in both SNUC and SMARCB1-deficient carcinoma.

Table 1. SNUC and SMARCB1-deficient carcinoma display immunoreactivity for INSM1. Histoscores (H-scores) were determined for INSM1 staining to reveal moderate intensity INSM1 staining in both SNUC and SMARCB1-deficient carcinoma. Significance was determined using an unpaired t-test ($p < 0.05$).

Histological Type	No. of Patients	H-Score		Negative or Weak Intensity (0-100)		Moderate Intensity (101-200)		Strong Intensity (201-300)		P - value
		Mean	STDEV	No.	%	No.	%	No.	%	
SNUC	27	144	89	16	59%	7	26%	4	15%	0.68
SMARCB1-Deficient	9	133	87	6	67%	2	22%	1	11%	

Abbreviations: Sinonasal undifferentiated carcinoma, SNUC; SWI/SNF related, matrix associated, actin dependent regulator of chromatin, subfamily B, member 1, SMARCB1, deficient carcinoma; insulinoma-associated 1, INSM1

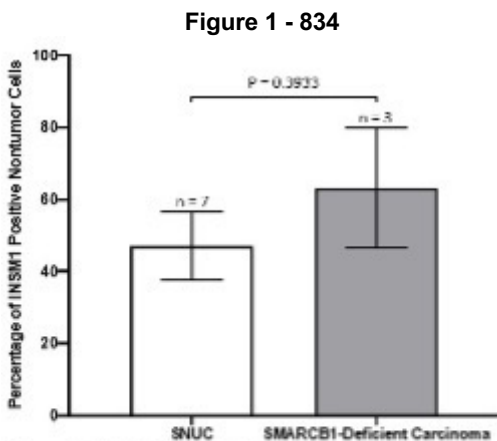


Figure 1. INSM1 demonstrates nonspecific staining of nontumor cells in both SNUC and SMARCB1-deficient carcinoma. Semiquantitative analysis of INSM1 immunoreactivity in nontumor cells in both SNUC and SMARCB1-deficient specimens was evaluated. Significance was determined using an unpaired t-test ($p < 0.05$).

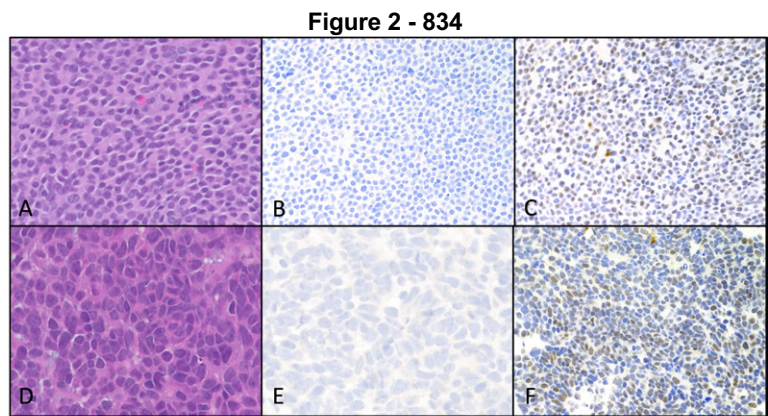


Figure 2: Neuroendocrine stains in sinonasal tumors. A. SMARCB1-deficient carcinoma, H&E, 40x. B. SMARCB1-deficient carcinoma, synaptophysin, 40x. C. SMARCB1-deficient carcinoma, INSM1, 40x. D. SNUC, H&E, 40x. E. SNUC, synaptophysin, 40x. F. SNUC, synaptophysin, 40x.

Conclusions: Our data suggest that INSM1 staining alone should be interpreted with caution to evaluate potential neuroendocrine differentiation in the diagnostic work-up of undifferentiated tumors of the head and neck. This is especially true in the absence of additional neuroendocrine markers such as synaptophysin or chromogranin. Care should be used when there is weak INSM1 staining or staining of background structures which are normally not considered to have neuroendocrine differentiation.

835 Immunophenotypic Analysis for the Reclassification Of Undifferentiated/Poorly Differentiated Carcinoma in the Sinonasal Tract

Tanya Sajan Ponnatt¹, Kelly Magliocca¹, Daniel Lubin², Scott Steward-Tharp¹, Xiaoqi Lin³, Azeem Kaka¹, Qiuying (Judy) Shi¹

¹Emory University, Atlanta, GA, ²Emory University Hospital, Atlanta, GA, ³Northwestern University, Chicago, IL

Disclosures: Tanya Sajan Ponnatt: None; Kelly Magliocca: None; Daniel Lubin: None; Scott Steward-Tharp: *Advisory Board Member*, Elsevier; Xiaoqi Lin: None; Azeem Kaka: None; Qiuying (Judy) Shi: None

Background: Sinonasal undifferentiated (SNUC) /poorly differentiated carcinomas (PDC) are aggressive neoplasms and are often challenging to diagnose. Molecular profiling of SNUC has resulted in the identification of a few distinct subentities, such as INI1/SMARCB1 deficient, NUT (midline), BRG1/SMARCA4 deficient, and IDH-mutant sinonasal carcinomas. We tried to reclassify SNUCs/PDCs by immunohistochemistry.

Design: 40 cases meeting the criteria for SNUC/PDC were selected from the Department’s archives between 2008-2020. The patients had an age range between 21-84 years old, with a mean of 52.5 years old and a 1.7:1 male to female ratio. This Cohort was composed of 7 SNUC, 8 PDC, 6 PDC with neuroendocrine differentiation (NED), 6 PDC favoring high grade neuroendocrine carcinoma (HG NEC), 5 PDC with glandular architecture (GA), and 8 PDC with squamous differentiation (SQD). Three sets of tissue microarrays (TMA) containing 121 cores (triplet of each case) were constructed from paraffin embedded tissue blocks at the Winship core lab. A panel of immunostains (AE1/AE3, p40, p63, synaptophysin, chromogranin, CD56, S100, NUT-1, INI-1, BRG-1, CD99, NSE, INSM1 and IDH2) were performed on the TMA sections with appropriate positive and negative controls.

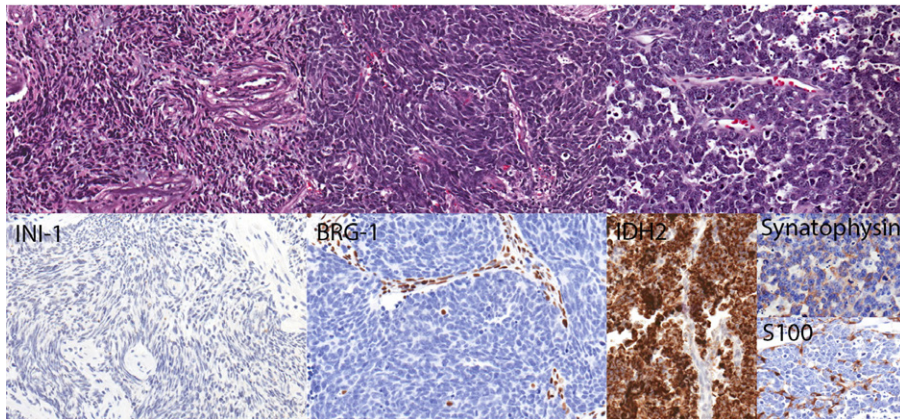
Results: Reclassification of these tumors is listed in Table 1 based on immunohistochemical results. There were 3 SMARCB1 deficient carcinomas and 2 SMARCA4 deficient carcinomas with the latter showing either synaptophysin immunoreactivity or focal positivity in other neuroendocrine markers. Seven IDH2 mutated carcinomas were identified with at least one positive neuroendocrine marker present and a sustentacular-like pattern of S100 positivity in 3 of the 4 cases (Fig. 1). Six favoring HG NEC were confirmed by at least two positive neuroendocrine markers and one of them had INI-1 loss identified. All cases were reclassified as PDC with NED showing at least one or focal positive neuroendocrine markers. All cases were NUT-1 and CD99 negative.

Table 1. Reclassification of SNUC and PDC based on immunostaining results

Original Diagnosis	No.	Reclassification	No.
SNUC	7	SNUC	3
		IDH2	4
PDC	8	PDC	4
		IDH2	1
		UC+NED	1
		UC+NED+SQD	2
PDC+NED	6	PDC+NED	3
		IDH2	1
		SMARCA4	2
PDC favoring HG NEC	6	HG NEC	5
		SMARCB1	1
PDC+Glandular Architecture	5	PDC	2
		SMARCB1	1
		PDC+NED	2
PDC+Squamous Differentiation	8	PDC+SQD	2
		PDC+NED+SQD	4
		IDH2	1
		SMARCB1	1

Figure 1 - 835

Fig. 1. Representative H&E with corresponding immunostaining for INI-1 and BRG1 deficient carcinoma and IDH2 mutated carcinoma on TMA.



Conclusions: The deficiency of SMARCB1 and SMARCA4 tumor suppressor genes and IDH2 mutations appear to be involved in the pathogenesis of subsets of sinonasal carcinomas. Detection of loss of SMARCB1 or SMARCA4 expression and expression of IDH2 by immunohistochemistry may play a significant role in the management of these highly aggressive tumors with targeted therapies. Diagnosing HG NEC by IHC could also be a useful guide in managing these tumors.

836 Sinonasal Tumors with Overlapping Neuroblastic and Epithelial Features Have Recurrent CTNNB1, SWI/SNF, and PPP2R1A Mutations: Validating the Concept of a True Olfactory Carcinoma?

Lisa Rooper¹, Jeffrey Gagan², Michiya Nishino³, Justin Bishop⁴

¹Johns Hopkins Hospital, Baltimore, MD, ²UT Southwestern Medical Center, Dallas, TX, ³Beth Israel Deaconess Medical Center, Harvard Medical School, Boston, MA, ⁴University of Texas Southwestern Medical Center, Dallas, TX

Disclosures: Lisa Rooper: None; Jeffrey Gagan: None; Michiya Nishino: None; Justin Bishop: None

Background: Sinonasal tumors that have morphologic features of olfactory neuroblastoma but show diffuse cytokeratin expression and gland formation are challenging to classify. Although often called olfactory carcinoma, it is unclear whether these tumors truly comprise a unique sinonasal carcinoma category or simply represent olfactory neuroblastomas with divergent epithelial differentiation. Recently, molecular analysis has clarified the pathogenesis of other high grade sinonasal tumors with neuroendocrine or neuroectodermal features. We aim to evaluate the molecular underpinnings of olfactory carcinomas to facilitate better classification.

Design: We identified 7 olfactory carcinomas from the authors' pathology archives and consultation files. For inclusion, we required tumors to show morphologic similarity to olfactory neuroblastoma and immunohistochemical evidence of neuroendocrine differentiation but also to display diffuse cytokeratin positivity and gland formation. Tumors with stromal elements were excluded. All cases underwent next generation sequencing (NGS) on the Illumina NextSeq 550 using a custom panel including all exons from >1425 cancer-related genes.

Results: The olfactory carcinomas arose in the superior nasal cavity of 6 men and 1 woman with a median age of 41 years (range 19-72). All 7 cases expressed synaptophysin and displayed nested growth and vascular stroma reminiscent of olfactory neuroblastoma with neurofibrillary stroma and rosette formation in 4 cases each. However, all 7 cases also were diffusely positive for AE1/AE3 and displayed well-formed glands, with cilia in 6 cases. On NGS, 4 cases had *CTNNB1* gene alterations, including missense mutations in 3 cases and copy number loss in 1 case; 1 case had concomitant *SMARCA4* inactivation and 1 also had *SMARCB1* mutation. 2 cases displayed *PPP2R1A* missense mutations and 1 had *ARID1A* deletion.

Conclusions: The majority of olfactory carcinomas show *CTNNB1* gene alterations, with frequent additional SWI/SNF complex mutations. These mutations are not known to be recurrent genetic events in olfactory neuroblastoma but have previously been implicated as common drivers of sinonasal neuroendocrine carcinomas and teratocarcinosarcoma, suggesting that olfactory

carcinoma is more closely related to these latter lesions and likely merits recognition as a sinonasal carcinoma. Recurrent mutations in *PPP2R1A* may play a parallel pathogenic role activating the Wnt pathway in *CTNNB1* wild type cases.

837 Characterization of the Diversity in the Lymphoid and Myeloid Lineage Cell Subsets from Premalignant Oral Lesion Cells versus Head and Neck Squamous Cell Carcinoma (HNSCC): The Peripheral Blood Immune Cell Profile

Sonia Sanadhya¹, John Basile¹, Dean Mann²

¹University of Maryland Baltimore, School of Dentistry, Baltimore, MD, ²University of Maryland Medical School of Medicine, Baltimore, MD

Disclosures: Sonia Sanadhya: None; John Basile: None; Dean Mann: None

Background: Head and neck squamous cell carcinoma (HNSCC) is known to be associated with an abnormal T cell immunoregulation. The immunologic milieu of the oral preneoplastic lesions needs to be explored in more detail to intercept precancerous lesions that are at high risk for progression to cancer and to overcome the immune escape mechanisms employed by cancers.

Design: We aimed to investigate the impact of mediators from oral premalignant lesion cells versus oral carcinoma cells on the phenotype of peripheral blood mononuclear cells (PBMCs) from healthy donors. Cells were cultured from human dysplastic oral mucosa, oral cancer and normal oral keratinocytes (NOKs) followed by collection of 96-hour supernatants and cytokine assessment by ELISA. PBMCs were cultured with these supernatants in 6-well tissue culture plates at 1 X 10⁶ cells/well for 72 hours at 37°C and flow cytometry was performed.

Results: We found that IL-6, IL-8 and IL-1β were profoundly elevated in the premalignant cell supernatants compared to HNSCC and NOK cells. Additional inflammatory cytokines IL-17, IL-23, TNF-alpha, GM-CSF, IFN-γ and immune suppressive cytokines IL 10 and IL-4 were below detection limits. These results confirm a less subversive and a varied premalignant immune landscape.

The total percentage population of CD3⁺, CD4⁺, CD8⁺ T cells was significantly decreased in presence of HNSCC cell conditioned media compared to premalignant and NOK cells. Interestingly at 20% the ratio of CD4⁺ and CD8⁺ T cells was nearly equal in cancer cells. A trend towards elevated percentages of myeloid cell populations CD14, CD19, CD38 was noted at 40% of HNSCC conditioned media. CD11C⁺ dendritic cells had a higher proportion in premalignancy.

PBMCs cultured with 10% and 20% of conditioned media from cancer cell lines exhibited an increased expression of total HLADR however there was a depletion at 40%. Increased percentages of dual HLADR⁺ CD3⁺ T cells were noted at all concentrations of malignant conditioned media versus preneoplastic cells. Furthermore, premalignant secretome induced a consistently greater expression of activation markers CD69, CD86 at all concentrations compared to HNSCC cells.

Comparison table for various markers at different concentrations of Supernatants for all cell lines								
Total Population	(Control) PBMCs only		Premalignant cells (DOK)		Malignant Cells (HN12)		Normal oral Keratinocytes (NOKs)	
	10%	40%	10%	40%	10%	40%	10%	40%
Lineage Markers								
CD3	78%	73.80%	70%	63%	51%	60%	80%	75.30%
CD14	7%	7.15%	18%	16.06%	11.37%	23.00%	4%	10.47%
CD11C	8%	10.30%	22.30%	24.60%	14%	21.22%	12.81%	10.52%
CD19	6%	4.20%	12%	9%	10.78%	15.15%	4%	7.24%
CD38	4%	14.20%	9.42%	8.80%	18.54%	20.86%	12.81%	7.75%
T- cell Subclass								
CD4	56%	48.95%	45.50%	39.06%	32%	40%	58.93%	46.80%
CD8	27%	24.83%	38.59%	30.84%	17.26%	33%	27.68%	35.41%
Activation Markers								
CD80	2.19%	1.46%	1.69%	4.80%	2.33%	9.64%	1.37%	1.65%
CD83	2%	15.64%	8%	4.88%	8%	11.10%	2.73%	3%
HLADR	75%	96.00%	38.30%	26.64%	66.10%	48.20%	90%	34.80%
CD86	31.50%	8.70%	18.38%	37%	11.07%	35.20%	24%	12.48%
CD69	78%	52.32%	48.20%	46.70%	44.50%	39%	60.23%	52.10%
CD25	4%	5%	5.47%	12.72%	10%	10.60%	4.08%	3.35%
Immune checkpoints								
PD-1	0.14%	1.00%	13%	16.80%	16%	20.84%	0.47%	1.68%
TIM-3	0.79%	3.85%	3.74%	15.26%	4.49%	29.41%	0.89%	2%

Conclusions: Our data suggests that although the premalignant immune landscape is more proinflammatory, increased expression of HLADR⁺ CD3⁺lymphocytes and myeloid cells in HNSCC are an index of systemic immune activation and could rescue the dampened immune status by regimes targeted at monitoring and augmenting these markers.

838 LRP1B May be an Important Suppressor Gene in the Transition of Pleomorphic Adenoma to Carcinoma Ex Pleomorphic Adenoma

João Scarini¹, Erika Egal², Sheila Nagamatsu¹, Luciana Mofatto¹, Rodrigo Maioral¹, Reydson de Lima-Souza¹, Marcelo Carazzolle¹, Luiz Coutinho³, Luiz Kowalski⁴, Albina Altemani⁵, Fernanda Mariano⁶

¹State University of Campinas (Unicamp), Campinas, Brazil, ²The University of Utah, Salt Lake City, UT, ³Piracicaba, Brazil, ⁴Faculdade de Medicina da USP, Campinas, Brazil, ⁵UNICAMP - Brazil, Brazil, ⁶Campinas, Brazil

Disclosures: João Scarini: None; Erika Egal: None; Sheila Nagamatsu: None; Luciana Mofatto: None; Rodrigo Maioral: None; Reydson de Lima-Souza: None; Marcelo Carazzolle: None; Luiz Coutinho: None; Luiz Kowalski: None; Albina Altemani: None; Fernanda Mariano: None

Background: Carcinoma ex-pleomorphic adenoma (CXPA) is a high-grade salivary gland carcinoma that arises from a pleomorphic adenoma (PA). The pathogenesis of malignant transformation remains a controversial issue. LRP1B is among the top 10 genes with significant mutation in human cancer, and is well recognized as a tumor suppressor gene in gastric cancer, oral squamous cell carcinoma, ovarian, and lung cancer.

Design: This study aims to investigate the *LRP1B* mutations based on Whole Exome Sequencing (WES). WES was successfully performed on DNA samples from 13 CXPA, 7 PA, and 5 residual PA individuals. Sequencing reads were aligned to the hg38 reference genome. Single nucleotide polymorphisms (SNPs) were identified for all samples. Quality and variant frequency filters were applied to the data.

Results: Mutated *LRP1B* was found in the three groups analyzed, with one high-impact (stop-gain) mutation in PA, four moderate-impact (missense) mutations in residual PA, and seven moderate-impact (missense) mutations in CXPA.

Conclusions: In glandular neoplasms, to our knowledge, the role of LRP1B has never been investigated. Here, unprecedentedly, we showed that the number of *LRP1B* mutations increased as malignant transformation occurred, suggesting that *LRP1B* might be an important gene in the adenoma-carcinoma transition, losing its suppressive role upon mutation.

839 Aberrant INSM1 Staining in Head and Neck Melanomas: A Potential Pitfall

Jesse Sheldon¹, Abberly Lott Limbach¹

¹The Ohio State University Wexner Medical Center, Columbus, OH

Disclosures: Jesse Sheldon: None; Abberly Lott Limbach: None

Background: INSM1 (insulinoma-associated protein 1) has been shown to be a sensitive and specific marker for neuroendocrine (NE) neoplasms. The majority of the literature focuses on tumors of known NE differentiation, but there is little data about the performance of INSM1 as part of a panel for tumors of uncertain differentiation. Recently data has emerged showing INSM1 may show focal staining in non-NE tumors in the lung and soft tissue. After observing INSM1 staining in an otherwise immunophenotypically characteristic sinonasal melanoma, we sought to examine the pattern of INSM1, synaptophysin and chromogranin staining in both mucosal and skin melanomas of the head & neck (H&N).

Design: The pathology LIS was searched for mucosal melanomas diagnosed in the H&N over a 5 year period. For comparison, melanoma arising in the skin of the H&N was also searched. The H&E slides were reviewed. The cases were screened for adequate tissue for ancillary testing. Synaptophysin, chromogranin, and INSM1 staining was performed, as needed, on each case. Staining intensity and percentage staining was recorded.

Results: The 29 cases included: 7 (24%) mucosal melanomas, 3 (10%) metastatic melanomas to the parotid gland, and 19 (66%) skin primaries. Chromogranin and synaptophysin were uniformly negative. INSM1 staining was present in 22 (76%) of cases of at least 1+ intensity (Table 1). The average percentage of tumor cells staining with INSM1 was 47% (range 5% - 95% of tumor cells). (Figure 1).

Table 1: Intensity of INSM1 staining in melanoma of the head & neck.

Histologic Type (N)	No staining (0)	Low intensity (1+)	Moderate Intensity (2+)	High Intensity (3+)
Mucosal Melanoma (7)	1	5	1 (focal 3+)	0
Non-mucosal Melanoma (22)	6	12	4	0

Figure 1 - 839

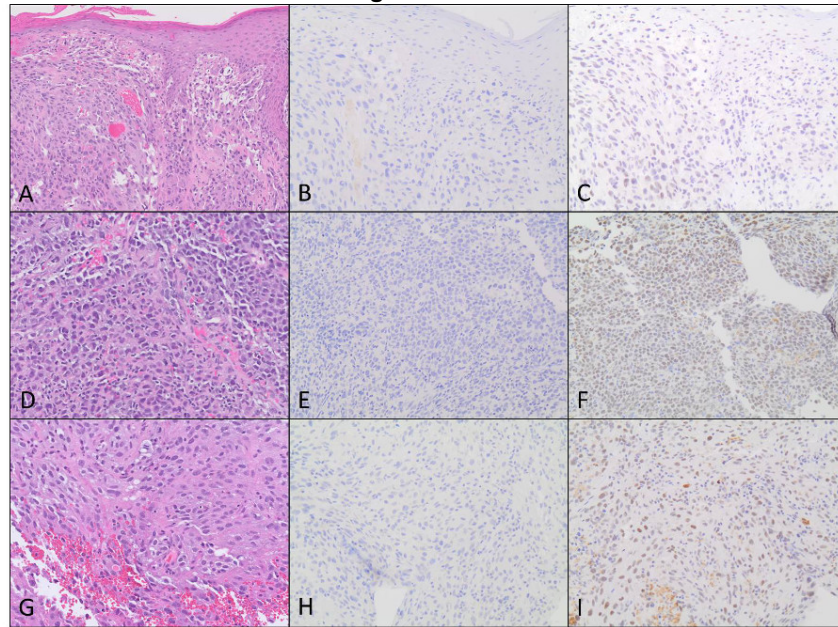


Figure 1: Melanoma cases with chromogranin and INSM1 staining. A. Melanoma of skin, H&E, 20x. B. Melanoma of skin, Chromogranin, 20x. C. Melanoma of skin, INSM1 (1+), 20x. D. Metastatic melanoma to parotid, H&E, 20x. E. Metastatic melanoma, Chromogranin, 20x. F. Metastatic melanoma, INSM1 (2+), 20x. G. Sinonasal melanoma, H&E, 20x. H. Sinonasal melanoma, Chromogranin, 20x. I. Sinonasal melanoma, INSM1 (3+), 20x.

Conclusions: Our data show INSM1 can weakly (1+) to moderately (2+) stains tumors which otherwise do not demonstrate NE differentiation. In addition, INSM1, when compared to other NE markers, is more likely to exhibit background and non-specific staining. For this reason, caution is urged when using INSM1 alone as part of a screening panel and the performance characteristics of INSM1 at each institution should be well studied. Given the emerging literature on INSM1 staining in tumors of the lung and soft tissue, caution should be used when using INSM1 as a solitary method of ruling out a neuroendocrine neoplasm in the head and neck region.

840 Surveying for Therapeutic Targets in Poorly Differentiated Carcinoma in the Sinonasal Tract: Immunohistochemical assessment of IDH2, SSRT2A, and CXCR4 in Tumors with Neuroendocrine Features

Scott Steward-Tharp¹, Tanya Sajan Ponnatt¹, Kelly Magliocca¹, Daniel Lubin², Zaid Mahdi², Faisal Saeed², Kartik Viswanathan¹, DI Ai², Qiuying (Judy) Shi¹

¹Emory University, Atlanta, GA, ²Emory University Hospital, Atlanta, GA

Disclosures: Scott Steward-Tharp: *Advisory Board Member*, Elsevier; Tanya Sajan Ponnatt: None; Kelly Magliocca: None; Daniel Lubin: None; Zaid Mahdi: None; Faisal Saeed: None; Kartik Viswanathan: None; DI Ai: None; Qiuying (Judy) Shi: None

Background: Poorly differentiated carcinomas of the sinonasal tract can be both diagnostically and therapeutically challenging. Recent studies have identified distinct molecular alterations within this broad group (e.g. IDH1/2) that allow for not only subcategorization, but also potential therapeutic targeting. Additionally, peptide receptor radionuclide therapy advances allow for selective targeting of neuroendocrine tumor cells (e.g. SSRT2A, CXCR4). We used immunohistochemistry to survey for potential therapeutic targets in a series of poorly differentiated sinonasal carcinomas with neuroendocrine features.

Design: The archives of Emory University Hospital (2008-2020) were searched for cases of sinonasal poorly differentiated carcinoma and tissue microarrays (TMA) were constructed from paraffin embedded blocks (triplicate cores when sufficient tumor). 22 cases exhibited histologic and immunohistochemical evidence of neuroendocrine differentiation. Immunohistochemistry for IDH2, SSRT2A, CXCR4, beta-catenin, and CD117/Kit were performed, as well as a panel of neuroendocrine markers.

Results: Five cases were IDH2 positive, four of which were suggestive of high-grade olfactory neuroblastoma, with sustentacular S-100 staining. Kit positivity was uniformly noted in this IDH2 positive population. IDH2 positive tumors were notably deficient in SSRT2A (0/5) and CXCR4 (1/5) expression. By comparison, either CXCR4 (13/17) or SSRT2A (9/17) were detected by immunohistochemistry in fifteen of seventeen IDH2 negative tumors. Nuclear beta-catenin marking was detected in only one of twenty-two cases.

Conclusions: Potential therapeutic targets were identified by immunohistochemistry in a number of poorly differentiated sinonasal carcinomas with neuroendocrine features. IDH mutations are found in a subset of tumors with immunophenotypic features of high-grade olfactory neuroblastoma with basal phenotype. Investigation of immunoexpression of SSRT2A, CXCR4 and other potential therapeutic targets on additional sinonasal tumors with neuroendocrine features, including low-grade olfactory neuroblastoma, will be worth further study.

841 Dominant SATB2 and PU.1 Expression, and Occult Odontogenic Epithelium, in Central and Peripheral Giant Cell Granulomas

Ivan Stojanov¹, Luvy Delfin Mendez¹, Vickie Jo²

¹Case Western Reserve University/University Hospitals Cleveland Medical Center, Cleveland, OH, ²Brigham and Women's Hospital, Harvard Medical School, Boston, MA

Disclosures: Ivan Stojanov: None; Luvy Delfin Mendez: None; Vickie Jo: *Stock Ownership*, Merck and Co

Background: Central giant cell granulomas (CGCG) are the most common of the giant cell lesions of the jaws. They are recently recognized as benign neoplasms harboring *TRPV4*, *KRAS* or *FGFR1* mutations in most cases, but their cellular composition apart from the well-recognized multinucleated giant cells (osteoclasts) remains unknown. Additionally, rare CGCG have been reported with an identifiable odontogenic epithelial component, termed hybrid CGCG/central odontogenic fibroma, but whether, or to what extent, occult odontogenic epithelium is associated with CGCGs in general is also unknown. Our aim was to evaluate CGCG and its extraosseous counterpart, peripheral giant cell granuloma (PGCG), using immunohistochemistry (IHC) for SATB2, PU.1 and AE1/AE3 to better characterize the cellular composition of these poorly understood tumors.

Design: 17 CGCG and 12 PGCG were retrieved from institutional archives. SATB2, PU.1 and AE1/AE3 IHC was performed on all 29 cases. SATB2 and PU.1 expression was scored as a percentage of all cellular constituents within the tumor and AE1/AE3 was scored as positive or negative.

Results: CGCGs occurred in 5 male and 12 female patients with a median age of 25 (range, 11-66) years. PGCGs occurred in 8 male and 4 female patients with a median age of 58 (range, 8-93) years. The mandible was involved in 15/17 CGCG and 9/12 PGCG, and tooth-bearing regions of the jaws were involved in all cases. The mononuclear tumor cell population showed consistent

staining for both SATB2 and PU.1, in differing proportions. SATB2 expression ranged from 60-80% of mononuclear cells in all CGCG (17/17) and PGCG (12/12). PU.1 uniformly highlighted osteoclasts and expression ranged from 5-10% of mononuclear cells in 16/17 CGCG and 12/12 PGCG, with 20% expression in one CGCG. Occult odontogenic epithelium was identified within or adjacent to the tumor in 4/17 (23.5%) CGCG and 3/12 (25.0%) PGCG, and occasionally identified retrospectively on H&E staining. At least focal intratumoral bone formation was present in 13/17 (76.5%) CGCG and 7/12 (58.3%) PGCG.

Conclusions: Cells of osteoblastic and macrophage/osteoclastic lineage (as highlighted by SATB2 and PU.1, respectively) comprise dominant cell populations in CGCG and PGCG, and intratumoral bone formation is common. Focal odontogenic epithelium is associated with a subset of these tumors and may, together with their anatomic predilection for tooth-bearing regions of the jaws, support an odontogenic or periodontal ligament origin for these unique neoplasms.

842 Insights Into the Molecular Underpinnings of Laryngeal Chondrosarcomas (LCs)

Kent Swimley¹, Daryoush Saeed-Vafa¹, Bruce Wenig¹, Juan Hernandez-Prera¹

¹H. Lee Moffitt Cancer Center & Research Institute, Tampa, FL

Disclosures: Kent Swimley: None; Daryoush Saeed-Vafa: None; Bruce Wenig: None; Juan Hernandez-Prera: None

Background: LCs are the most common malignant mesenchymal tumor affecting the larynx. Their etiology remains unknown, and they appear to be molecularly distinct from central-type conventional chondrosarcoma which are commonly associated with isocitrate dehydrogenase 1 and 2 (*IDH1/IDH2*) gene mutations. We aim to investigate the molecular profile of LCs.

Design: Nine cases of LC were identified in our database from 2010 to 2021. The clinical-pathological features were summarized, and all cases were subjected to a DNA and RNA-based next-generation sequencing (NGS) assay covering 170 different cancer-related genes, including *IDH1/IDH2*.

Results: There were 7 men and 2 women with a mean age at onset of 67 years (range 48-87 years). A majority of tumors arose in the cricoid cartilage (8/9). A majority (6/9) followed a stable, localized clinical course with multiple recurrences over a range of 2 to 8 years. One patient was free of disease 3 years after surgery; two patients were lost to follow-up. Morphologically, the tumors were predominantly low-grade (7/9, grade 1), characterized by a paucicellular neoplastic chondrocyte proliferation with mild nuclear cytologic atypia, binucleate cells, rare mitosis, and no necrosis. Two cases were intermediate-grade (grade 2) characterized by increased cellularity and nuclear atypia. No cases were high-grade (grade 3). NGS was successful in 8 cases with adequate DNA/RNA quality metrics. None of the cases had recurrent pathogenic *IDH1/IDH2* mutations. One case harbored an *IDH2* p.T435M alteration, which has been identified in 0.4% of the general population (gnomAD) and reported in the germline as benign/likely benign by ClinVar (ID:158664). Interestingly, 2 cases harbored significant variants associated with hereditary cancer-predisposing syndromes: 1 case showed an *MUTYH* missense mutation (p.G393D) and another showed a frameshift deletion in *CHEK2* (p.T410Mfs*15). Both variants have been reported in the literature as pathogenic germline mutations; however, these 2 patients have not undergone genetic testing.

Conclusions: *IDH1/IDH2* mutations are not characteristic of chondrosarcomas arising from the laryngeal cartilages. Our findings support the observation that this group of neoplasms are molecularly distinct from tumors arising in the appendicular and axial skeleton, suggesting an alternate tumorigenesis. Whether LCs belong to the spectrum of malignancies associated with germline variants in *MUTYH* and *CHEK2* remains unclear and warrants further investigations.

843 PD-L1 Expression and Microsatellite Stability Status in HPV-related Multiphenotypic Sinonasal Carcinomas, our Experience

Justyna Szafranska¹, Eva Chenu², Eduard Neumann¹, Juan Ramon Gras Cabrerizo¹, Silvia Bague³, Laura Lopez-Vilaro²

¹Hospital de la Santa Creu i Sant Pau, Barcelona, Spain, ²Hospital Sant Pau, Barcelona, Spain, ³Hospital de la Santa Creu i Sant Pau

Disclosures: Justyna Szafranska: None; Eva Chenu: None; Eduard Neumann: None; Juan Ramon Gras Cabrerizo: None; Silvia Bague: None; Laura Lopez-Vilaro: None

Background: HPV-related Multiphenotypic Sinonasal Carcinoma (HMSC) is a rare neoplasm, despite that the sinonasal tract has been identified as another "hot spot" for these tumors according to recent published series. The aim of this study was to analyze

the characteristics of HMSC resected in our institution and their association with PD-L1 expression, the presence of Tumor Infiltrating Lymphocytes (TILs), Microsatellite Stability Status (MSS) and its prognostic impact.

Design: We reviewed clinical, histological and immunochemistry findings of 9 HMSC diagnosed within the period of 2007-2019.

Results: The study included 7 males and 2 females with a median age of 54 years and a median tumor size of 2,5 cm, 4 of which were localized in nasal cavity, 4 in ethmoid and 1 in maxillary sinus. 5 patients presented nasal obstruction, 2 nasal epistaxis, 1 epiphora and 1 was asymptomatic. Histologically 7 out of 9 cases had adenoid cystic carcinoma-like features and 2 were poorly differentiated squamoid-like carcinomas. All cases proved positive for p16 immunostaining, and HPV genomic PCR was obtained in 4 cases showing the presence of 33, 54, 16 and 11 HPV genotypes. In the other cases, determination of HPV was not possible due to PCR artifacts, probably related to DNA fragmentation. Using CPS score for evaluating PD-L1 expression we observed one strong and two weak positive stainings in our cases. All tumors showed microsatellite stability with the presence of few intraepithelial lymphocytes (0-2/hpf). 60% of patients were treated with surgery and adjuvant radiotherapy, 10% with surgery and adjuvant chemoradiotherapy, 20% with neo and adjuvant chemotherapy and 10% just underwent surgical resection. Three patients presented local recurrence, 2 of which were PD-L1 positive tumors associated with HPV 16 and 11 genotype, and were treated with surgery and radiotherapy. Four tumors didn't recur and one of them was PD-L1 positive. Two patients developed metastatic disease and had PD-L1 negative tumors, one with HPV 33 genotype presenting a more aggressive progression than expected (central nervous system and lung metastasis) compared to series previously published by Bishop.

Case	Sex	Age	Presentation	Site	Stage	Treatment	p16	HPV type	PD-L1 CPS score	MSS	TILs	Histology	Size (cm)	Follow-up
1	M	54	Nasal obstruction	Ethmoid	T3N0M0	Surgery+RT	positive		<1	stable	0-2/hpf	HMSC-ACC like	4	NED (127)
2	M	45	Nasal obstruction	Nasal cavity	T4aN0M0	CT+RT	positive		<1	stable	0-2/hpf	HMSC-ACC like	1,5	NED (156)
3	M	44	Nasal obstruction	Ethmoid	T4aN0M0	CT+RT	positive	33	<1	stable	0-2/hpf	HMSC-ACC like	1,3	LR (60), NED (126)
4	F	43	Epiphora	Maxillary sinus	T3N0M0	Surgery+RT	positive		<1	stable	0-2/hpf	HMSC-ACC like	4	DM (42), DM (48), DM(51), DM (53), DM (61); (42)
5	F	48	Nasal obstruction	Nasal cavity	T1N0M0	Surgery+RT	positive		<1	stable	0-2/hpf	HMSC-ACC like	3	NED (84)
6	M	47	Asymptomatic	Nasal cavity	T1N0M0	Surgery+RT	positive		>1(1)	stable	0-2/hpf	HMSC-SC like	0,6	NED (66)
7	M	48	Nasal obstruction	Ethmoid	T2N0M0	Surgery+RT	positive	33, 54	<1	stable	0-2/hpf	HMSC-ACC like	6,5	DM (12), NED (16)
8	M	83	Epistaxis	Nasal cavity	T2N0M0	Surgery	positive	16	>1(50)	stable	0-2/hpf	HMSC-SC like	1	LR (3)
9	M	82	Epistaxis	Ethmoid	T2N0M0	Surgery+RT	positive	11	>1(1)	stable	0-2/hpf	HMSC-ACC like	1	LR (47), LR (67), LR(82)

Conclusions: Our findings suggest that there may be modification of the outcomes depending on PD-L1 status in HMSC. Further investigation is needed given the limited number of cases presented in our series.

844 Sinonasal Mucosal Melanoma, PD-L1 Expression, Tumor Infiltrating Lymphocytes, and BRAF V600E Mutations: A 10-Year Experience at a Single Institution

Jana Tarabay¹, Ifegwu Ibe², Sherehan Zada³, Robert Edwards², Jeff Chan³, Edward Kuan⁴, Beverly Wang³
¹University of California, Irvine, Irvine, CA, ²UC Irvine Health, Orange, CA, ³UCI Medical Center, Orange, CA, ⁴University of California, Irvine, CA

Disclosures: Jana Tarabay: None; Ifegwu Ibe: None; Sherehan Zada: None; Robert Edwards: None; Jeff Chan: None; Edward Kuan: *Consultant, Stryker ENT; Advisory Board Member, Optinose*; Beverly Wang: None

Background: Sinonasal mucosal melanoma (SNMM) is a rare malignancy that accounts for less than 1% of all melanomas. Due to its high metastatic potential, late clinical presentation, and the lack of standardized treatment guidelines, SNMM is known to have an aggressive clinical behavior. Immunotherapy has been introduced to the management of SNMM, however, given the rarity of

this entity, data on the response to different treatment regimens and the prognostic value of various histopathologic factors remains unclear. To date, little data originates from small cohorts from around the world.

Design: An observational cross-sectional study was performed. Institutional Review Board (IRB) approval was obtained to review clinical characteristics, treatment modalities, outcomes, and prognostic factors of every patient treated in our institution for SNMM from 2011 to 2021. Survival outcomes among different treatment modalities and numerous histopathologic factors were analyzed using the Kaplan–Meier method and log-rank test.

Results: In total, twelve patients were included; median age was 70.0 years (range 53-96 years). All the tumors were in the nasal cavity. Mean tumor size was 3.5 cm (range 0.8-6.3 cm). Eight patients (67%) developed metastasis to the brain, liver, bone, lymph nodes, and lungs. Nine patients underwent endoscopic surgical resection while palliative care was provided to one patient who had presented with a stage IV disease. Out of the twelve cases, five (41.7%) showed a brisk infiltration by lymphocytes. BRAF V600E Melanoma mutational analysis was performed on all cases and the mutation was not detected in any. PD-L1 was performed on ten cases and showed a positivity defined by $\geq 1\%$ was detected in half of the cases. Kaplan-Meier analysis (Figure 1) showed that a brisk tumor infiltrating lymphocytes (TIL) was strongly associated with better survival (Log-Rank, $p=0.036$). PD-L1 positivity and immunotherapy with anti-PL1 agents did show better survival rates. (Log-Rank, $p=0.188$ and $p=0.695$ respectively).

Age		
Median (year)	70	
Range (year)	53-96	
	Number of patients	Percentage (%)
Gender		
Female	10	83.3
Male	2	16.7
Tumor Stage		
T2	1	8.3
T3	6	50
T4a	2	16.7
T4b	3	25
Local recurrence		
	5	41.7
Metastasis		
	8	66.7
Regional lymph node	2	25
Distant	6	75
Site of metastasis		
Lung	2	33.3
Brain	1	16.7
Liver	2	33.3
Bone	1	16.7
Multiple	2	33.3
Treatment		
Surgical resection	9	75
Radiotherapy	5	41.7
Immunotherapy	8	66.7
TIL		
Brisk	5	41.7
Non-brisk	7	58.3

Figure 1 - 844

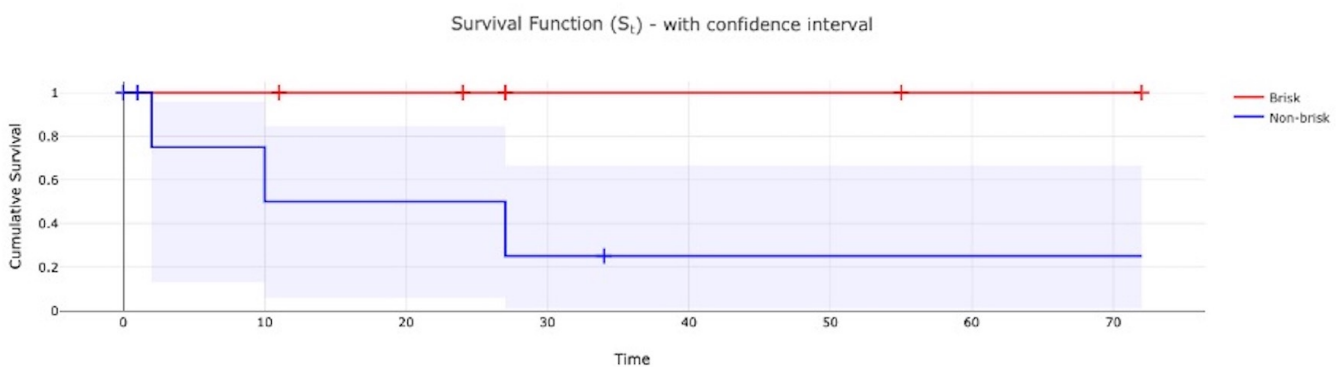
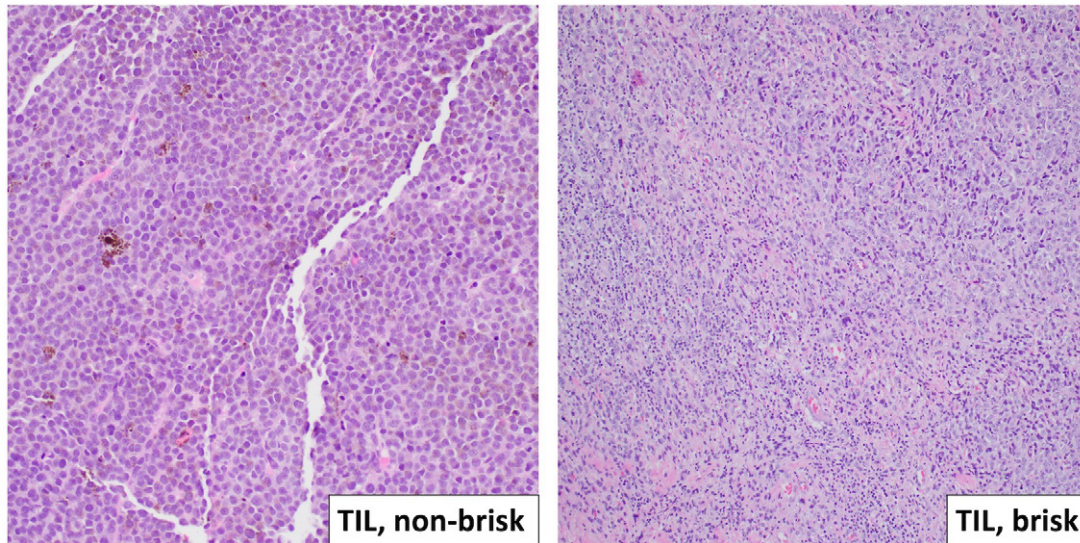


Figure 2 - 844



Conclusions: Our results indicate that a brisk TIL is a strong factor for longer survival in SNMM. Prospective studies with larger sample size are needed to determine whether TILs should be included in future staging guidelines and to highlight the clinical value of anti-PD-L1 treatment.

845 Osteosarcoma of the Jaw: The Better Twin - An Institutional Experience of 38 Cases

Immanuel Thayakaran¹, Shailee Mehta¹, Kanwalpreet Kaur¹, Priti Trivedi¹, Amisha Gami¹
¹Gujarat Cancer Research Institute, Ahmedabad, India

Disclosures: Immanuel Thayakaran: None; Shailee Mehta: None; Kanwalpreet Kaur: None; Priti Trivedi: None; Amisha Gami: None

Background: Although osteosarcoma is the commonest primary bone tumour, osteosarcoma of the jaw (JOS) is relatively rare comprising 6 to 7% of all osteosarcomas. In contrast to the long bone osteosarcoma, JOS albeit malignant has a milder disease course owing to a myriad of factors namely early detection facilitating complete surgical removal and less tumour vascularity diminishing the risk of distant metastasis. The histopathological implication is that JOS can be misdiagnosed as any other spindle cell lesion affecting the oral cavity on a small biopsy. We aim to study the clinicopathologic features of 38 cases of JOS and thereby broadening our awareness regarding this peculiar yet a relatable entity.

Design: The clinical, radiological and histopathologic records of JOS were obtained from the archives of department of pathology retrospectively between the period 2010 to 2021. The data was analysed with regard to age, gender, location of tumour, histopathologic type and grade with clinical data. Immunohistochemistry was done as and when required.

Results: A total of 38 cases of JOS were identified from 2010 to 2021. The median age was 30 years (range 10 to 76 years) with male female ratio being 0.8:1. Mandibular involvement was seen in 73% of tumours while maxillary involvement was seen in 27%. Histological subtypes noted were osteoblastic, chondroblastic, fibroblastic, epithelioid and small cell variant.

Radiography showed cortical breach with soft tissue component in 66% cases and one case showed extension to skull base. AJCC TNM staging was available for 68% cases out of which 62% presented with AJCC TNM stage I and 38% cases with AJCC stage II. Adjuvant chemotherapy was rendered in 63% of cases. Local recurrence was seen in 28% cases and 2 cases had lung metastasis (5%). Two cases had putative factors with one being radiation induced osteosarcoma (45-year-old male with prior history of oral squamous cell carcinoma 3 years back) and another being a malignant transformation of fibrous dysplasia.

Table 1: Clinicopathologic Features of 38 cases of Osteosarcoma of the Jaw

Clinicopathologic Features	
Osteosarcoma of Jaw (JOS)	
Median age (range)	30 years (10-76)
Sex	
Male	44% (17/38)
Female	56% (21/38)
Site	
Mandible	73% (28/38)
Maxilla	27% (10/38)
Laterality	
Left	(14/38)
Right	(15/38)
Cortical breach with soft tissue extension	66% (25/38)
Histopathologic subtypes	Osteoblastic Chondroblastic Fibroblastic Epithelioid Small cell
AJCC TNM Stage	
T1	62% (16/26)
T2	38% (10/26)
Adjuvant chemotherapy	63% (24/38)
Local recurrence	28% (11/38)
Lung metastasis	5% (2/38)
Putative risk factors	Radiation induced secondary osteosarcoma (1) Malignant transformation of fibrous dysplasia (1)

Conclusions: Osteosarcoma of the jaw comprise a distinct group of tumours differing from their long bone counterpart in terms of later age of onset, early presentation, local recurrence, lower metastatic spread and better overall survival. A high degree of suspicion for osteosarcoma of the jaw (JOS) is imperative when encountering a spindle cell lesion in a small biopsy from the maxillomandibular region facilitating an expedited diagnosis with timely and optimal patient management.

846 Salivary Glant Neoplasms in Major and Minor Salivary Glands: A 5-year Retrospective Study of 1,799 Cases from a Private Practice Group

Lester Thompson, Head and Neck Pathology Consultations, Woodland Hills, CA

Disclosures: Lester Thompson: None

Background: Epidemiology data about salivary gland neoplasms identified within a large private practice health care delivery system without referral bias has not been reported.

Design: All head and neck salivary gland sites were reviewed retrospectively to determine the clinicopathologic features (tumor site, tumor type, patient sex and age) of neoplasms identified over 5 consecutive years (2015 to 2019) from the medical centers of the Southern California Permanente Medical Group. Of the 2,749,467 accessioned surgical cases, 1,799 represented neoplasms affecting salivary glands (0.00065%) removed from 4,226,728 patient members on average at the mid-point of each calendar year: 8.5 tumors/100,000 patient years.

Results: Overall, 905 tumors were in females and 894 in males, with benign tumors (38.9% vs 32.9%) more common in females and malignant tumors (16.8% vs. 11.4%) more common in males. Benign tumors and malignant tumors represented 71.8% and 28.2%, respectively. Pleomorphic adenoma (68.9% of benign and 49.4% of all tumors) was the most common tumor in major and minor salivary gland sites, followed by Warthin tumor (14.9% of benign and 10.7% of all tumors), identified only in major salivary

gland sites. For malignant tumors (% of all malignant tumors followed by % of all tumors, respectively), metastatic squamous cell carcinoma was most common (32.1% and 9.1%), while of primary salivary gland-type tumors, mucoepidermoid carcinoma (23.9% and 6.7%), adenoid cystic carcinoma (11.6% and 3.3%), and acinic cell carcinoma (9.1% and 2.6% of all tumors) were most common. Of major salivary glands, 89.1% affected the parotid gland; of minor salivary gland subsites, the hard palate was most commonly affected (24.3%). Overall, the mean age at presentation was 55.3 and 57.3 years, respectively for benign and malignant tumors, with specific findings for each tumor category. Pediatric patients represented 1.5% of benign and 1.8% of malignant tumors, with benign tumors twice as common as malignant.

Histologic Category	Histologic Diagnosis	Sex		Age in years, mean (SD)			Anatomic Site		Grand Totals
		Female	Male	Female	Male	Total	Major	Minor	
Benign (% of Category)									
(68.8%)	Pleomorphic adenoma	562	327	52.1 (16.1)	50.5 (17.2)	51.5 (16.5)	803	86	889 (49.4%)
(14.9%)	Warthin tumor	47	146	64.4 (11.7)	64.3 (9.8)	64.3 (10.3)	193	0	193 (10.7%)
(6.3%)	Oncocytoma	35	46	70.5 (10.7)	66.2 (12.6)	68.0 (11.9)	80	1	81 (4.5%)
(3.1%)	Basal cell adenoma	23	17	61.5 (12.3)	59.2 (15.4)	60.6 (13.6)	37	3	40 (2.2%)
(2.5%)	Cystadenoma	14	18	48.6 (18.7)	67.1 (9.6)	59.0 (16.8)	12	20	32 (1.8%)
(1.6%)	Sialolipoma	3	18	52.0 (19.2)	59.2 (10.0)	58.2 (11.3)	21	0	21 (1.2)
(0.9%)	Canalicular adenoma	7	4	68.9 (10.6)	70.3 (7.8)	69.4 (9.3)	0	11	11 (0.6%)
(0.9%)	Hemangioma	5	6	51.0 (7.6)	43.2 (16.7)	46.7 (13.4)	11	0	11 (0.6%)
(0.5%)	Myoepithelioma	0	6	na	58.8 (11.7)	58.8 (11.7)	5	1	6 (0.3%)
(0.3%)	Lymphadenoma	1	3	88.0 (na)	67.7 (3.8)	72.8 (10.6)	4	0	4 (0.2%)
(0.2%)	Sclerosing polycystic adenoma	2	0	34.0 (14.1)	na	34.0 (14.1)	2	0	2 (0.1%)
(0.2%)	Intercalated duct adenoma*	2	0	53.0 (15.6)	na	53.0 (15.6)	2	0	2* (0.1%)
(0.1%)	Solitary fibrous tumor	1	0	79.0 (na)	na	79.0 (na)	1	0	1 (0.06%)
(0.1%)	Sialadenoma papilliferum	0	1	na	54.0 (na)	54.0 (na)	0	1	1 (0.06%)
	Totals for benign neoplasms	700 (38.9%)	592 (32.9%)	54.3 (16.4)	56.4 (16.3)	55.3 (16.4)	1169 (65.0%)	123 (6.8%)	1292 (71.8%)
Malignant (% of Category)									
(32.1%)	Metastatic squamous cell carcinoma	25	138	74.8 (11.2)	74.2 (9.6)	74.3 (9.8)	163	0	163 (9.1%)
(23.9%)	Mucoepidermoid carcinoma	67	54	55.4 (17.1)	53.4 (17.7)	54.7 (17.3)	68	53	121 (6.7%)
(11.6%)	Adenoid cystic carcinoma	36	23	57.4 (18.0)	60.5 (13.2)	58.6 (16.2)	16	43	59 (3.3%)
(9.1%)	Acinic cell carcinoma	24	22	56.9 (18.2)	51.0 (17.4)	54.1 (17.9)	46	0	46 (2.6%)
(7.1%)	Carcinoma ex pleomorphic adenoma	14	22	60.0 (14.1)	58.9 (17.1)	59.3 (15.8)	31	5	36 (2.0%)
(5.1%)	Secretory carcinoma	15	11	48.9 (16.2)	39.8 (16.6)	45.0 (16.7)	19	7	26 (1.4%)
(4.5%)	Salivary duct carcinoma	8	15	63.3 (13.1)	76.7 (7.7)	72.0 (11.7)	23	0	23 (1.3%)
(3.0%)	Polymorphous adenocarcinoma	9	6	65.9 (11.0)	61.8 (11.4)	64.3 (11.0)	0	15	15 (0.8%)
(1.8%)	Basal cell adenocarcinoma	4	5	58.3 (21.2)	63.4 (10.7)	61.1 (15.3)	8	1	9 (0.5%)
(0.6%)	Myoepithelial carcinoma	1	2	63.0 (na)	59.5 (3.5)	60.7 (3.2)	2	1	3 (0.2%)
(0.4%)	Lymphoepithelial carcinoma	1	1	50.0 (na)	71.0 (na)	60.5 (14.8)	2	0	2 (0.1%)
(0.2%)	Sebaceous adenocarcinoma	0	1	na	82.0 (na)	82.0 (na)	0	1	1 (0.06%)
(0.2%)	Intraductal carcinoma	0	1	na	89.0 (na)	89.0 (na)	1	0	1 (0.06%)
(0.2%)	Hyalinizing clear cell carcinoma	0	1	na	63.0 (na)	63.0 (na)	0	1	1 (0.06%)
(0.2%)	Mucinous adenocarcinoma	1	0	67.0 (na)	na	67 (na)	0	1	1 (0.06%)
	Totals for malignant neoplasms	205 (11.4%)	302 (16.8%)	59.0 (17.2)	65.0 (16.8)	62.6 (17.2)	379 (21.1)	128 (7.2%)	507 (28.2%)
	Grand totals	905 (50.3%)	894 (49.7%)	55.4 (16.7)	59.3 (16.9)	57.3 (16.9)	1548 (86.0%)	251 (14.0%)	1799 (100%)

Conclusions: In conclusion, while pleomorphic adenoma was the most common tumor, it represented only 49.4% of all tumors, while metastatic squamous cell carcinoma to the parotid gland was the most common malignant tumor identified in salivary glands. Overall, salivary gland benign and malignant tumors are very rare, representing only 0.00065% of all surgical pathology cases.

847 Extranodal Follicular Dendritic Cell Sarcoma of the Head and Neck region: A Clinicopathological Study of 6 cases

Nasir Ud Din¹, Zubair Ahmad², Muhammad Usman Tariq¹, Arsalan Ahmed¹
¹Aga Khan University Hospital, Karachi, Pakistan, ²Aga Khan Hospital, Karachi, Pakistan

Disclosures: Nasir Ud Din: None; Zubair Ahmad: None; Muhammad Usman Tariq: None; Arsalan Ahmed: None

Background: Follicular dendritic cell sarcoma (FDCS) is a rare lymphoid neoplasm which commonly arises in lymph nodes but can also occur at extranodal sites. Common extra-nodal sites include gastrointestinal tract (GIT) and head and neck (HAN) region.

Design: Cases of FDCS diagnosed in our lab were searched electronically and extranodal cases involving head and neck region were segregated. Patient demographics, tumor site and size were recorded. Glass slides were reviewed by the two pathologists to confirm the diagnosis and histological features. Follow up was obtained.

Results: A total of 57 cases of FDCS were reported during the study period (2005-2021). Six cases occurred in the HAN region. The age of patients ranged from 12 to 79 years (mean 40; median 44 years). Five patients were males, and one was female. Tumor involved parapharyngeal space and tonsil in 2 cases each. Oropharynx and parotid were involved in one case each. 5 cases were received as resection specimens. Gross tumor size ranged from 2.4 to 5.5 cm (mean 4.1 cm). Histologically, tumors were composed of a mixture of spindle to epithelioid cells arranged in whorls, syncytia and nests. Focal multinucleated tumor cells were seen. Sprinkling of lymphocytes was seen in all cases. Encapsulation was noted in two cases. Nodal involvement noted in one parapharyngeal case. Mitotic figures ranged from 3 to 18/10HPFs (mean 8/10HPFs). Immunohistochemical stains CD21 and CD23 were positive in all cases. S100 was positive in 1/6 cases. LCA, ASMA, CD34, Desmin and CD68 were negative in cases performed. Follow up was available in 4 patients and ranged from 9 to 180 months (mean 61 months). Female patient with tonsil tumor experienced two recurrences at 33 and 45 months after primary surgery. She received radiation therapy and is alive after 180 months. Another patient with tonsillar tumor died 16 months after surgery. He had received radiation therapy and treatment for concomitant pulmonary Tuberculosis as well. One patient with parapharyngeal tumor died 9 months after surgery, he received 7 cycles of chemotherapy. Patient with oropharyngeal tumor is alive at 39 months without surgical excision or chemo-radiation with progression of disease

Conclusions: Tonsil and parapharyngeal space were most common locations. Male predominance was noted in our cases. Both patients who died had a tumor size of >5 cm and mitoses >15/HPFs. Oropharyngeal patient was alive thus confirming a relatively better prognosis for this site as noted in the literature.

848 A Comparison Of Tumor Infiltrating Lymphocytes With Pathological Stage In Predicting The Prognosis Of Oral Squamous Cell Carcinoma

Aparna Valsan¹, Garima Goel¹, Vikas Gupta¹, Joshi Deepti², Neelkamal Kapoor²
¹Bhopal, India, ²All India Institute of Medical Sciences, New Delhi, India

Disclosures: Aparna Valsan: None; Garima Goel: None; Vikas Gupta: None; Joshi Deepti: None; Neelkamal Kapoor: None

Background: Carcinoma of the oral cavity is the sixth most common malignancy reported worldwide. More than 90 % of oral cancers are squamous cell carcinoma but the prognosis has not improved even after the advances in treatment modalities. Tumor infiltrating lymphocytes (TIL) are important component of tumor microenvironment which helps in altering the prognosis of the patient. The present study was conducted with an aim to assess the role of TIL subsets in comparison to the pathological tumor and nodal stage of oral squamous cell carcinoma(OSCC) in predicting the prognosis of the tumor.

Design: A retrospective cross-sectional study on 56 operated cases of OSCC was carried out in a tertiary care center. The haematoxylin and eosin slides of the cases were examined and section which had areas with TIL that are surrounded by tumour on all four sides were selected for analysis. The type of tumour area was grouped as cell rich, moderate, stroma rich and percentage for TIL as low(0-30%), moderate(30-70%), high(>70%). Immunohistochemistry for CD3, CD4, CD8 and FOXP3 was performed and

evaluated for positive expression of tumour cells and the ratio of CD3/FOXP3, CD4/FOXP3, CD8/FOXP3 was calculated using morphometry software. The TIL subsets were correlated with the pathological tumour and nodal stage of OSCC. Statistical analysis was carried out using Chi-square test for categorical data and unpaired sample t-test for bivariate data. The Kruskal Walli's test was used for multivariate analysis. A p value of <0.05 was considered as significant.

Results: The CD4 (p value 0.004) and CD8 (p-0.045) cell density had a significant correlation with tumour stage. The CD3 (p-0.034) cells showed a higher density of expression in early stage (T1,T2) tumour as compared to the advanced (T3,T4) tumours. CD4 (p-0.039) cells had significantly lower density of expression in cases with no nodal metastasis. The ratio of CD3/FOXP3 (p-0.005) and CD8/FOXP3 (p-0.048) was significantly higher in cases with no nodal metastasis compared to cases with metastasis. The expression of CD3 (p 0.034) and CD8 (p-0.020) had statistically significant correlation with patterns of WPOI.

Conclusions: TIL can be used as prognostic and predictive marker in the oral squamous cell carcinoma. A better understanding of the tumour microenvironment and complex interplay amongst the cytokine, chemokine, regulatory and effector T cells may help in development of immunotherapy for patients with oral squamous cell carcinoma making it more responsive to conventional radiation and chemotherapy.

849 Sinonasal Myxoma: A Distinct Entity or a Myxoid Variant of Desmoid Fibromatosis? A Morphological and Genetic Study

Jaylou Velez Torres¹, Douglas Mata², Laurence Briski³, Elizabeth Montgomery¹, Andrew Rosenberg³
¹University of Miami Miller School of Medicine, Miami, FL, ²Foundation Medicine, Inc., Cambridge, MA, ³University of Miami Health System, Miami, FL

Disclosures: Jaylou Velez Torres: None; Douglas Mata: *Employee*, Foundation Medicine, Inc.; *Speaker*, Astellas Pharma, Inc.; Laurence Briski: None; Elizabeth Montgomery: None; Andrew Rosenberg: None

Background: Myxomas of the sinonasal cavity and maxillary sinus are rare non-odontogenic osseous tumors that occur in infancy and early childhood. Sinonasal myxoma (SNM) is currently reported in the literature as a specific entity but its molecular characteristics have not been previously described.

Design: Lesions diagnosed as SNMs were identified from participating institution pathology files. Hybrid capture-based next-generation sequencing (NGS) using DNA and RNA extracted from formalin-fixed, paraffin-embedded tissue was performed in all cases. The clinicopathologic and genomic features of the cases were evaluated.

Results: Three males with a mean age of 23.6 months (range, 20.3-25.8) with SNMs arising from the bones of the sinonasal cavity or maxilla were identified. Two lesions were initially classified as odontogenic myxoma (OM) and odontogenic fibromyxoma (OFM). The tumors were circumscribed, surrounded by a rim of reactive woven bone, and composed of a moderately cellular proliferation of spindled and/or stellate cells with small hyperchromatic nuclei and thin delicate cytoplasmic processes. The spindle cells were oriented in intersecting fascicles in a variably rich myxoid stroma that contained collagen fibers, prominent small-caliber blood vessels, and foci of extravasated erythrocytes. Rare mitotic figures and keloidal-type collagen were present. No necrosis or odontogenic epithelium were identified. One case tested showed strong nuclear immunohistochemical expression of β -catenin. The tumors resembled desmoid fibromatosis (DF) but contained more prominent myxoid stroma that could lead to a lack of accurate recognition. NGS confirmed this impression. The three tumors exhibited intragenic deletions of *APC* exons 5-6, 9 and 15, or 16, respectively, with concurrent loss of the other wild type copy of *APC*, predicted to result in biallelic inactivation. The deletions were identical to those that may occur in DF and copy-number analysis suggested that they were germline in origin.

Conclusions: SNM has been considered a distinct entity. However, our study indicates that it is an infantile myxoid variant of DF involving the facial bones often misdiagnosed as OM or OFM. It can be distinguished from these tumors based on age, morphology, nuclear β -catenin expression, and *APC* alterations. Because the *APC* alterations might be germline, these tumors may be an early manifestation of familial adenomatous polyposis and germline testing should be considered.

850 The Prognostic Impacts of Extranodal Extension (ENE) in P16/HPV-Positive Oropharyngeal Squamous Cell Carcinoma (OPSCC) with Nodal Metastasis

Bin Xu¹, Maelle Saliba², Mohammed Alghamdi¹, Bayan Alzumaili³, Snjezana Dogan¹, Ronald Ghossein¹, Nora Katabi¹
¹Memorial Sloan Kettering Cancer Center, New York, NY, ²Columbia University Irving Medical Center, New York, NY, ³Mount Sinai Hospital, New York, NY

Disclosures: Bin Xu: None; Maelle Saliba: None; Mohammed Alghamdi: None; Bayan Alzumaili: None; Snjezana Dogan: None; Ronald Ghossein: None; Nora Katabi: None

Background: Extranodal extension (ENE) is a significant prognostic factor for HPV-negative head and neck squamous cell carcinoma and is incorporated into AJCC pN stage. It remains controversial whether ENE is prognostically relevant in p16/HPV+ oropharyngeal squamous cell carcinoma (OPSCC).

Design: A detailed clinicopathologic review was conducted in a large retrospective cohort of 206 patients with p16/HPV+ OPSCC and nodal metastasis. Unknown primaries and p16/HPV-negative cases were excluded.

Results: Sixty-two patients had ENE. The median vertical extent of ENE was 2.5 mm (range 0.3-20.3 mm) and the median horizontal span of ENE was 3.2 mm (range: 0.3 -23.2 mm). Compared to cases without ENE, those with ENE were associated with higher number of positive lymph nodes ($p<0.001$), lymphovascular invasion ($p=0.005$), perineural invasion ($p=0.003$), AJCC pT stage ($p=0.041$) and larger primary tumor size ($p<0.002$).

Follow up was available for 192 patients, with a median follow up of 41 months (range 3-289 months). Univariate survival analysis using log rank test showed that ENE was associated with significantly shortened overall survival (OS), disease specific survival (DSS), and recurrence free survival (RFS, $p<0.001$). The 5-year OS, DSS and RFS were 95%, 97% and 89% for ENE(-) group, and 68%, 75%, and 69% in ENE(+) group. Other significant prognostic factors identified were nodal laterality, number of positive lymph nodes, number of lymph nodes with ENE, extent of ENE, tissue invaded by ENE, irregular soft tissue deposit, perineural invasion, and AJCC pN and pT stage.

ENE was further divided into major and minor ENE using a vertical extent of 2.8 mm, a cutoff determined using ROC analysis for RFS. Irregular soft tissue deposits were considered as major-ENE. Among the 62 tumors with ENE, 30 (48%) had major-ENE. Log rank pairwise test showed that major-ENE was associated with decreased OS and DSS compared with minor-ENE and decreased OS, DSS and DFS compared with no-ENE; whereas minor-ENE was associated with decreased OS compared with no-ENE ($p<0.05$).

Multivariate survival analysis using Cox proportional hazard model showed that major-ENE was an independent prognostic factor for OS (hazard ratio [HR]=19.443, 95% confidence interval [CI] 5.113-73.930, $p<0.001$), DSS (HR=59.150, 95% CI 5.523-633.438, $p=0.001$) and RFS (HR=5.806, 95% CI 1.968-17.130, $p=0.001$), whereas minor-ENE was an independent prognostic factor for OS only (HR=8.867, 95% CI 2.210-35.574, $p=0.002$).

Conclusions: ENE is an independent prognostic factor in p16/HPV+ OPSCC. Furthermore, major-ENE, defined as a vertical extent > 2.8 mm and/or irregular soft tissue deposit, is associated with shortened survival compared with minor-ENE. Therefore, we propose to document the presence and extent of ENE for p16/HPV+ OPSCC. Consideration may be given for AJCC 9th edition to include ENE into pN stage of p16/HPV+ OPSCC.